Biochemical analysis revealing
the molecular actions of *Escherichia coli*
DNA polymerase III and IV
at the replication fork

Le Thi Thanh

Nara Institute of Science and Technology

Graduate School of Biological Sciences

Supervisor: Professor Hisaji Maki

Graduate School of Biological Sciences　Doctoral Thesis Abstract

Lab name (Supervisor)	Microbial molecular genetics (Professor Hisaji Maki)		
Name (surname) (given name)	Le Thi Thanh	Date	(2016/12/13)
Title	Biochemical analysis revealing the molecular actions of *Escherichia coli* DNA polymerase III and IV at the replication fork		

In *Escherichia coli,* DNA polymerase III (Pol III) is known as the primary enzyme for the genomic replication which rapidly replicates DNA with very high processivity and fidelity. However, Pol III is stalled when it encounters a blockage on template DNA, such as a DNA lesion (a DNA damage). One biological process known to rescue the stalled Pol III at a lesion site is the translesion synthesis (TLS), in which a specialized polymerase for TLS comes to take over the primer terminus from Pol III and synthesizes DNA across the lesion site instead of Pol III. This polymerase exchange process is called as "polymerase switch". DNA polymerase IV (Pol IV) is one of the TLS polymerases in *E. coli.* Previous studies revealed that Pol IV is involved in TLS of some special lesions such as N^2-dG adducts or alkylation damage. However, until now how the Pol III-Pol IV polymerase switch occurs is poorly understood.

Interestingly, it is reported that the overexpression of Pol IV strongly reduces the replication-fork speed and significantly increases the mutation frequency. Compared to Pol III, Pol IV can just slowly synthesize DNA with a small track and exhibits no proof reading activity. These data imply that slowing down of the replication fork movement and increment of the mutation rate observed when Pol IV is overexpressed may be caused by the participation of Pol IV in the genomic synthesis. Hence, I hypothesized that using its special ability to execute the polymerase-switch event, Pol IV may not only switch places with the stalled Pol III at some certain lesion sites during TLS but also replace the ongoing Pol III during the normal genomic replication. However, Pol III is very stable on the DNA template with a processivity of more than 50 kb per binding event because it forms a tight complex with the primer terminus and the sliding clamp that encircles template DNA. Therefore, it is interesting to know whether the polymerase switch between Pol III and Pol IV occurs without a lesion, and if it does, it is important to investigate how Pol IV displaces Pol III from the template DNA and how it switches the role with an ongoing Pol III on the template DNA, because such a mechanism would be used for the polymerase switch during TLS.

First, to figure out the molecular mechanism by which Pol IV gains access to the primer terminus during the polymerase-switching event, I aimed to find a condition that stimulates the switch between Pol IV and the ongoing Pol III on the sliding clamp.

I hypothesized that some difficult structures on template DNA, such as a hairpin structure, could be a trigger of the polymerase switch, because Pol III slows down the chain-elongation speed when it encounters such an obstacle on template DNA. By a synchronized DNA synthesis assay, so called the burst DNA synthesis assay, with a singly-primed, circular single-stranded DNA containing a short inverted repeat as a template DNA, I found that the polymerase switch between Pol III and Pol IV was strongly stimulated at the short hairpin site. My data suggest that the polymerase switch occurs when Pol III needs to overcome the hairpin structure by the strand displacement activity. I speculate that during the strand displacement synthesis, Pol III changes the conformation from the normal synthesis mode to the proofreading mode, and this transition may make the enzyme complex unstable and give Pol IV a chance to take over the primer terminus.

Second, I tested whether the polymerase switch between Pol III and Pol IV takes places not only at the burst DNA synthesis assay but also at the replication fork. From the biochemical analyses using *E. coli* replication fork reconstituted *in vitro*, I found that Pol IV indeed switches the place with Pol III at the normal replication fork and inhibits the fork progression. Notably, the inhibitory effect of Pol IV on leading synthesis seems to be stronger than that on lagging synthesis. In the presence of Pol IV, the lagging strand synthesis continues while producing shorter Okazaki fragments. On the other hand, the leading strand synthesis was turned off and the uncoupling of leading- and lagging-strand synthesis was induced. This implies that the role of Pol III on the leading strand may not be substituted by Pol IV.

Finally, I tried to answer an important, yet unsolved question in the study of Pol III-Pol IV switch: the fate of Pol III after the polymerase switch by Pol IV in the replication fork; whether Pol III still stays in the replication machinery or already dissociates from it. Using the reconstituted replication fork and a novel method developed in this study to isolate the replication intermediate, I observed that at a high concentration of Pol IV, Pol III detached from the fork by the intensive polymerase switch by Pol IV. This suggests that a new Pol III needs to be recruited to re-form the replisome to resume the normal replication.

As conclusions of my study, by biochemical analyses using *in vitro* DNA replication systems, I demonstrated that Pol IV has an ability to switch with ongoing Pol III on template DNA without a lesion. My data provide insights into the molecular mechanism of Pol III-Pol IV switch on the sliding clamp using a hairpin structure as a virtual trigger for the polymerase switch. In addition, consistent with the *in vivo* observation that Pol IV slows down the fork speed, I found that even at the normal replication fork the deleterious polymerase switch between Pol III and Pol IV takes place and thus Pol IV strongly inhibits the replication depending on its protein concentration.

List of contents

List of tables

List of figures

Chapter 1: Introduction

1.1. Genome maintenance by DNA replication in *E. coli* cell

Organisms faithfully maintain their DNA genome by DNA replication - a biological process whereby two copies of DNA are produced from the original one. *Escherichia coli* (*E. coli)* genome is composed of one circular chromosome and replication of the genome starts from the single origin sequence as called as *oriC* (Mott & Berger, 2007).

To initiate the replication process, the initiator proteins (DnaA is the major component) bind to DnaA boxes within the *oriC* region to form a protein/DNA complex where DNA wraps around the initiator proteins (Figure 1.1). This complex then directly catalyzes melting of an AT rich sequence in the *oriC*, leading to a recruitment of DNA helicase (DnaB) with help of the helicase loader (DnaC). Subsequently, DNA helicase opens the duplex DNA, recruits primase (DnaG) to form the primosome and synthesizes a RNA primer. Next, DNA polymerase (Pol) III holoenzyme comes to the RNA primer and starts DNA chain elongation. Finally, two replication forks are formed from the *oriC* and proceed in the opposite directions. Therefore, replication model of *E. coli* cell is also known as the bidirectional replication (Alberts, Johnson, & Lewis, 2002; Mott & Berger, 2007; Ozaki & Katayama, 2009).

The chain-elongation step is carried out by a replisome that is constructed by multiple proteins. On the replisome, DNA helicase lies on lagging template strand and unwinds parental duplex DNA in 5'-3' direction, produces two single-stranded templates for DNA synthesis by Pol III. This partial separation results in a Y-shaped structure as called replication fork. The duplex unwinding reaction by DNA helicase accumulates some torsional stress in front of the replication fork, which is later released by a topoisomerase II - DNA gyrase. Following helicase, asymmetric dimeric Pol III simultaneously incorporates nucleotides to both newly synthesized strands in 5'-3' direction. Therefore, the synthesis of the 3'-5' template strand is performed continuously and generates only a long leading product (this template strand is called as leading template). The synthesis of the 5'-3' template strand is discontinuously and results in a plenty of short Okazaki fragments (this template strand is called as lagging template). This semi-discontinuous replication manner exposes a segment of single-stranded DNA on lagging

template, which is covered by <u>S</u>ingle <u>S</u>tranded-DNA <u>B</u>inding protein, SSB. In *E. coli* cell, the length of the Okazaki fragments varies from 1000 - 2000 nucleotides. To mature lagging product, RNA primer in each Okazaki fragment is removed by RNase H and 5'-3' exonuclease activity of DNA Polymerase I (Pol I). After that, the gap is filled by Pol I and finally the nick is sealed by DNA ligase (Alberts et al., 2002; Lewis, Jergic, & Dixon, 2016).

Two replication forks move equally and stop when they encounter the termination complex, which is made by the binding of the termination protein (Tus) to the termination sequence (*terB*) after half way of the circular chromosome. In *E. coli* cell, replication of genomic DNA takes approximate 20 minutes (Dewar & Walter, 2017; Neylon, Kralicek, Hill, & Dixon, 2005).
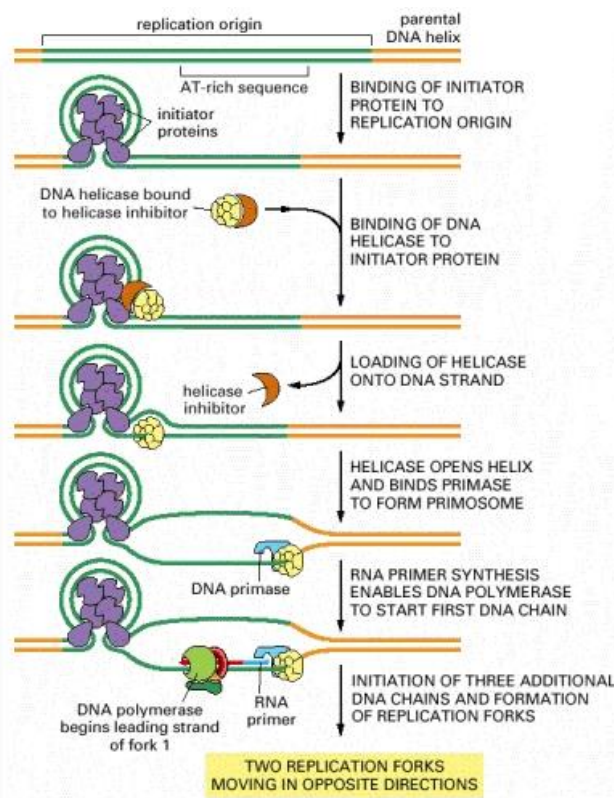
Figure 1.1. Progression of replication initiation in *E. coli* cell (Alberts et al., 2002). Replication starts from the single origin sequence called as *oriC*. Initially, the initiator proteins bind to the specific site within the *oriC* region to form a protein/DNA complex. This complex unwinds a short AT rich sequence in *oriC* and recruits DNA helicase. DNA helicase separates the duplex DNA and recruits primase to form a primosome. After that, primosome synthesizes a RNA primer and recruits replicative DNA polymerase III to start chain-elongation. Finally, two replication forks are created and move in the opposite directions.
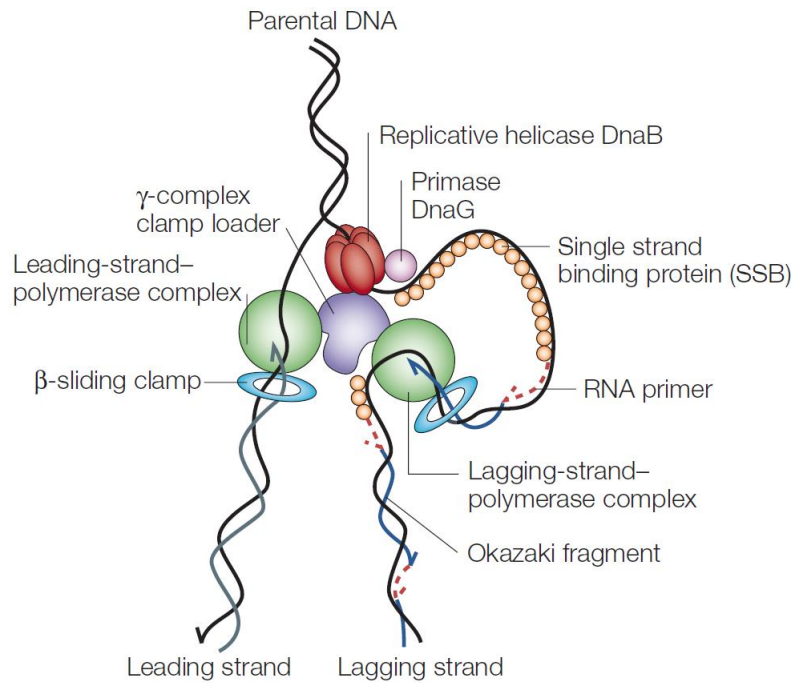
Figure 1.2. *E. coli* replisome structure (McGlynn & Lloyd, 2002). At the replication fork, DNA helicase unwinds duplex DNA, exposes two single-stranded templates for DNA polymerase III. Following DNA helicase, replicative DNA polymerase III synthesizes daughter strands in 5'-3' direction. On lagging template, a single-stranded region is generated which is covered by the single stranded-DNA binding protein SSB. On the replisome, the primase binds DNA helicase and serves for RNA primer synthesis of each Okazaki fragment. The leading polymerase, lagging polymerase and DNA helicase are coordinated by the clamp loader of DNA polymerase III holoenzyme.

1.2. DNA polymerase III holoenzyme

DNA polymerase III holoenzyme (Pol III HE) is the primary enzyme for DNA replication. The enzyme consists of 15 subunits with three subassemblies: two αεϴ polymerase cores for leading- and lagging synthesis, two β clamps for tethering leading- and lagging polymerases and a $\tau_2\gamma\delta\delta'\psi\chi$ clamp loader complex (DnaX complex) for β clamp loading (Figure 1.3) (H. Maki & Furukohri, 2013; McHenry, 2011). On the replisome, the β clamp tightly encircles template DNA strand with help of the clamp loader complex. Each polymerase core is tethered to the β clamp hence smoothly slides along the template DNA strand during chain-elongation step. The leading- and lagging polymerase cores are connected by the τ subunits of the clamp loader that enables the coupling DNA synthesis. In addition, Pol III HE also interacts with other components of the replication machinery, such as with the DNA helicase via the τ subunits- and with SSB on the lagging strand template via the subunit χ of the clamp loader (H. Maki & Furukohri, 2013; McHenry, 2011). All of these interactions allow the enzyme to synthesize DNA with a very high speed (approximate 1000 nucleotide per second) and a high processivity (more than 50 kb per binding event) (Lewis et al., 2016; McHenry, 2011).

Pol III possesses two activities, a 5'-3' polymerase activity by α subunit that drives the polymerization reaction and a 3-5' exonuclease activity by ε subunit that drives the proof reading reaction . Both α and ε subunits interact with two protein-binding pockets on the cleft of β clamp through their Clamp-Binding Motif CBM (Fernandez-Leiro, Conrad, Scheres, & Lamers, 2015; Scotland et al., 2015) (Figure 1.4). During normal elongation process, α subunit takes the primer terminus and synthesizes the daughter strand by addition of complementary nucleotides to newly strand in 5'-3' direction. The accuracy of nucleotide insertion is detected by the structure between the finger and the thumb domain, which holds DNA and scans the fit of a complementary nucleotide. When the enzyme made a misincorporation, it performs proofreading reaction to remove the incorrect nucleotide using 3-5' exonuclease activity and re-incorporates the correct one (Figure 1.5). This editing ability makes Pol III synthesize DNA with very high fidelity (approximate 1 mistake per 10^6 incorporation events) (Bloom et al., 1997; Fijalkowska, Schaaper, & Jonczyk, 2012a; H. Maki, Akiyama, Horiuchi, & Sekiguchi, 1990).

Beside polymerase and proofreading activities, Pol III also has another activity called as strand displacement activity, which allows the enzyme to overcome a secondary structure on template DNA such as a hairpin. Using the strand displacement activity, Pol III unwinds a hairpin or displaces downstream duplex DNA on template strand in a helicase-independent manner through DNA synthesis. Compare to the normal processive chain-elongation, the strand displacement reaction proceeds with slower rate (approximate 150 nucleotides/second) and lower processivity (approximate 300 nucleotides per binding event) (Yuan & McHenry, 2009). The molecular mechanism underlying strand displacement activity is not clear yet, but it is believed to occur through a link between the subunits τ-Ψ-χ of the clamp loader and the Single Stranded-DNA Binding protein, SSB (Yuan & McHenry, 2009) and requires the interaction between ε subunit of polymerase core and β clamp (Jergic et al., 2013).
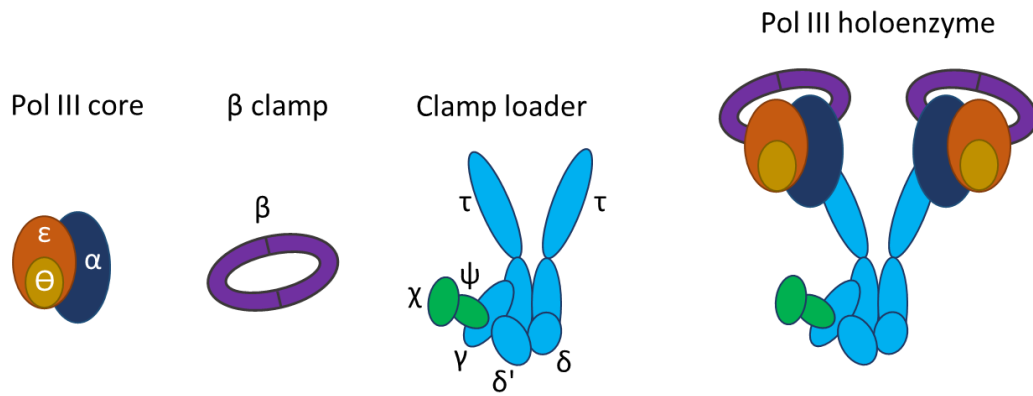
Figure 1.3. Structure of DNA polymerase III holoenzyme. Pol III HE consists of 15 subunits with 3 assemblies: two polymerase cores (αεϴ), two β clamps and a clamp loader (τ₂γδδ'ψχ) (H. Maki & Furukohri, 2013).
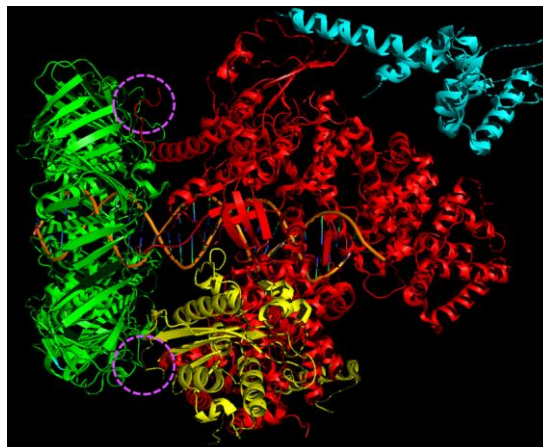
Figure 1.4. Crystal structure representing the interactions between Pol III core and β clamp. α (red)- and ε (yellow) subunits interact each other and both bind to the protein-binding pocket on the cleft of β clamp (green) though the Clamp-Binding Motif (CBM) (marked by pink circles). Brown helix represents for DNA and Cyan helix represents for τ subunit. This model was built using MacPyMOL Molecular Graphics System and the previously published data for the Pol III core-β clamp-DNA binding (Fernandez-Leiro et al., 2015).
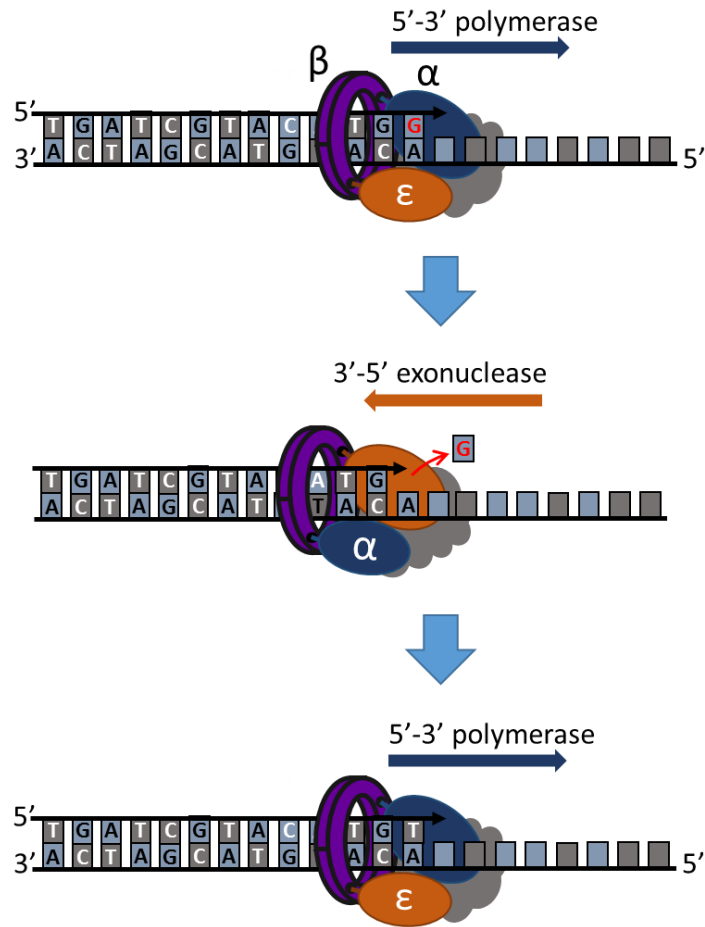
Figure 1.5. Proof reading activity of Pol III. During chain-elongation, Pol III incorporates complementary nucleotides to a nascent strand in 5'-3' direction by 5'-3' polymerase activity of α subunit. However, when the enzyme makes a mis-insertion, it changes the conformational mode from elongation to proofreading. In the proofreading mode, Pol III excises the incorrect nucleotide using 3'-5' exonuclease activity by ε subunit. Subsequently, Pol III returns to the elongation mode to add a correct nucleotide to the newly synthesized strand (H. Maki & Kornberg, 1987; Ozawa et al., 2013).

1.3. Damage tolerance pathways and translesion synthesis

Genome of all living cells is always exposed to both exogenous and endogenous sources of spontaneous damaging-agents that cause the formation of various damages in DNA. Even every cell possesses sufficient repair systems, which detect and remove these damages, damages sometimes evade and display during DNA replication. The faithful replication of genome is undertaken by the replicative DNA polymerase, which carries an editing ability allowing the enzyme to accurately copy new DNA strands with minimum rate of mistake. However, this high intrinsic fidelity of the replicative DNA polymerase faces to the cost that they cannot bypass an abnormal structure on template DNA such as a DNA lesion. The stalling of the replicative DNA polymerase leads to the stalling of the replication fork movement and consequently may cause cell death. To avoid the deleterious effects of a stalled replication fork, cell has several mechanisms to help the replicase bypass a damage, called as damage tolerance. Damage tolerance consists of two pathways, recombinational pathway and translesion synthesis (Fuchs, 2016; Ghosal & Chen, 2013). In recombinational pathway, the stalling of replicative DNA polymerase induces uncoupling of leading and lagging strand synthesis, hence exposes an abnormal single-stranded DNA segment on leading template. This appearance of single-stranded DNA segment is a signal for SOS response (Ghosal & Chen, 2013; Kreuzer, 2013). Consequently, a double stranded DNA break is created and this initiates the recombination process. On the other hand, translesion synthesis is believed to directly rescue the stalled replication fork, by involvement of specialized polymerases that has an ability to synthesize DNA across a lesion (Fuchs, 2016; Ghosal & Chen, 2013).

Translesion synthesis is a conserved mechanism in all organisms from bacteria to mammals. When replicative DNA polymerase stalls at an obstacle on template DNA, a specialized polymerase (translesion synthesis polymerase) comes to exchange with the stalled replicative DNA polymerase and keeps elongating the daughter strand across the lesion. After that, the replicative DNA polymerase returns to the primer terminus and resumes processive DNA replication as usual (Figure 1.6). The polymerase exchange event at the primer terminus is called as "polymerase switch" (Furukohri, Goodman, & Maki, 2008).
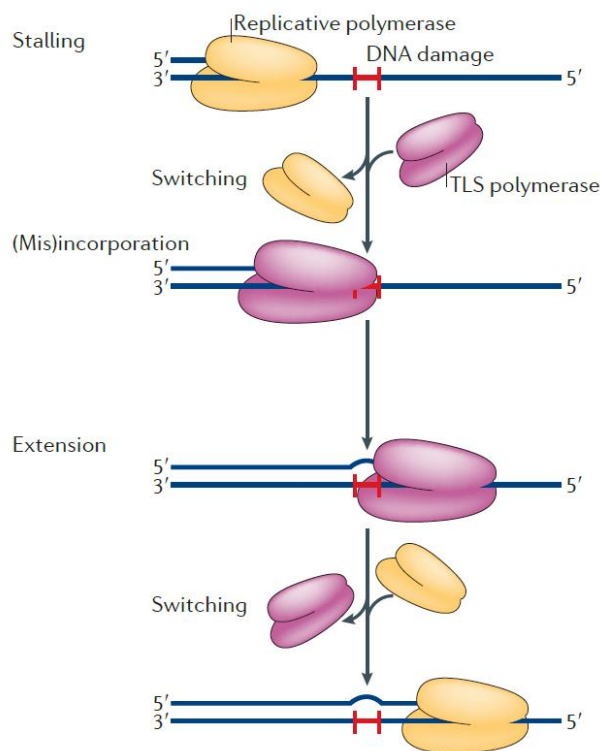
Figure 1.6. The basic mechanism of translesion synthesis (Sale, Lehmann, & Woodgate, 2012). When the replicative polymerase stalls at a site of the DNA damage, a TLS polymerase comes to switch the place of the stalled Pol III and synthesizes bypassing the lesion in either error-prone or error-free manner. After that, Pol III comes back to the primer terminus and resumes DNA synthesis.

Perhaps the feature that makes the translesion polymerases are able to elongate a daughter strand across a lesion is because unlike the replicative DNA polymerase, they lack a sufficient function to scan an incorrect nucleotide and a 3′-5′ exonuclease activity therefore synthesize DNA with very low fidelity. Depending on the situation, the lesion bypass by translesion synthesis may result in error-free or error-prone hence may cause mutagenesis. Translesion DNA polymerases synthesize DNA with very low speed and processivity.

There are three translesion synthesis DNA polymerases found in *E. coli*: DNA Polymerase II (Pol II), DNA Polymerase IV (Pol IV) and DNA Polymerase V (Pol V). Each polymerase works in translesion synthesis of different type of DNA lesion. Pol II is involved in bypassing of UV-induced damage. Pol IV is involved in translesion synthesis of N^2-dG adducts or alkylation damage. Pol V takes part in translesion synthesis of UV-induced pyrimidine dimers and abasic sites (Goodman & Woodgate, 2013; Sale et al., 2012; Uchida et al., 2008). Pol IV and Pol V are known as the main translesion synthesis DNA polymerases and upregulated during SOS

induction (Sale et al., 2012; Uchida et al., 2008). Among these three DNA polymerases, Pol IV is extremely abundant in both normal- and SOS-induced cells (Layton & Foster, 2003; Uchida et al., 2008) but its cellular function is still unclear.

1.4. DNA polymerase IV

DNA polymerase IV (Pol IV or DinB) is a product of *dinB* gene, which consists of 352 amino acids (including methionine) (Goodman & Woodgate, 2013; Layton & Foster, 2003). Pol IV belongs to the Y family polymerase and is conserved among three domains of life with the DpoIV ortholog in Archaea and Pol κ ortholog in human cell (Goodman & Woodgate, 2013; Sale et al., 2012) (Figure 1.7).

Like other TLS polymerases, Pol IV carries only 5'-3' polymerase activity and exhibits no proof reading activity. Depending on the type of DNA damage or the sequence context, Pol IV may carry out an error-prone or error-free translesion synthesis. So far it has been found that Pol IV is involved in bypassing of N^2-dG adducts or alkylation damages as cells lacking *dinB* gene display very high sensitivities with these agents, such as NFZ or MMS (Goodman & Woodgate, 2013; Scotland et al., 2015).

Pol IV contains all domains required for polymerase activity in the N-terminal half of the protein, including the finger, the thumb and the palm domain. The C-terminal contains an additional, Y-family specific domain, called little finger domain, serving to achieve TLS and the β clamp binding. Litter finger domain also stabilizes the enzyme on DNA at a damage site (Goodman & Woodgate, 2013; Sale et al., 2012; Scotland et al., 2015).

The interaction of Pol IV to the β clamp increases the enzyme's processivity but compared to Pol III HE, these interactions are weaker (Fernandez-Leiro et al., 2015). Co-crystal structure analysis of Pol IV little finger domain - β clamp reveals that Pol IV has several interaction sites to the β clamp (Bunting, Roe, & Pearl, 2003; Scotland et al., 2015) (Figure 1.8). For DNA synthesis, Pol IV is required to bind to the protein-binding pocket on the cleft of the β clamp through the hexameric Clamp-Binding Motif (CBM) 346-351 at the C-terminal (James et al., 2014; Scotland et al., 2015). The same binding pocket of the β clamp is used for both Pol III α and ε subunits to interact with the clamp via their CBM (Bunting et al., 2003) (Fig 1.8). Pol IV

also can bind to the position E93 and L98 on the rim of the β clamp (Scotland et al., 2015). Several groups revealed that these rim interactions is important for the polymerase switch between Pol III and Pol IV (Gabbai, Yeeles, & Marians, 2014; J. M. Heltzel, Maul, Scouten, & Sutton, 2009; James et al., 2014; Justin, Robert, David, & Mark, 2012).

In a normal cell, the protein concentration of Pol IV is detected at a concentration of approximately 200-250 nM, however, the enzyme is produced by 10-fold higher during SOS induction and its cellular concentration becomes more than 2000 nM (Layton & Foster, 2003; Uchida et al., 2008).
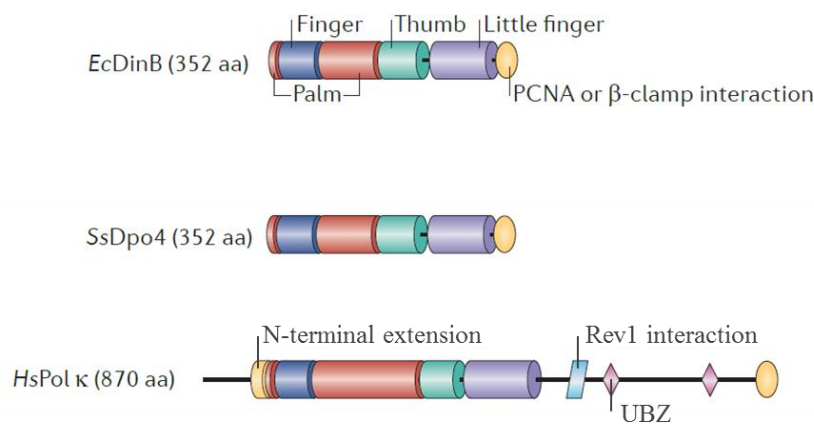
Figure 1.7. Domain organization of *E. coli* Pol IV (DinB) and its ortholog (Sale et al., 2012). The domains that require for polymerase activity including the palm, the thumb and the finger are located at the N-terminal. C-terminal domain serves for β clamp interaction. Compare to the replicative polymerase, Pol IV-group has an additional domain called litter finger. Human Polκ carries two additional domains: Rev1 interaction and UBZ (ubiquitin-binding motifs). *Ec*, *Escherichia coli*; *Ss*, *Sulfolobus solfataricus; Hs, Homo sapiens;* aa, amino acid.
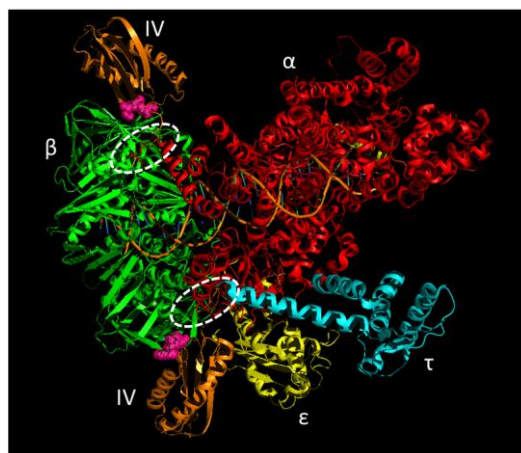
Figure 1.8. Co-crystal structure representing the co-interactions of Pol IV and Pol III core to β clamp. Pol IV has several interaction sites to the β clamp. On one hand, Pol IV can bind to the protein-binding pocket on the cleft of

the β clamp through the hexameric Clamp-Binding Motif (CBM) 346-351 at the C-terminal (white ellipse). This binding is required for DNA synthesis. However, Pol III α and ε subunits also bind to these binding pockets of the β clamp via their CBM during DNA synthesis (white ellipse). On the other hand, Pol IV also can bind to the position E93 and L98 on the rim of the β clamp (highlighted in pink). Brown helix represents for DNA. This model was built using MacPyMOL Molecular Graphics System and the previously published data for the binding of Pol III core, Pol IV to β clamp and DNA (Bunting et al., 2003; Fernandez-Leiro et al., 2015).

1.5. Earlier studies about the polymerase switch between Pol III and Pol IV

It has been classically believed that Pol IV is involved in translesion synthesis of some special DNA lesions such as N^2-dG adducts or alkylation damage (Goodman & Woodgate, 2013; Sale et al., 2012; Shrivastav et al., 2014; Uchida et al., 2008). When replicative Pol III stalls at a lesion on template DNA, Pol IV comes to exchange with the stalled Pol III at the replication fork and elongates the daughter strand to bypass the lesion *in vitro* (Ikeda et al., 2014).

Besides Pol IV's known function for TLS, Furukohri et al. revealed that Pol IV strongly inhibited DNA synthesis by Pol III on a normal template DNA without any lesion by *in vitro* primer-extension analysis, called Burst DNA synthesis assay, which allows the analysis of the chain-elongation reaction of Pol III on a singly primed-circular single-stranded template DNA, (Furukohri et al., 2008). In line of this inhibition, they found that the presence of Pol IV, even at low concentration, led to an appearance of particular intermediate-sized replication products of Pol III, suggesting that the elongation reaction of Pol III is inhibited by Pol IV at a particular location of template DNA. This finding imply that Pol IV might switch the place with an ongoing Pol III at that site on the template strand. It is predicted that the template DNA might contain some kinds of trigger that stimulates Pol III-Pol IV switch at the location. However, due to the limitation of the study, they were unable to figure out what is the detail of the trigger.

On the other hand, several *in vivo* studies reported that the overexpression of Pol IV strongly reduced replication-fork speed and significantly increased mutation frequency (Ikeda et al., 2012; Kuban et al., 2005; Kuban, Banach-Orlowska, Schaaper, Jonczyk, & Fijalkowska, 2006; Mori et al., 2012; Tan, Pham, Furukohri, Maki, & Akiyama, 2015). As mentioned previously, compared to Pol III, Pol IV slowly synthesizes DNA with a small tract and exhibits

no proof reading activity. These data suggests that the slowing down of the replication fork movement and increment of the mutation rate observed when Pol IV is overexpressed may be caused by the participation of Pol IV in the genomic synthesis. Taken together, I speculates that Pol IV may not only switch places with the stalled Pol III at some certain lesion sites during TLS but also can exchange with an ongoing Pol III at the replication fork.

However, this hypothesis has never been seriously discussed so far, because during DNA replication, it is well-known that Pol III stably binds to template strand with the processivity of more than 50 kb per binding event (Furukohri et al., 2008; Toste Rego, Holding, Kent, & Lamers, 2013). One of the features that contribute to the processive synthesis of Pol III is the tethering between the polymerase core and the sliding β clamp during DNA synthesis (LaDuca, Crute, McHenry, & Bambara, 1986; Lewis et al., 2016; H. Maki & Furukohri, 2013; Stukenberg, Studwell-Vaughan, & O'Donnell, 1991). As mentioned in chapter 1.2, the polymerase core of Pol III, which catalyzes the enzyme activity, is composed of three subunit: α subunit that drives the polymerization reaction, ε subunit functions in proofreading reaction and a small θ subunit with an unclear function. In the replisome, both α and ε subunits bind to two protein-binding pockets on the cleft of dimeric β clamp and during normal elongation mode, α subunit stably stays on the primer terminus (Scotland et al., 2015). Therefore, it seems to be difficult for Pol IV to just exchange the place with Pol III core on the clamp during normal DNA synthesis, and thus it is very important to know how Pol IV can displace Pol III from the template and gain access to the primer terminus without any lesion. However, so far the molecular basis underlies the polymerase switch between Pol III and Pol IV is largely unclear. As mentioned above in chapter 1.4, Pol IV can binds to the two different region of the β clamp, the cleft and the rim (Bunting et al., 2003). Recent studies by Dr Sutton's group proposed that while the binding of Pol IV to the cleft of β clamp is important for Pol IV DNA synthesis, the polymerase switch between Pol III and Pol IV requires both interactions: Pol IV to the cleft and Pol IV to the rim of β clamp (James et al., 2014; Scotland et al., 2015). In addition, biochemical studies revealed that the β clamp can simultaneously carries two different polymerases during DNA synthesis (Indiani, McInerney, Georgescu, Goodman, & O'Donnell, 2005; James et al., 2014). Jergic et al. also revealed that within Pol III holoenzyme, while the interaction between α subunit and

the β clamp is very strong to undertake the processive elongation, the interaction between ε subunit and the β clamp is weaker (Jergic et al., 2013). These characteristics may give a chance for a second polymerase to gain access to the primer terminus.

In terms of studying Pol III-Pol IV switch, an important but still remain unanswered question is what happens to Pol III after Pol III-Pol IV switch occurs at the replication fork. Whether Pol III still stays in the replisome or is pushed away from the fork by Pol IV. Using the single molecule analysis, James et al. found that at a high concentration of Pol IV, Pol IV significantly reduced the processivity of Pol III (James et al., 2014).. From this observation they suggested that Pol IV might push away Pol III from the primer template junction. However, this suggestion was not evidenced enough, because the reduction of the Pol III processivity can be explained by any causes rather than the dissociation of Pol III from the primer terminus. In addition, the system that they used is just a simple primer-extension reaction of Pol III on a primed-single stranded template, which was not able to represent a precise *E. coli* replication fork. On the replisome, besides the binding with the template strand, Pol III holoenzyme also interacts with other protein components such as DNA helicase or SSB, those enhance the stability of Pol III holoenzyme on the replisome (McHenry, 2011).

1.6. Thesis rationale

In the first part of this study, using Burst DNA synthesis assay, I firstly tested whether Pol IV has a potential to switch the place with an ongoing Pol III and if it is the case, what is the trigger on the template DNA. Because Pol III slowed down when it encounters the secondary structures on the template DNA such as a hairpin, I speculated that hairpin DNA maybe a trigger for Pol III-Pol IV switch. I next studied the molecular mechanism of how Pol IV displaces Pol III from the template DNA and gains access to the primer terminus.

In the second part, to explain the *in vivo* data about the increment of untargeted mutation rate and decrement of replication-fork speed when Pol IV was overproduced by the hypothesis that Pol IV enters to the replisome in the replication fork by Pol III-Pol IV switch, I tested the ability of Pol IV to enter a normal replication fork without any lesion using *E. coli* reconstituted replication assay. In this part, I also monitored how Pol IV affects DNA synthesis by Pol III at

the replication fork in detail.

Regarding to the *in vitro* studies using *E. coli* reconstituted replication assay, it is very important for accurate analysis to synchronize all the replisome those are formed on a plenty of template DNA molecules. In addition, to study the individual replication protein's function, it is also important to have a method to isolate the replication intermediate from other components. In this study, I tried to establish a novel system that allowed me to synchronize the replication fork and isolate the replication intermediate from the reaction mixture.

Using the novel established system mentioned above, I aimed to study the fate of Pol III after Pol III-Pol IV switch at the replication fork: whether Pol III still stays on the replisome or dissociated. As mentioned in chapter 1.2, Pol III holoenzyme consists of 3 subassemblies: the polymerase core, the sliding clamp and the clamp loader complex, and within the enzyme complex, the leading- and lagging polymerase cores are tightly anchored by the clamp-loader and the clamp. In addition, in the replisome, Pol III holoenzyme also interacts with other replication components through the clamp loader such as DNA helicase or SSB on the lagging template. Therefore, I speculated that even Pol IV displaces Pol III from the primer terminus, Pol III may still stay in the replisome through these interactions and soon comes back to the primer terminus when Pol IV dissociates.

Chapter 2: Materials and methods

2.1. Materials

2.1.1. Chemicals, reagents and enzymes

Chemicals and reagents used in this study were purchased from Wako and Sigma.

Restriction enzymes were from New England Biolabs and Takara. T4 DNA ligase was from Takara. T4 polynucleotide kinase were from Toyobo. PCR kits were from Takara or Bio Academia. DNA polymerase Stoffel fragment was from Thermo Fisher Scientific. Therminator™ DNA Polymerase was from New England Biolabs. Dynabeads M280 streptavidin was from Thermo Fisher Scientific.

DNA markers were from Takara. Protein markers were from Bio-Rad. Columns for DNA or protein purification were from GE Healthcare.

2.1.2. *E. coli* strains and bacteriophage

E. coli JM109 strain was used for construction and maintenance of the plasmids pMS2-AIR12-12, pMS2-AIR6-6, pMS2-NIR15-3-15. *E. coli* XL1-Blue MRF' strain was used for amplification of VCSM13 helper phage. *E. coli* W3110 *tus*::Km strain was used for maintenance and amplification of the plasmid pMOL7. *E. coli* Biotin Xcell strain was used for construction and maintenance of the overexpression vector carrying the *tus* gene - pAV-*tus,* overexpression and *in vitro* biotinylation of the protein Tus.

VCSM13 helper phage was used to prepare the single stranded template DNA for Burst DNA synthesis.

E. coli strains, bacteriophage used in this study and their brief descriptions are listed in Table 2.1.

Table 2.1. List of *E. coli* strains and bacteriophage used in this study.

Name	Genotype	Description	Source
***E. coli* strain**			
JM109	endA1 glnV44 thi-1 relA1 gyrA96 recA1 mcrB$^+$ Δ(lac-proAB) e14- [F' traD36 proAB$^+$ lacI^q lacZΔM15] hsdR17(r$_K^-$m$_K^+$)		Laboratory stock
JM109/pMS2		JM109 strain carries the plasmid pMS2	Furukohri,A. (unpublished data)
JM109/ pMS2-AIR23-23		JM109 strain carries the plasmid pMS2-AIR23-23	The plasmid was from (Masaaki Moriya, 1993). Noted that the original name was pMS2 but renamed as pMS2-AIR23-23 in this study
JM109/ pMS2-AIR12-12		JM109 strain carries the plasmid pMS2-AIR12-12	This study
JM109/ pMS2-AIR6-6		JM109 carries the plasmid pMS2-AIR6-6	This study
JM109/ pMS2-NIR15-3-15		JM109 strain carries the plasmid pMS2-NIR15-3-15	This study
XL1-Blue MRF'	Δ(*mcrA*)*183* Δ(*mcrCB-hsdSMR-mrr*)*173 endA1 supE44 thi-1 recA1* gyrA96 relA1 lac *[F' proAB* lacI^q*ZΔM15 Tn*10 *(Tet^r)]*	For amplification of VCSM13 helper phage	Stratagene
W3110 *tus*::Km/pMOL7	*LAM-*, in(rrnD-rrnE)1, rph-1, r+m+Tus::km	*E. coli* strain carries the plasmid pMOL7	(Higuchi et al., 2003)
Biotin Xcell	MC1061 [F´ pro A+B+ lacIqZΔM15::Tn10 (TetR)] araD139 Δ(ara-leu)7696 Δ(lac)l74 galU galK hsdR2(rK- mK+) mcrB1 rpsL (StrR) birA		Lucigen
Biotin Xcell/ pAV-*tus*		Biotin Xcell strain carries the plasmid pAV-*tus*	This study
Bacteriophage			

Name				Source
M13VCS helper phage			For preparation of the single stranded plasmid	Stratagene

2.1.3. Plasmids

Plasmids used in this study including the template DNA for *in vitro* replication assays and vector for protein expression are listed in Table 2.2.

Table 2.2. List of plasmids used in this study and their descriptions.

Name	Size	Description	Source
Template for Burst DNA synthesis assay			
pMS2	5.2 kb	Hairpin-free template.	Furukohri,A. (unpublished data)
pMS2-AIR23-23	5.2 kb	Template carries a perfect inverted repeat AIR23-23 (23 nucleotides long in each arm).	(Masaaki Moriya, 1993). Noted that the original name was pMS2 but renamed as pMS2-AIR23-23 in this study
pMS2-AIR12-12	5.2 kb	Template carries a perfect inverted repeat AIR12-12 (12 nucleotides long in each arm).	This study
pMS2-AIR6-6	5.2 kb	Template carries a perfect inverted repeat AIR6-6 (6 nucleotides long in each arm).	This study
pMS2-NIR15-3-15	5.2 kb	Template carries a natural inverted repeat NIR15-3-15 (15 nucleotides long in each arm and 3 nucleotides spacer).	This study
Template for *oriC* assay			
pMOL7	4.4 kb	Template carries a replication origin site - *oriC* and a replication termination site - *terB* of *E. coli.*	(Higuchi et al., 2003)
Other plasmid			
pAV-tus		Expression vector carries the *tus* gene	This study

i. Construction of the template containing the shorter inverted repeat pMS2-AIR12-12 and pMS2-AIR6-6

Inside the sequence of the inverted repeat A23-23, there are two symmetric recognition

sites of *Sal*I and two symmetric recognition sites of *Eco*RV (Figure 2.1). Therefore, to shorten the length of the original inverted repeat, I digested the plasmid pMS2-AIR23-23 by restriction enzyme *Sal*I or *Eco*RV and re-ligated the plasmid by T4 DNA ligation. Cleavage by *Sal*I removed 11 nucleotides in each arm at the central of the inverted repeat A23-23, resulted in a new plasmid, pMS2A12-12, which carries a shorter inverted repeat with 12 nucleotides long in each arm (as named as A12-12). In the other hand, cleavage by *Eco*RV cut down 17 nucleotides in each arm at the central of the inverted repeat A23-23, generated a new plasmid, pMS2A6-6, which carries a much shorter inverted repeat with 6 nucleotides long in each arm (as named as AIR6-6). After getting the double stranded plasmid having the desire inverted repeats, respective single stranded template DNA for Burst DNA synthesis assay were prepared using VCS helper phage infection.
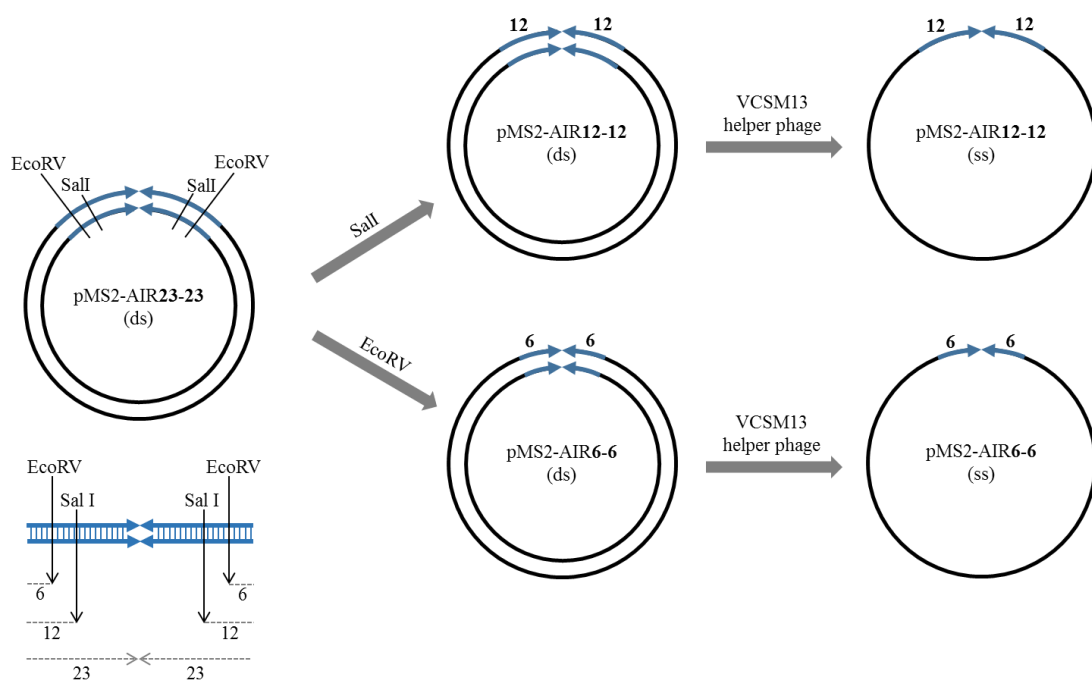
Figure 2.1. Construction of the template DNA containing the shorter inverted repeat by restriction enzyme digestion and T4 DNA ligation. After making the double stranded plasmid carries the shorter inverted repeat, the respective single stranded template DNA was prepared using VCS helper phage infection.

ii. Construction of the template containing an E. coli endogenous inverted repeat pMS2-NIR15-3-15.

An *E. coli* endogenous inverted repeat contains 15 nucleotides in each arm and a 3

nucleotides spacer (so called NIR15-3-15), which is located from nucleotide position 1790249 to 1790281 in MG1655 genome, was amplified by PCR using the forward primer carries a *Kpn*I recognition site at 5' end (NIR15-3-15 FOR) and the reverse primer carries a *Apa*I recognition site at 5' end (NIR15-3-15 REV). Subsequently, the PCR product was digested by these two restriction enzymes, *Kpn*I and *Apa*I. On the other hand, the hairpin-free plasmid pMS2 was also digested by the same restriction enzyme. Finally, the digested- PCR product and pMS2 was ligated and transformed into the *E. coli* strain JM109. For single stranded template preparation, VCSM13 helper phage infection was used.

2.1.4. Oligonucleotides

The oligonucleotides used in this study including the primers for Burst DNA synthesis assay, PCR amplification and the probes for Southern blot analysis are listed in Table 2.3.

Table 2.3. List of oligo DNA used in this study and their descriptions.

Name	Sequence (5'-3') and length (nt)	Description
Primers for Burst DNA synthesis assay		
pri-pMS2-AIR1	AGAGCAGCCGATTGTCTGTTGT GCC (25 nt)	For studying effect of the inverted repeats to Pol III-Pol IV switch (artificial inverted repeats)
pri-pMS2-AIR2	AGCGATTGCATAAGCTTTTGCC ATTC (26 nt)	For studying effect of the strand displacement activity of Pol III to Pol III-Pol IV switch
pri-pMS2-NIR	AATCATGCGAAACGATCCTCATC CTG (26 nt)	For studying effect of the inverted repeat to Pol III-Pol IV switch (natural inverted repeat)
Primers for PCR amplification		
NIR15-3-15-FOR	TGCAGGTACCTTAGATTATCCT GATTATAAACG (33 nt)	For PCR amplification of the natural inverted repeat NIR15-3-15 from MG1655 genome.
NIR15-3-15-REV	GACTGGGCCCTGATGCGTTCCT CACTTG (28 nt)	
Probes for Southern blot analysis		
Probe A	CGATGTAACCCACTCGTGCACC CAACTGATCTTCAG (36 nt) Located from position 4051-4086 on pMOL7	For detecting the leading product of the counter clock-wise replication fork on pMOL7
Probe A'	GAGTGATAACACTGCGGCGAAC TTACTTCTGACAACGATCG (41 nt) Located from position 3501-3541 on pMOL7	For detecting the Okazaki fragments of the counter clock-wise replication fork on pMOL7

2.1.5. Replication proteins

Proteins for *in vitro* replication assays performed in this study, including Burst DNA synthesis assay and *oriC* assay are listed as below:

DnaA (300 ng/μl), HU (80 ng/μl), γ complex (880 ng/μl) were a kindly gift from Prof. Katayama in Kyushu University. Wild type Tus was a generous gift from Prof. Hidaka in National institute for Basic Biology.

DNA gyrase (His-GyrA, 2200 ng/μl; His-GyrB, 1100 ng/μl), β clamp (400 ng/μl), SSB (570ng/μl), Pol III* fraction IV (80 units/μl), HolDCBP-tagged-Pol III* (12 units/μl), DnaB (980 ng/μl), DnaC (333 ng/μl), DnaG (980 ng/μl) were previously purified in my laboratory or purified in this study.

Biotinylated Tus was purified in this study as described in Chapter 3.

HolD-CBP-tagged-DnaE173 Pol III was previously purified by Furukohri, A. et al. Pol IV (wild type and the mutants D8A, △C5) were previously purified by (Furukohri et al., 2008).

2.2. Methods

2.2.1. Burst DNA synthesis assay

Preparation of the γ- ^{32}P labeled primed-single stranded circular template DNA

The primers pri-pMS2-AIR1 and pri-pMS2-NIR were labeled with ^{32}P at 5' end by T4 polynucleotide kinase (Toyobo) at 37°C for 30 min followed by G25 column (GE healthcare) purification. To make the primed-single stranded template DNA, the suitable radiolabeled primer was mixed with the respective single stranded template at the molecular ratio of 3:1 in the presence of 265 mM NaCl. The mixture was incubated at 96°C for 3 min, 56°C for 10 min and slowly cooled down to room temperature for overnight. To remove the unbound primers, the solution was loaded onto a Microspin S-400 HR column (GE Healthcare).

Burst DNA synthesis assay

7.5 μl of buffer 1 containing 20 mM Tris-Cl (pH 7.5), 4% glycerol, 8 mM DTT, 80 μg/mL BSA, 8 mM $MgCl_2$, 1 mM ATP, 100 μM each of dATP, dGTP, dCTP, 0.03 pmol primed-single stranded template DNA, 147 nM SSB, 4 nM β clamp, 20 units of HolD-Pol III* was incubated at 30°C for 3 min to form the initiation complex. After that, the DNA chain-elongation process was started by addition of 22.5 μl of 30°C pre-warm buffer 2 containing 20 mM Tris-Cl (pH 7.5), 4% glycerol, 8 mM DTT, 80 μg/mL BSA, 8 mM $MgCl_2$, 1 mM ATP, 100 μM each of dATP, dGTP, dCTP, 133 μM dTTP and incubated at 30°C for some certain time points. The reaction was stopped by adding 140 μl of stop solution containing 50 mM EDTA, 0.15% SDS, pH 8.0. The proteins were degraded by treatment with Proteinase K (33 μg/mL) at 55°C for 30 min. The products was then purified by phenol/chloroform extraction, ethanol precipitation and resuspended in 2 μl of sample buffer containing 98% formamide, 10 mM EDTA, 0.05% bromophenol blue, 0.05% xylene cyanol.

In the experiment checking the behavior of Pol III at the inverted repeat site, SSB was added to Burst synthesis assay to the final concentration of 0, 37, 74, 147, 265 nM.

In the experiments studying Pol III-Pol IV switch at the hairpin structure, Pol IV was added to the buffer 1 or buffer 2 with some indicated concentrations.

To check the behavior of Pol IV alone at the hairpin structure, instead of Pol III, 100 nM of Pol IV was used. The γ complex was added to load the β clamp onto the DNA template.

2.2.2. Strand displacement assay

The experimental procedure is same as for Burst DNA synthesis assay, except that two primers, pri-pMS2-AIR1 with 5' ^{32}P labeling and pri-pMS2-AIR2 without labeling were annealed into the single stranded hairpin-free template pMS2 with the molecular ratio of 1.5:3:1, respectively. In addition, a double amount of HolD-Pol III* and β clamp was added into the reaction mixture.

2.2.3. *In vitro oriC*-plasmid replication assay (*oriC* assay)

This assay reconstitutes the bidirectional replication system of *E. coli in vitro* by using an *oriC* plasmid mimicking *E. coli* genome as template DNA and the proteins involved in *E. coli* replication.

The standard reaction mixture (15 μl) contained 40 mM HEPES-KOH (pH 7.6), 0.1 mg/mL BSA, 10 mM DTT, 10 mM magnesium acetate, 2mM ATP, 1 mM GTP, 1 mM CTP, 1 mM UTP, 4 mM creatine phosphate, 40 μg/mL creatine kinase, 50 μM NAD, 100 μM of each dNTPs, pMOL7 (120 ng), DnaA (60 ng), SSB (174 ng), HU (10.2 ng), DnaG (194 ng), DnaB (90 ng), DnaC (55.2 ng), DNA Gyrase subunit A (108 ng), DNA Gyrase subunit B (216 ng), Polymerase III* (14.4 units), β clamp (30 ng), Tus (67.2 ng). The reaction was assembled on ice in the absence of DnaA. The replication process was started by addition of DnaA and incubated at 30ºC for 15 min. The reaction was stopped by addition of an equal volume of Stop solution containing 50 mM EDTA (pH 8.0) and 0.15% SDS. In the case when the *oriC* product was subjected to Pull-down assay, the stop solution contained only EDTA (50 mM). The proteins were degraded by incubating with 0.15% SDS and 50 μg/mL proteinase K at 55ºC for 30 min. After that, the DNA was purified by phenol/chloroform extraction, ethanol precipitation and resuspended in 10 μl of 1/10 TE solution containing 1mM Tris-HCl (pH 8.0), 0.1 mM EDTA. For total products analysis, the replication reaction was performed in the presence of α-^{32}P dATP.

2.2.4. Pull down assay

i. Pull down assay for checking the biotinylation efficiency of the biotinylated Tus

30 µl of the Dynabeads M280 Streptavidin (Thermo Fisher Scientific) was washed by 1 ml of 1X Hepes buffer containing 40 mM Hepes-KOH, 100 µg/mL BSA, 10 mM DTT. After that, 100 ng of the protein (wild type Tus or biotinylated Tus) was mixed with the washed bead in the buffer containing 1X Hepes and 100 mM NaCl at room temperature for 2 min. The tube was then placed on a magnetic separation rack for 1 min and the supernatant and pellet were separated. The pellet was washed 4 times by 100 µl of 1X Hepes buffer and resuspended in 5 µl of 1X Hepes buffer. The protein was released from the beads by adding the SDS sample buffer to final concentration of 62.5 mM Tris-Cl pH 6.8, 2.5% SDS, 0.002% Bromophenol Blue, 5% β-mercaptoethanol, 10% glycerol and heating at 100ºC for 5 min. The solution containing the protein was withdrawn using the magnetic separation rack. The supernatant was also mixed with the SDS sample buffer to final concentration of 62.5 mM Tris-Cl pH 6.8, 2.5% SDS, 0.002% Bromophenol Blue, 5% β-mercaptoethanol, 10 % glycerol. The samples from both supernatant and pellet were subjected to a 15% SDS polyacrylamide gel. The electrophoresis of the proteins was carried out at 20 mA for 2 hours in a SDS-PAGE running buffer containing 25 mM Tris, 192 mM glycine, 0.1% SDS. After electrophoresis, the proteins were stained by PlusOne Silver Staining Kit (GE healthcare). The gel was dried by Gel Air Drier (Bio-Rad).

ii. Pull down assay for isolation of the replication intermediates from oriC assay

30 µl of the Dynabeads M280 Streptavidin (Thermo Fisher Scientific) was washed by 1 ml of 1X Hepes buffer containing 40 mM Hepes-KOH, 100 µg/mL BSA, 10 mM DTT. 15 µl of the *oriC* reaction was added into the washed beads. The mixture was incubated at room temperature for 1 min. After that, the tube was placed on a magnetic separation rack for 1 min and the supernatant and pellet was separated. The supernatant was kept on ice (named as S1). The pellet was washed by 300 µl of 1X Hepes.

To analyze the recovery rate of the replication intermediates in the pellet, the DNA was released from the beads by adding 100 µl of the releasing solution (2% SDS, 30 mM biotin, 6 M urea, 2 M thiourea, 137 mM NaCl, 2.7mM KCl, and 11.9 mM phosphates, pH 12), and

incubating at room temperature for 15 min, 96ºC for 15 min. Afterwards, the solution was withdrawn using the magnetic separation rack.

To restart the isolated replication intermediates, the pellet was resuspended by 15 µl of a buffer containing 40 mM HEPES-KOH (pH 7.6), 0.1 mg/mL BSA, 10 mM DTT, 10 mM magnesium acetate, 2mM ATP, 1 mM GTP, 1 mM CTP, 1 mM UTP, 4 mM creatine phosphate, 40 µg/mL creatine kinase, 50 µM NAD, 100 µM of each dNTPs, SSB (174 ng), HU (10.2 ng), DnaG (194 ng), DNA Gyrase subunit A (1080 ng), DNA Gyrase subunit B (2160 ng); and incubated at 30ºC for 5 min or 10 min. The pellet was collected and the supernatant was removed using the magnetic separation rack. The DNA in the pellet was released from the beads by adding 100 µl of the releasing solution (2% SDS, 30 mM biotin, 6 M urea, 2 M thiourea, 137 mM NaCl, 2.7mM KCl, and 11.9 mM phosphates, pH 12), followed by incubating at room temperature for 15 min, 96ºC for 15 min. The solution was withdrawn using the magnetic separation rack.

The supernatant (S1) and the solution from the pellet were treated with Proteinase K (50 µg/mL) at 55ºC for 30 min to degrade the proteins. After that, the DNA was purified by phenol/chloroform extraction, ethanol purification and resuspended in 5 µl of 1/10 TE solution (1mM Tris-HCl pH 8.0, 0.1 mM EDTA). The products were analyzed by 0.9% alkaline agarose gel electrophoresis, followed by Southern blot analysis.

2.2.5. Sequencing gel electrophoresis analysis

The products of Burst DNA synthesis assay was resuspended in 2 µl of a sample buffer containing 98% formamide, 10 mM EDTAs, 0.05% bromophenol blue, 0.05% xylene cyanol and loaded to a denaturing polyacrylamide gel (7.5% polyacrylamide. 8M urea, 6.3M formamide, 1X TBE). Electrophoresis was carried out at 35W for 1.5 hours in 1X Tris-borate-EDTA (TBE) buffer containing 89 mM Tris, 89 mM boric acid and 2 mM EDTA, pH 8.0. A ^{32}P-labeled 20 bp marker was used as the DNA size standards. After electrophoresis, the gel was dried on the DE81 paper (Whatman) using the Vacuum gel drier (Bio-Rad). The result was visualized by BAS2500 phosphorimager (Fuji Film).

2.2.6. Alkaline agarose gel electrophoresis analysis

The electrophoresis was carried out at an alkaline condition therefore the double stranded DNA was denatured to the single stranded DNA. The single stranded DNA was then migrated from cathode to anode according to their size. The purified product from *oriC* assay or Pull down assay was mixed with a loading dye to the final concentration of 30 mM NaOH, 30 mM EDTA, 10% sucrose and 0.1% bromocresol green before loading to a 0.9% alkaline agarose gel. Electrophoresis was performed at 3.6V/cm for 4 hours in the alkaline electrophoresis buffer containing 30 mM NaOH and 1 mM EDTA. *Eco*T14I digested-λ DNA marker with 5' labeled by ^{32}P was used as the DNA size standards.

After electrophoresis, the gel was either fixed in 7% TCA solution for 20 min, pressed for 30 min and dried using the Vacuum gel drier (Bio-Rad); or proceeded to Southern blot analysis.

2.2.7. Southern blot analysis

After separation by alkaline agarose gel electrophoresis, the DNA was transferred onto a Hybond N$^+$ nylon membrane (GE healthcare) by capillary method using 10X Saline-Sodium Citrate (SSC) buffer (1.5 M NaCl, 150 mM $Na_3C_6H_5O_7$, pH 7.0); and cross-linked by UV radiation at 120 mJ for 2 min. The replication product was then hybridized with the suitable 5' ^{32}P labeled probe in a hybridization buffer containing 6X SSC (0.9 M NaCl, 90 mM $Na_3C_6H_5O_7$, pH 7.0), 5X Denhardt's solution (0.1% Bovine Serum Albumin (BSA), 0.1% Ficoll, 0.1% Polyvinylpyrrolidone (PVP)), 0.1 mg/mL Salmon sperm DNA and 0.5% SDS at 55ºC for overnight. The membrane was washed 4 times with the washing solution (0.1X SSC, 0.1% SDS). The hybridized products were visualized by BAS2500 phosphorimager (Fuji Film). Analysis of the autoradiogram was carried out using Image Gauge software (Fuji film).

2.2.8. SDS polyacrylamide gel electrophoresis analysis

Protein samples were mixed with the SDS sample buffer to final concentration of 62.5 mM Tris-Cl pH 6.8, 2.5% SDS, 0.002% Bromophenol Blue, 5% β-mercaptoethanol, 10 % glycerol. The mixture was subjected to a SDS polyacrylamide gel (12% or 15%). The electrophoresis of the proteins was performed at 20 mA for 2 hours in a SDS-PAGE running buffer containing 25

mM Tris, 192 mM glycine, 0.1% SDS. After electrophoresis, the proteins were stained by Coomassie Brilliant Blue or Silver. The gel was dried the Vacuum gel drier (Bio-Rad).

2.2.9. Preparation of DNA markers for electrophoresis

i. Radiolabeled EcoT14-digested λ DNA marker

2.65 μg of λ DNA was digested by 1.25 units of *Eco*T14I restriction enzyme (Takara) in the reaction buffer for 2 hours at 37°C. For alkaline gel electrophoresis, the digested bands were labeled by ^{32}P at 5' end using T4 polynucleotide kinase (Toyobo).

ii. Radiolabel 20 bp DNA ladder

For sequencing gel electrophoresis analysis, the 20 bp DNA ladder (Takara) was labeled by ^{32}P at 5' end using T4 polynucleotide kinase (Toyobo).

iii. Radiolabel 1-nucleotide laddering marker for sequencing gel electrophoresis analysis

The sequencing marker for sequencing gel electrophoresis analysis was prepared based on Sanger sequencing method, whereby each of the ddNTPs was added into the reaction mixture to block the chain-elongation of polymerase. A ^{32}P-labeled primer was annealed to the single stranded circular template DNA. Afterwards, the primer extension reaction was performed in 20 μl of the reaction buffer containing 0.25 pmol of the primed-single stranded template, 1 unit of DNA polymerase Stoffel fragment (Thermo Fisher Scientific) or Therminator™ DNA Polymerase (New England Biolabs), 2.5 mM MgCl$_2$, dNTPs (2 μM in the case of DNA polymerase Stoffel fragment and 100 μM in the case of Therminator™ DNA Polymerase) and each of four dideoxynucleotides, 60 μM ddATP or 80 μM ddTTP or 20 μM ddGTP or 40 μM ddCTP at 74°C for 5 min. The reaction was stopped by addition of an equal volume of stop solution containing 50 mM EDTA. The product was purified by phenol/chloroform extraction, ethanol precipitation and resuspended in 2 μl of sample buffer containing 98% formamide, 10 mM EDTA, 0.05% bromophenol blue, 0.05% xylene cyanol.

Chapter 3: Results

Part I: Study of the molecular mechanism underlying Pol III-Pol IV switch using Burst DNA synthesis assay

As described in the Experimental procedure, Burst DNA synthesis assay allows a simple chain-elongation reaction of Pol III on a singly primed-single stranded circular template DNA (Figure 3.1). Briefly, the singly primed-single stranded circular template DNA was pre-incubated with ATP, three deoxyribonucleotides dACGTPs, single stranded-DNA binding protein (SSB) and Polymerase (Pol) III holoenzyme at 37ºC for 3 min. During this process, SSB covered the single stranded template DNA while Pol III holoenzyme formed an initiation complex at the primer terminus. When the ford deoxyribonucleotide - dTTP was added, Pol III holoenzyme started elongation process. To analyze the elongated product, the primer was labeled by γ-^{32}P at 5' end.
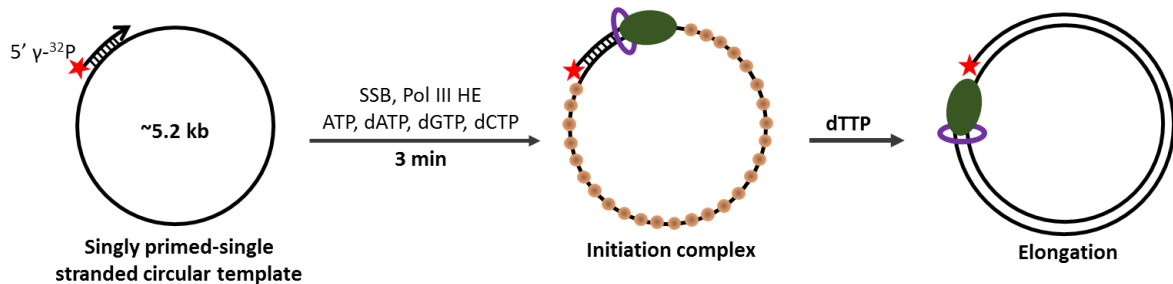
Figure 3.1: Schematic diagram showing the principle of Burst DNA synthesis assay. To form the initiation complex, the singly primed-single stranded circular template DNA was pre-incubated with ATP, three deoxyribonucleotides dACGTPs, single stranded-DNA binding protein (SSB) and Pol III holoenzyme for 3 min at 37ºC. When dTTP was added, Pol III holoenzyme started chain-elongation from primer terminus. To analyze the elongated product, the primer was labeled by γ-^{32}P at 5' end.

To study the molecular mechanism of how Pol IV takes over the primer terminus from the ongoing Pol III on the sliding clamp, first, I needed to find a condition that stimulates the switch. It has been well known that replicative DNA polymerase (Pol) III rapidly synthesizes DNA with a chain-elongation rate of approximate 1000 nucleotides per second (Fijalkowska, Schaaper, & Jonczyk, 2012b). However, when the enzyme encounters some obstacles on the template DNA such as a hairpin structure, it slows down the speed (Yuan & McHenry, 2009). Therefore, I

asked whether a hairpin structure could be a trigger for the polymerase switch between Pol IV and an ongoing Pol III.

I.1. Effect of the DNA hairpin structure on Pol III-Pol IV switch

A hairpin loop is a kind of DNA secondary structure, which is extruded by self-pairing of two arms of an inverted repeat on the single-stranded DNA (ssDNA). In order to test whether a hairpin structure on the template DNA stimulates the polymerase switch between Pol III and Pol IV during DNA synthesis, I carried out Burst DNA synthesis assay in the presence of Pol IV using a single stranded circular plasmid containing a short inverted repeat as the template DNA.

First, a perfect short-inverted repeat that consists of 23 nucleotides in each arm (named as AIR23-23) was tested. A circular, single stranded template DNA containing this repeat (named as pMS2-AIR23-23) was annealed with a 25-nucleotide, $5'\gamma$-^{32}P-labeled primer, which was located 120-nucleotides upstream of the inverted repeat. A control template without insertion of any inverted repeat (named as pMS2) was also used (Figure 3.2 A).

I.1.1. Behavior of Pol III at the inverted repeat AIR23-23 in the absence of SSB

When Pol III meets a secondary structure on the template DNA such as a hairpin, the enzyme needs to synthesize DNA using the strand displacement reaction, which strictly requires single stranded-DNA binding protein, SSB (Yuan & McHenry, 2009). To confirm whether the inverted repeat AIR23-23 can form a hairpin structure under my experimental condition, I tested the behavior of Pol III at this inverted repeat in the absence of SSB. I speculated that if a hairpin structure was extruded on the template DNA but SSB was absent, Pol III stalls at the hairpin site.

The standard concentration of SSB in Burst DNA synthesis assay was previously determined as a sufficient amount to cover the whole single-stranded region of the template DNA (147 nM SSB monomer/1 nM template DNA). In this experiment, behavior of Pol III at the inverted repeat AIR23-23 was examined under various concentrations of SSB, from excessive to none (265 nM, 147 nM, 74 nM, 37 nM, 0 nM). The chain-elongation was

conducted for 10 seconds and the replication products were analyzed by 7.5% sequencing gel electrophoresis (Figure 3.2). As a result, when SSB was sufficient (265 nM or 147 nM), Pol III smoothly extended the primer, resulted in a majority of the full-length products in the cases of both control template pMS2 (Figure 3.2C, lanes 1, 2) and template pMS2-AIR23-23 (Figure 3.2C, lanes 6, 7). However, when the concentration of SSB was insufficient or SSB was omitted, Pol III exhibited its difficulty to synthesize the DNA, resulting the production of short, intermediate products and the inhibition of the full-length product's formation (Figure 3.2C, lanes 3, 4, 5 for template pMS2 and lanes 8, 9, 10 for template pMS2-AIR23-23). Notably, stalled replication products with the size of 145-155 nucleotides were specifically observed only when pMS2-AIR23-23 was used as the template (compare blue square-dot box with black square-dot box in Figure 3.2C), suggesting that Pol III frequently stalled within this region. The locations of Pol III arrest were fit to that of the inverted repeat on the template pMS2-AIR23-23. Moreover, by compared between the products and 1-nt TACG laddering markers, I confirmed that Pol III stalled within the first 11 nucleotides of the upstream arm of the inverted repeat. These data indicate that a hairpin structure was extruded from the inverted repeat AIR23-23 on the single-stranded circular template DNA but Pol III overcame this structure using the strand displacement reaction with the help of SSB.

In the other hand, appearance of other intermediate products rather than the pausing at the inverted repeat site suggests that within the sequence of the plasmid pMS2, there were also some other difficult sequences, which potentially formed some structures that hampered Pol III synthesis in the absence of SSB.
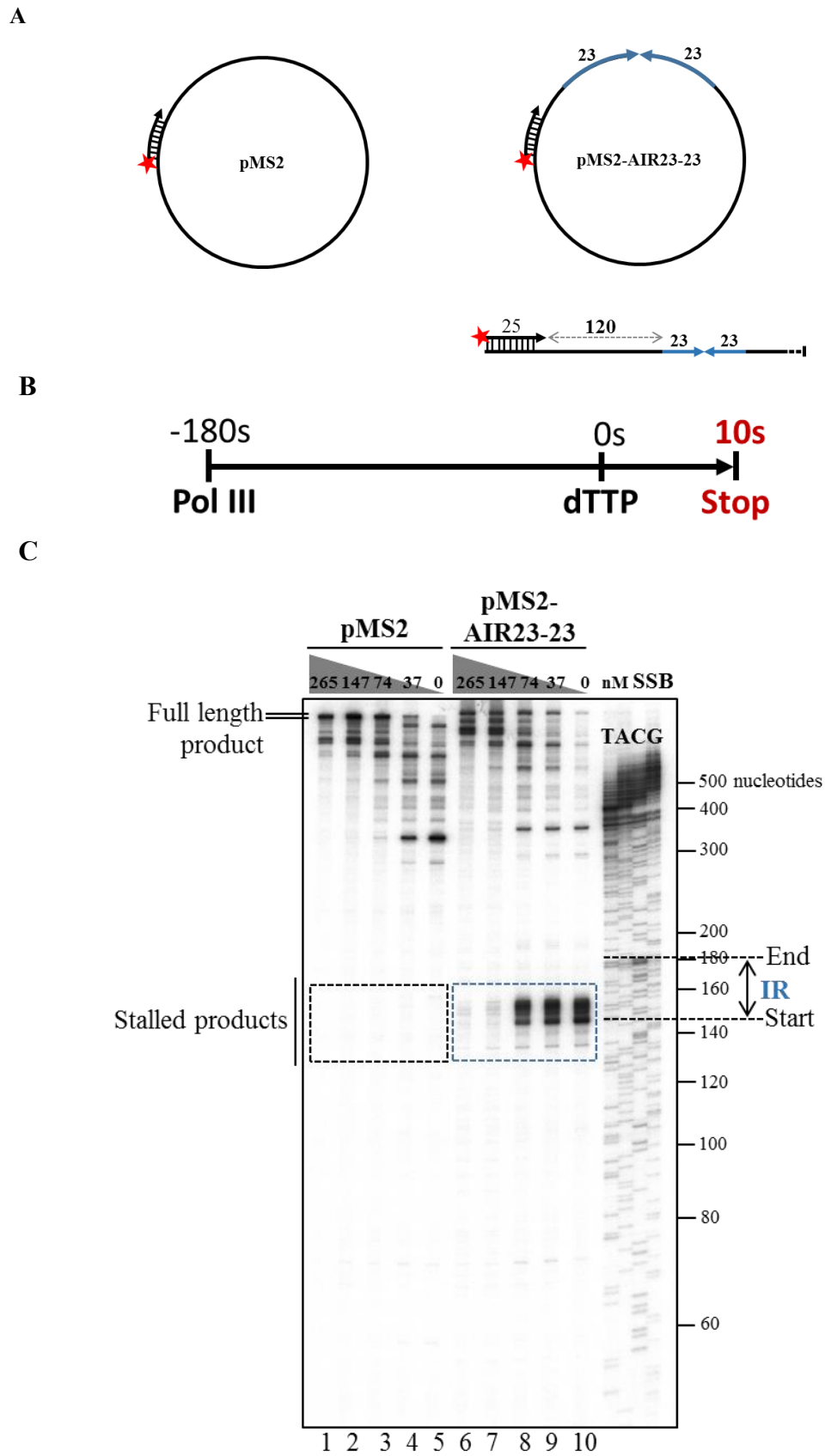
Figure 3.2. Checking the behavior of Pol III at the perfect inverted repeat AIR23-23 in the absence of single stranded-DNA binding protein (SSB). (**A**) Simple schematic diagram representing for the primer/template design. A 25-nucleotides, 5'γ-^{32}P labeled primer was annealed to the control single stranded circular template DNA pMS2

(left panel) or the single stranded circular template DNA containing a perfect inverted repeat pMS2-AIR23-23 (right panel). In the case of the template pMS2-AIR23-23, the distance from the 3' end of the primer to the inverted repeat site was 120 nucleotides. (**B**) Schematic diagram representing the experimental procedure: The initiation complex was formed in the absence of dTTP for 3 min. After that, dTTP was added to start chain-elongation and incubated for 10 seconds. The reaction was stopped by adding 140 µl of Stop solution containing 50 mM EDTA, 0.15% SDS, pH 8.0. Notably, in this experiment SSB was added into the reaction mixture with different concentrations as indicated. (**C**) The replication products were analyzed by 7.5% sequencing gel analysis. Lanes 1-5: control template pMS2 with SSB concentration was 265 nM, 147 nM, 74 nM, 37 nM, 0 nM, respectively. Lanes 6-10: template pMS2-AIR23-23 with SSB concentration was 265 nM, 147 nM, 74 nM, 37 nM, 0 nM, respectively. IR: inverted repeat. For 1-nucleotide TACG laddering marker preparation, template pMS2-AIR23-23 was used.

I.1.2. Effect of Pol IV on Pol III synthesis at the hairpin structure

Next, to study the effect of Pol IV to Pol III synthesis at the hairpin structure, I carried out Burst DNA synthesis assay in the presence of Pol IV. The wild-type Pol IV was added together with Pol III and SSB to the final concentration of 0, 10, 50, 100 and 200 nM, respectively. After initiation, chain-elongation process was started by addition of dTTP and lasted for 10 seconds. The replication products were analyzed by 7.5% sequencing gel electrophoresis as shown in Figure 3.3C.

Like previously shown in Figure 3.2C, in the absence of Pol IV, Pol III smoothly synthesized DNA to form a significant amount of the full-length products within 10 seconds (Figure 3.3 C, lane 1 for pMS2 and lane 6 for pMS2-AIR23-23). However, when Pol IV was added into the reaction, at the location of the hairpin site, the stalled products with the various sizes between 145-160 nucleotides appeared in the case of the repeat template pMS2-AIR23-23 (Figure 3.3 C, lanes 7, 8, 9 and 10), but not in the case of the control template pMS2 (Figure 3.3 C, lanes 2, 3, 4 and 5). The band intensity of the paused products proportionally increased when the concentration of Pol IV was increased. This result indicates that Pol IV did inhibit the elongation reaction of Pol III at the hairpin structure. The presence of minor laddering products observed upstream and downstream of the hairpin site in both templates suggests that the inhibitory effect of Pol IV on Pol III are also observed at some other locations, probably at some naturally formed secondary structures on the template DNA.

A
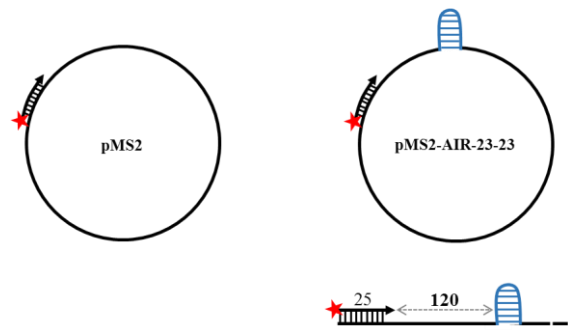
B
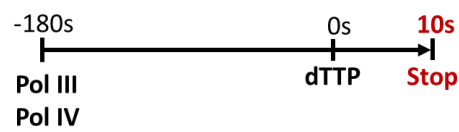
C

Figure 3.3. Checking effect of Pol IV to Pol III synthesis at the hairpin structure. (**A**) Simple schematic diagram representing for the primer/template design. A 25-nucleotides, 5'γ-^{32}P labeled primer was annealed to the control

single stranded circular template DNA pMS2 (left panel) or the single stranded circular template DNA containing a hairpin structure pMS2-AIR23-23 (right panel). In the case of the template pMS2-AIR23-23, the distance from the 3' end of the primer to the hairpin site was 120 nucleotides. (**B**) Schematic diagram representing the experimental procedure. Indicated concentration of the wild type Pol IV was added together with Pol III, SSB. The initiation complex was formed in the absence of dTTP for 3 min. After that, dTTP was added to start chain-elongation and incubated for 10 seconds. The reaction was stopped by adding 140 μl of Stop solution containing 50 mM EDTA, 0.15% SDS, pH 8.0. (**C**) The replication products were analyzed by a 7.5% sequencing gel electrophoresis. Lanes 1-5: control template pMS2 with Pol IV concentration was 0, 10, 50, 100, 200 nM, respectively. Lanes 6-10: template pMS2-AIR23-23 with Pol IV concentration was 0, 10, 50, 100, 200 nM, respectively. IR: inverted repeat. For 1-nucleotide TACG laddering marker preparation, template pMS2-AIR23-23 was used.

On the other hand, the behavior of Pol IV alone at the hairpin structure was also tested in a time course experiment. Instead of Pol III, 100 nM of the wild type Pol IV was added to the Burst DNA synthesis assay. In addition, because Pol IV itself was unable to load the processive β clamp on the primer/template junction, the clamp loader (γ complex) of Pol III was also added. After initiation, chain-elongation was started by adding dTTP and further incubated for 20, 35, 60, 90 seconds. The replication products were analyzed by 7.5% sequencing gel electrophoresis as shown in Figure 3.4C. From the length of Pol IV's elongation product at each time point, the chain-elongation speed of Pol IV was determined around five nucleotides per second at the normal template region (upstream or downstream of the hairpin site). This observation was consistent with the previous studies (Furukohri et al., 2008). However, at the hairpins site the chain-elongation speed of Pol IV was strongly slowed down (to approximate one nucleotide per second). This data suggests that Pol IV had some difficulties to overcome the hairpin structure even in the presence of SSB, probably due to a weak strand displacement reaction.

Taken together, I speculated that the inhibitory effect of Pol IV on Pol III at the hairpin site might cause by the polymerase switch between Pol III and Pol IV. It was possible that Pol IV took over the primer terminus from Pol III at the hairpin. However, because Pol IV itself had some difficulties to synthesize across the hairpin structure (even in the presence of SSB), a high intensity of the paused products at the hairpin site was exposed. In the next chapter, I tested this possibility using several types of mutant Pol IV in the same reaction condition.
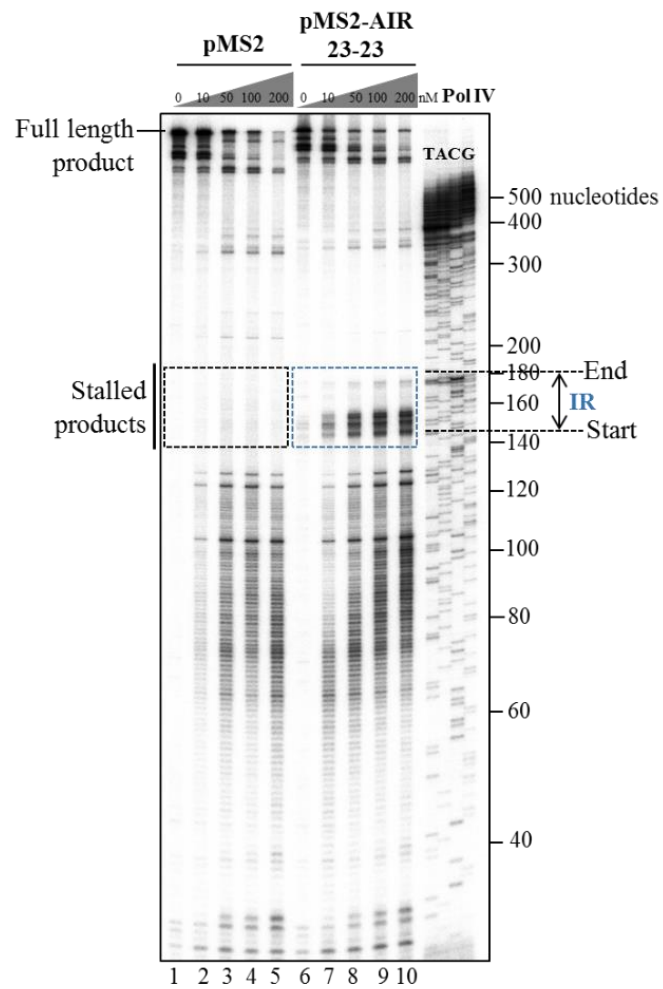
A

B

C

D
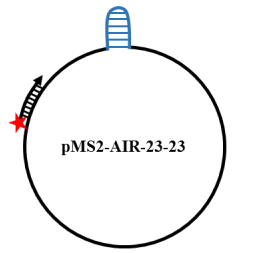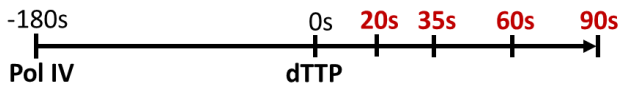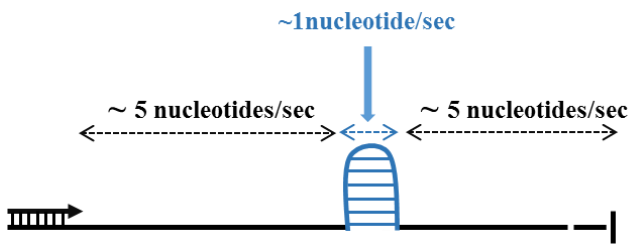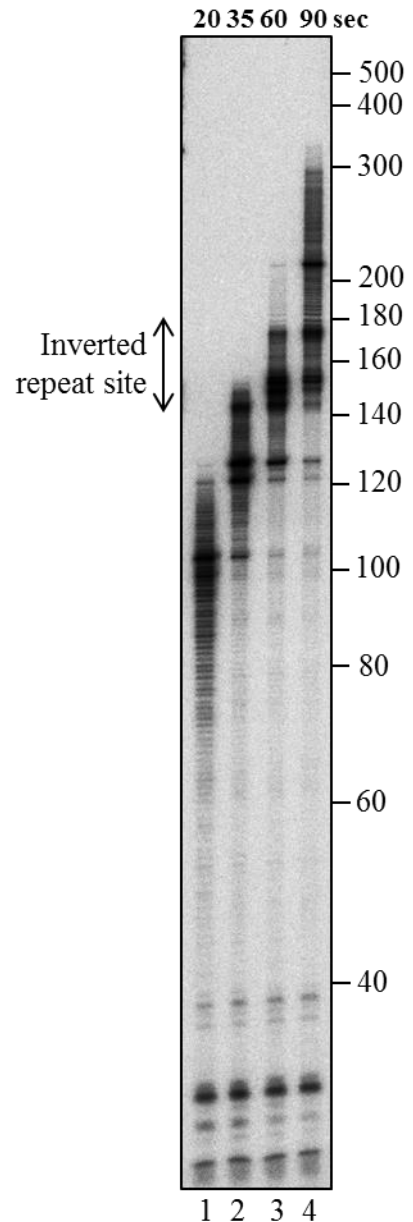
Figure 3.4. Checking the behavior of Pol IV at the hairpin structure. (**A**) Simple schematic diagram representing for the primer/template design. A 25-nucleotides, 5'γ-^{32}P labeled primer was annealed to the single stranded circular template DNA containing a perfect inverted repeat pMS2-AIR23-23 whereby the distance from the 3' end of the primer to the hairpin site was 120 nucleotides. (**B**) Schematic diagram representing the experimental procedure: Instead of Pol III, Pol IV was used to perform DNA synthesis. Initiation complex was formed in the absence of dTTP for 3 min. After that, dTTP was added to start chain-elongation and incubated for 20, 35, 60, 90 seconds. The reaction was stopped by adding 140 μl of Stop solution containing 50 mM EDTA, 0.15% SDS, pH 8.0. (**C**) The replication products were analyzed by a 7.5% sequencing gel electrophoresis. Lanes 1-4: chain-elongation time was 20, 35, 60, 90 seconds, respectively. (**D**) Schematic diagram summarizing the chain-elongation speed of Pol IV at the normal template region and at hairpin structure.

I.1.3. The ongoing Pol III was changed with Pol IV at the hairpin structure.

Pol IV carries the domains for polymerase activity at N-terminal and β clamp interaction at C-terminal (Figure 3.5, A (Furukohri et al., 2008)). An amino acid substitution (D8→A) at the N-terminal resulted in a polymerase-dead mutant as called as D8A. In the other hand, deletion of five amino acids (347-351) at the C-terminal generated a β clamp interaction deficient mutant as called as ∆C5. In order to further confirmed whether the inhibitory effect of Pol IV to Pol III at the hairpin structure was a consequence of Pol III-Pol IV switch, the effect of wild type Pol IV was compared with that of two mutants (D8A and ∆C5). Because the interaction between Pol IV and β clamp is required for Pol III-Pol IV switch, I expected that the stalled products at the hairpin site could be observed in the case of the wild type Pol IV and the mutant D8A, but could not observed in the case of the mutant ∆C5.
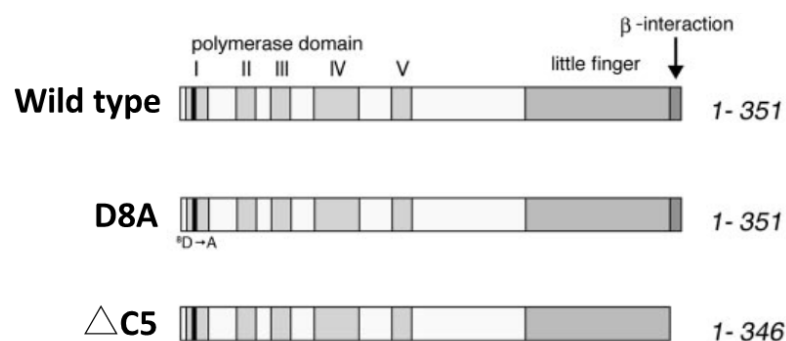
Figure 3.5. Domains organization of the wild type Pol IV and two mutants (Furukohri et al., 2008). The wild type Pol IV carries domains for polymerase activity at the N-terminal and β clamp interaction at the C-terminal. The polymerase-dead mutant D8A contains an amino acid substitution (D8→A) at the N terminal. In the β clamp interaction deficient mutant ∆C5, five amino acids at the C terminal was deleted.

100 nM of the wild type Pol IV or each mutant was added into the reaction mixture together with Pol III. After initiation, chain-elongation process was conducted for 90 seconds. The replication products were analyzed by 7.5% sequencing gel electrophoresis. The result was shown is Figure 3.6C. Similar to the previous results, without addition of Pol IV, Pol III smoothly bypassed the hairpin structure in the presence of SSB but strongly stalled there when SSB was omitted (Figure 3.6 C, lanes 1 and 2). As predicted, when the polymerase-dead mutant (D8A mutant) or the wild-type Pol IV were added into the reaction mixture, a significant amount of paused products was observed at the hairpin site (Figure 3.6 C, lanes 4 and 6), however no

significant pausing was observed in the case of ΔC5 mutant (Figure 3.6 C, lane 5). These results suggest that at the hairpin site, Pol IV replaced Pol III via the interaction with the β clamp. In addition, at lane 6 when the wild type Pol IV was used, long products downstream of the hairpin site (red asterisks) showed the similar band pattern when compared with the product pattern of Pol IV alone (Figure 3.6 C, lane 3). This result indicates that after taking over the primer terminus from Pol III at the beginning of the hairpin site, wild-type Pol IV kept synthesizing DNA for some length instead of Pol III, hence it reduced the intensity of stalling products but the mutant D8A was unable to do it. Because the mutant D8A lost the polymerase activity, the observation of the polymerase switch between Pol III and Pol IV at the hairpin site suggests that Pol IV exchanged with an ongoing Pol III at the hairpin structure.
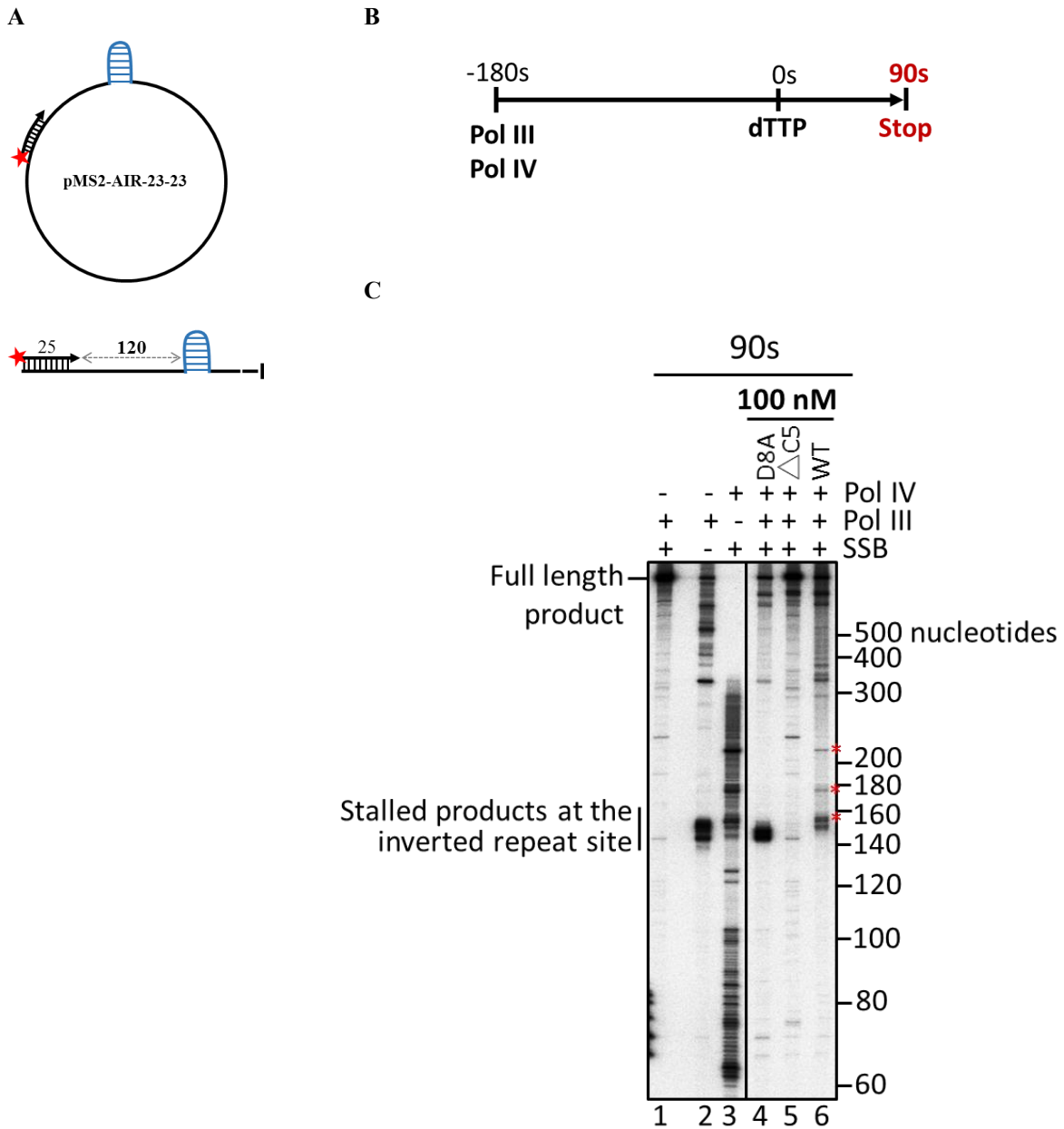
Figure 3.6. Comparison between effect of the wild type (WT) Pol IV and two mutants (D8A and ΔC5) to Pol III at the hairpin structure. (**A**) Simple schematic diagram representing for the primer/template design. A 25-nucleotides, 5'γ-^{32}P labeled primer was annealed to the template pMS2-AIR23-23 whereby the distance from the 3' end of the primer to the hairpin site was 120 nucleotides. (**B**) Schematic diagram representing the experimental procedure. 100 nM of Pol IV (WT or D8A or △C5) was added into the reaction mixture together with Pol III. Initiation complex was formed in the absence of dTTP for 3 min. After that, dTTP was added to start chain-elongation and incubated for 90 seconds. The reaction was stopped by adding 140 μl of Stop solution containing 50 mM EDTA, 0.15% SDS, pH 8.0. (**C**) The replication products were analyzed by a 7.5% sequencing gel electrophoresis. Lanes 1-2: Burst DNA synthesis of Pol III alone in the presence- or absence of SSB, respectively. Lane 3: Burst DNA synthesis of Pol IV alone in the presence of SSB. Lanes 4, 5, 6: 100 nM of Pol IV D8A or △C5 or the wild-type was added to the reaction mixture together with Pol III, respectively.

I.1.4. The polymerase switching by Pol IV at the hairpin structure occurred quickly but was transient

Now it becomes clear that the polymerase switch between Pol III and Pol IV takes places at the hairpin site. After taking over the primer template junction from Pol III, Pol IV itself synthesizes DNA instead of Pol III. To know whether Pol III again takes back the primer terminus from Pol IV and if it does, how long Pol IV keeps the primer terminus, a time course experiment was carried out. 100 nM of the wild-type Pol IV was added into the reaction mixture together with Pol III and after initiation, elongation was conducted for 10s, 30s, 90s and 150s. The replication products were analyzed by 7.5% sequencing gel electrophoresis (Fig 3.7C). As the result, after 10-second incubation, stalled products was accumulated at the hairpin site and just a few amount of full-length product was produced, indicating that Pol IV rapidly displaces most of ongoing Pol III at the hairpin site within several seconds (Fig 3.7C, lane 1). When incubation time was prolonged, the amount of paused products at the hairpin site gradually decreased and disappear after 150s (Fig 3.7C, lanes 2, 3, 4, red dot-square box). In addition, while the reduction of paused products was observed, the full-length product was accumulated accordingly (Fig 3.7C, lanes 2, 3, 4, blue dot-square box). Because of the slow chain-elongation speed, Pol IV was unable to synthesize the full-length products within indicated time. These data suggest that the polymerase switch reaction from Pol III to Pol IV at the hairpin was rapid and efficient but transient. Pol IV kept the primer terminus for a while, but Pol III soon took back the primer terminus and resumed the elongation process.
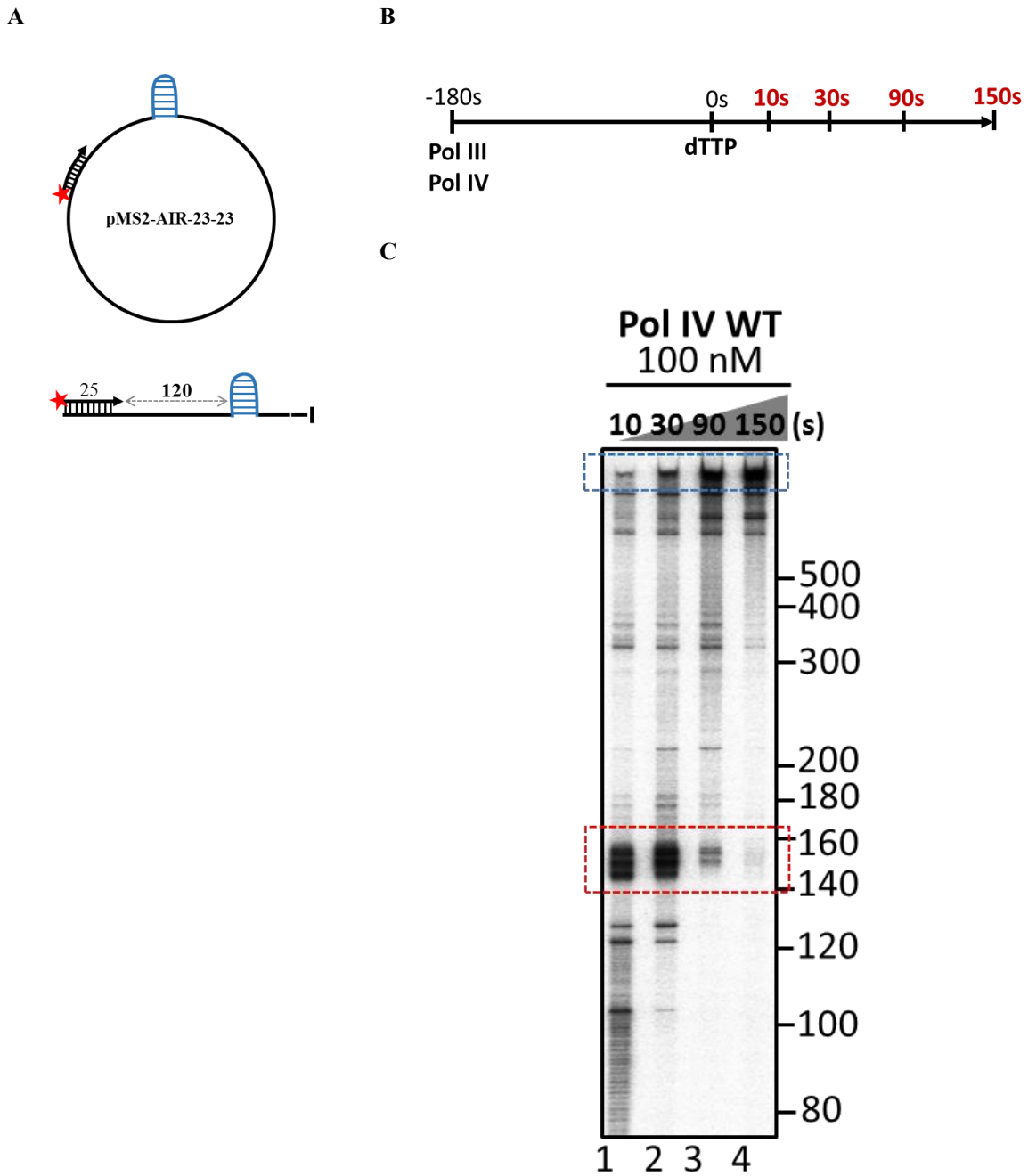
Figure 3.7. Checking the ability to re-gain access to the primer terminus of Pol III after Pol III-Pol IV switch at the hairpin structure. (**A**) Simple schematic diagram representing for the primer/template design. A 25-nucleotides, 5'γ-^{32}P labeled primer was annealed to the template pMS2-AIR23-23 whereby the distance from the 3' end of the primer to the hairpin site was 120 nucleotides. (**B**) Schematic diagram representing the experimental procedure. 100 nM of the wild type Pol IV was added into the reaction mixture together with Pol III. Initiation complex was formed in the absence of dTTP for 3 min. After that, dTTP was added to start chain-elongation and incubated for 10, 30, 90, 150 seconds. The reaction was stopped by adding 140 μl of Stop solution containing 50 mM EDTA, 0.15% SDS, pH 8.0. (**C**) The replication products were analyzed by a 7.5% sequencing gel electrophoresis. Lanes 1-4: chain-elongation time was 10, 30, 90, 150 seconds, respectively.

I.1.5. Analysis of Pol III-Pol IV switch using other types of inverted repeat

I found that Pol IV causes the polymerase switch from Pol III to Pol IV at the perfect inverted repeat AIR23-23 (each arm is composed of 23-nucleotide repeat unit). From the results obtained so far, I speculated that the trigger for Pol III-Pol IV switch was the formation of a hairpin structure from the inverted repeat on the template DNA, because it was confirmed that Pol III strongly stalled within the inverted repeat sequence in the absence of the single stranded-DNA binding protein SSB. In this chapter, to investigate how long is the sufficient length of the inverted repeat to cause Pol III-Pol IV switch, template DNA with various sizes of inverted repeats was tested. In addition, because these data could not deny the possibility that Pol III-Pol IV switch observed in the inverted repeat AIR23-23 was sequence-dependent, not structure-dependent. I tested the Pol III-Pol IV switch using the other inverted-repeat containing a different DNA sequence in the same assay system.

i. Study of Pol III-Pol IV switch at the shorter inverted repeats

To investigate whether Pol III-Pol IV switch is observed at the shorter inverted repeats, I shortened the length of the inverted repeat A23-23 in the plasmid pMS2-AIR23-23 by restriction enzyme digestion followed by a self-ligation reaction as explained in Materials and methods (Figure 2.1). Resulting new ssDNA template, pMS2-AIR12-12, having a short inverted repeat with 12-nucleotides repeat unit in each arm and pMS2-AIR6-6, having a short inverted repeat with 6-nucleotides repeat unit in each arm (Figure 2.1) were used in Burst DNA synthesis assay to test the effect of Pol IV on Pol III as previously described. Indicated concentration of the wild type Pol IV was added to the reaction mixture together with Pol III. After initiation, chain-elongation process was lasted for 10 seconds. The replication products were analyzed by 7.5% sequencing gel electrophoresis as shown in Figure 3.8B.

In the control experiment with the template pMS2, no significant pausing was detected at around the inverted repeat site even in the presence of Pol IV (Figure 3.8B, lane 1). Similar to the result of AIR23-23 (lane 7-8), the AIR12-12 also caused Pol III-Pol IV switch in a Pol IV concentration-dependent manner but the efficiency was much lower compared to AIR23-23 (Figure 3.8B, compare lanes 5, 6 with 7, 8). Notably, the smallest inverted repeat AIR6-6 did

not induce Pol III-Pol IV switch even at higher concentration of Pol IV (Figure 3.8B, lanes 2, 3, 4).

The T_m of double-stranded region of hairpin stem is estimated as 66.6°C for the AIR23-23, 36°C for the AIR12-12 and 18°C for the AIR6-6. As our experimental condition is 30°C, I speculated that the inverted repeats AIR23-23 and AIR12-12 formed hairpin structures on template DNA in our assay and thus triggered Pol III-Pol IV switch, but the smallest one AIR6-6 could not. To test this possibility, I carried out the experiment to examine the behavior of Pol III with these inverted repeats in the absence of SSB (Figure 3.8 C). In the presence of SSB, Pol III smoothly bypasses all the inverted repeats (Figure 3.8 C, lane 4, 6 and 8). However, in the absence of SSB, although Pol III exhibited some difficulty to synthesize the full length product in all the cases, the stalling at the inverted-repeat site was observed only in the cases of AIR12-12 (Figure 3.8 C, lane 5) and AIR 23-23 (Figure 3.8 C, lane 7), but not in the case of the AIR6-6 (Figure 3.8 C, lane 3). This data supports my speculation above that there was no hairpin extruded at the small inverted repeat AIR6-6. Effects of different inverted repeat sizes used in this experiment are summarized in Table 3.1.
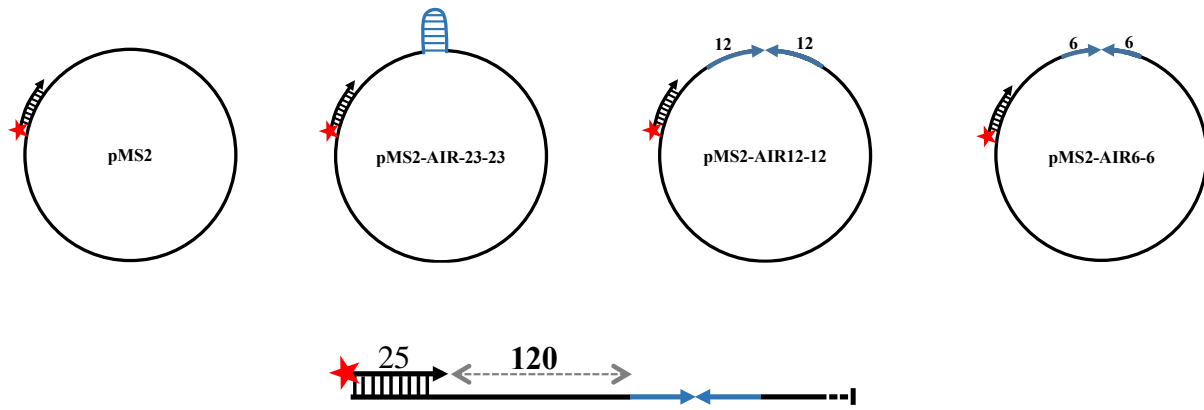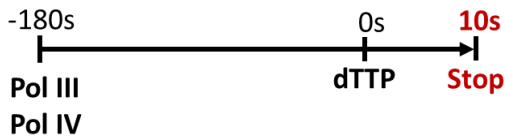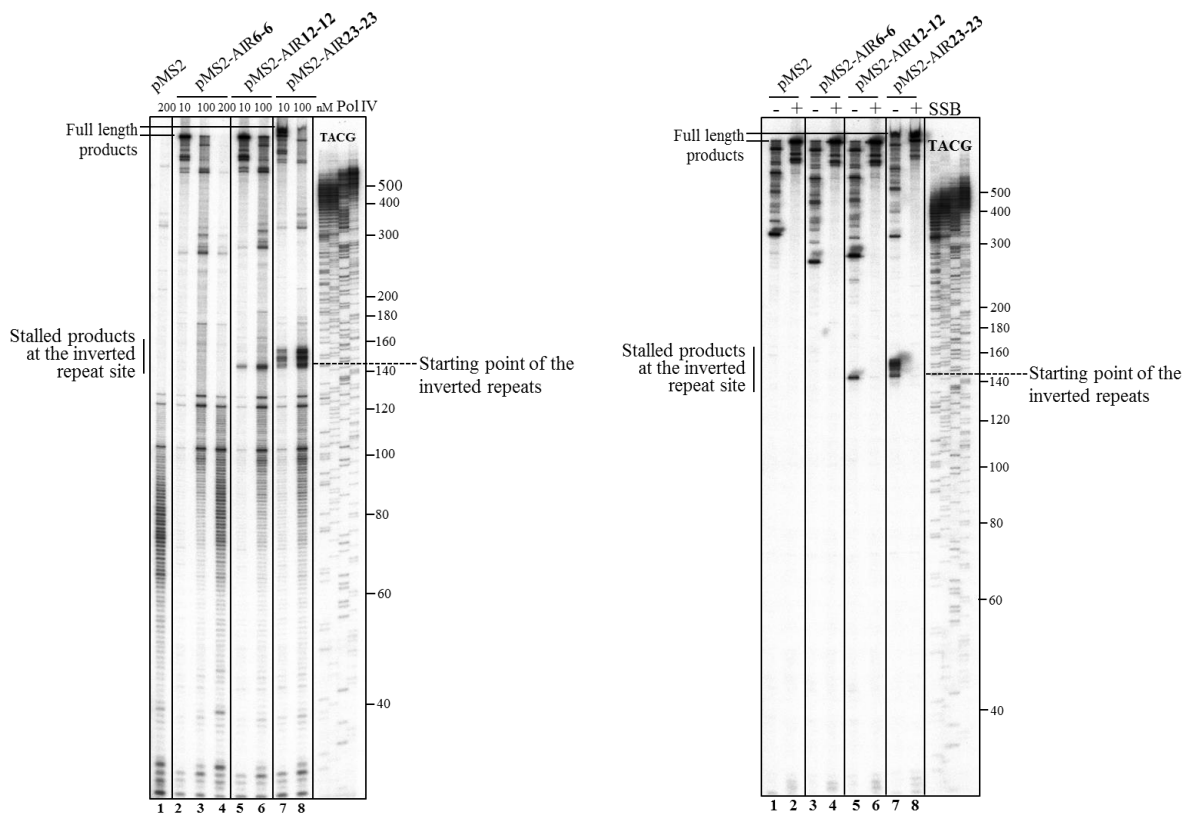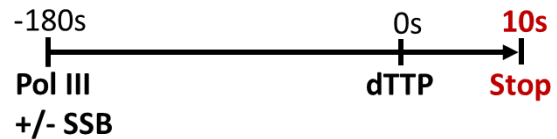
Figure 3.8. Checking Pol III-Pol IV switch and the behavior of Pol III at the shorter inverted repeats.

(**A**) Simple schematic diagram representing for the primer/template design. A 25-nucleotides, 5' γ-^{32}P labeled primer was annealed to the template pMS2, pMS2-AIR23-23, pMS2-AIR12-12, pMS2-AIR6-6. In all templates containing the inverted repeat the distance from the 3' end of the primer to the inverted repeat was 120 nucleotides.

(**B**) Checking Pol III-Pol IV switch at the shorter inverted repeats. Upper panel: Schematic diagram representing

the experimental procedure. Indicated concentration of the wild type Pol IV was added into the reaction mixture together with Pol III. Initiation complex was formed in the absence of dTTP for 3 min. After that, dTTP was added to start chain-elongation and incubated for 10 seconds. The reaction was stopped by adding 140 µl of Stop solution containing 50 mM EDTA, 0.15% SDS, pH 8.0. Lower panel: The replication products were analyzed by a 7.5% sequencing gel electrophoresis. Lane 1: control template pMS2 with addition of 200 nM of Pol IV. Lanes 2, 3, 4: Template pMS2-AIR6-6 with Pol IV concentration was 10, 100 and 200 nM, respectively. Lanes 5, 6: Template pMS2-AIR12-12 with Pol IV concentration was 10, 100 nM, respectively. Lanes 7, 8: Template pMS2-AIR23-23 with Pol IV concentration was 10, 100 nM, respectively. For 1-nucleotide TACG laddering marker preparation, template pMS2AIR12-12 was used.

(**C**) Checking the behavior of Pol III at the shorter inverted repeats. Upper panel: Schematic diagram representing the experimental procedure. Burst DNA synthesis assay was carried out in the absence or presence of SSB. Initiation complex was formed in the absence of dTTP for 3 min. After that, dTTP was added to start chain-elongation and incubated for 10 seconds. The reaction was stopped by adding 140 µl of Stop solution containing 50 mM EDTA, 0.15% SDS, pH 8.0. Lower panel: The replication products were analyzed by a 7.5% sequencing gel electrophoresis. Lanes 1, 2: Pol III synthesis on the control template pMS2 in the absence or presence of SSB, respectively. Lanes 3, 4: Pol III synthesis on the template pMS2-AIR6-6 in the absence or presence of SSB, respectively. Lanes 5, 6: Pol III synthesis on the template pMS2-AIR12-12 in the absence or presence of SSB, respectively. Lanes 7, 8: Pol III synthesis on the template pMS2-AIR23-23 in the absence or presence of SSB, respectively. For 1-nucleotide TACG laddering marker preparation, template pMS2AIR12-12 was used.

Table 3.1. Summarization of the effect of different inverted repeat sizes to Pol III-Pol IV switch.

Template	pMS2-AIR 23-23	pMS2-AIR 12-12	pMS2-AIR 6-6
Inverted repeat size	23-23	12-12	6-6
Hairpin's Tm (°C)	66.6	36	18
Pausing of Pol III at the inverted repeat site in the absence SSB	+++	++	-
Pol III-IV switch at the inverted repeat	+++	++	-

ii. Study of Pol III-Pol IV switch at an E. coli endogenous inverted repeat

I also tested the ability of Pol IV to replace Pol III at another inverted repeat having a different DNA sequence. A short inverted repeat with the size of 15 nucleotides for each arm linked by 3 nucleotides spacer (so called as NIR15-3-15) found in *E. coli* genome was introduced into the control plasmid pMS2, resulting a new ssDNA template as named as pMS2-AIR15-3-15. This template was used as DNA template in Burst DNA synthesis assay. Indicated concentrations of the wild type Pol IV or two mutants (D8A or ΔC5) were added to the reaction mixture together with Pol III. After initiation, chain-elongation process was conducted for 10 seconds. The replication products were analyzed by 7.5% sequencing gel electrophoresis. As a result, I found that in the absence of SSB, the inverted repeat NIR15-3-15 also caused the pausing of the elongation reaction of Pol III (Figure 3.9 C, lane 1), suggesting that a hairpin structure was also formed at this inverted repeat in our experimental condition. When the wild-type Pol IV or the polymerase-dead mutant D8A was added into the reaction, a significant amount of paused products was observed (Figure 3.9 C, lanes 3-5), but was not detected when ΔC5 mutant was used (Figure 3.9 D, lane 6). This data suggests that the endogenous inverted repeat NIR15-3-15 also causes Pol III-Pol IV switch by formation of a hairpin structure.

As summary, the inverted repeats that can form a hairpin structure are trigger for Pol III-Pol IV switch. This effect is not dependent on the DNA sequence context or the spacer between two repeated units.
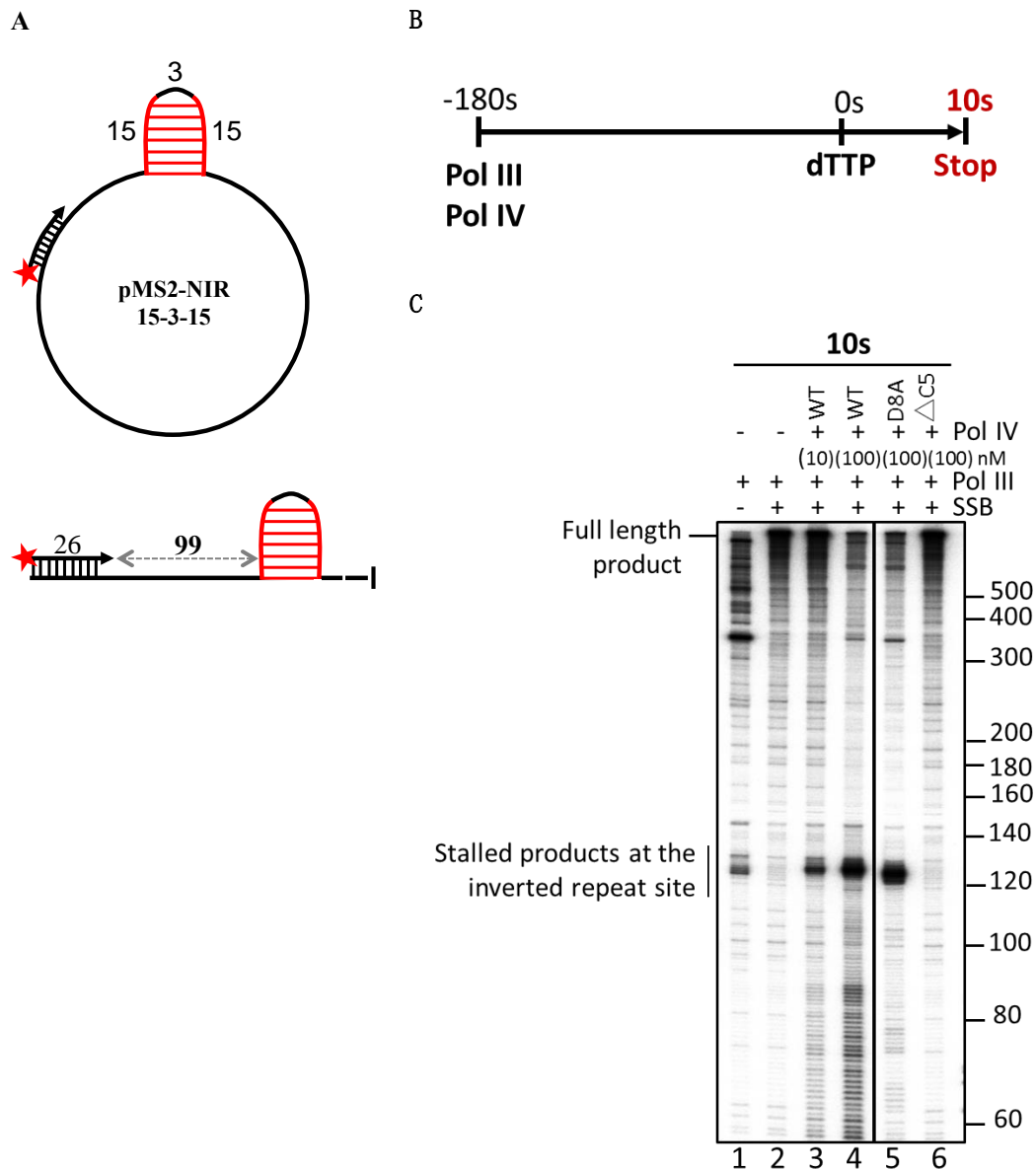
Figure 3.9. Checking Pol III-Pol IV switch with an *E. coli* endogenous inverted repeat. (**A**) Simple schematic diagram representing for the primer/template design. A 26-nucleotides, 5' γ-^{32}P labeled primer was annealed to the template pMS2-NIR15-3-15 whereby the distance from the 3' end of the primer to the inverted repeat was 99 nucleotides. (**B**) Schematic diagram representing the experimental procedure. Indicated concentrations of the wild type Pol IV or each mutant (D8A or ΔC5) were added into the reaction mixture together with Pol III. Initiation complex was formed in the absence of dTTP for 3 min. After that, dTTP was added to start chain-elongation and incubated for 10 seconds. The reaction was stopped by adding 140 μl of Stop solution containing 50 mM EDTA, 0.15% SDS, pH 8.0. (**C**) The replication products were analyzed by a 7.5% sequencing gel electrophoresis. Lanes 1-2: Burst DNA synthesis of Pol III alone in the absence or presence of SSB, respectively. Lanes 3, 4: 10 or 100 nM of the wild type Pol IV was added into the reaction mixture, respectively. Lane 5: 100 nM of Pol IV mutant D8A was added into the reaction mixture. Lane 6: 100 nM of Pol IV mutant $\triangle$C5 was added into the reaction mixture.

I.2. Study of the molecular mechanism underlying Pol III-Pol IV switch using the hairpin-mediated polymerase switch as a model system

I.2.1. Pol IV initiated Pol III-Pol IV switch when Pol III executed the strand-displacement reaction

When Pol III encounters a hairpin structure, it changes the mode from normal chain-elongation to strand displacement (Yuan & McHenry, 2009). Therefore, I hypothesized that the switching activity by Pol IV was allowed to be effective on Pol III at the hairpin site when Pol III changed the elongation mode for the strand-displacement reaction.

To further confirm the above hypothesis, I tested the effect of Pol IV on Pol III when Pol III carried out the strand displacement reaction. Hence, a hairpin-free, circular ssDNA template annealed with two primers was prepared and used in Burst DNA synthesis assay as explained in the Experimental procedure (Chapter 2.2.2). Briefly, a double amount of Pol III was added to the reaction mixture to allow Pol III to extend 3'-ends of both primers equally (Figure 3.10A). The first primer was radio labeled by ^{32}P at 5'-end, but the second one was not labeled, so only the elongation products of first primer was detected when the replication products were analyzed by 7.5% sequencing gel electrophoresis. When the elongation reaction is started, the elongation complex of Pol III on the first primer collided with the 5'-end of the second primer after several-seconds incubation. Then Pol III needed to elongate DNA using the strand displacement activity while removing the 2nd-primer. However, because the second primer was also elongated by Pol III similarly, Pol III at the first primer needed to keep elongating the primer by the strand displacement activity even after removing the 2nd-primer region. The length of the first primer was 25 nucleotides and the distance between the first and the second primer was 120 nucleotides, so that the labeled products longer than 145 nucleotides represented the strand displacement's product (Figure 3.10C).

The elongation reaction of Pol III from γ^{32}P-labeled primer on this double-primed template was firstly analyzed in Burst DNA synthesis assay in the absence of Pol IV (Figure 3.10C, lane 1). Pol III was unable to produce one-circle, full-length products within 10 seconds because of the presence of the products of second primer on the template, resulting a significant amount of stalled product at the 2nd primer site and intermediate-sized product downstream of the 2nd

primer. This was because the normal-elongation speed of Pol III is very high (1000 nt/sec) but the speed of strand-displacement reaction is much slower (150 nt/sec) (Yuan & McHenry, 2009). When the chain-elongation time was prolonged, the amount of stalled or intermediate products gradually decreased and the significant amount of full-length product was accumulated accordingly (Figure 3.10C, lanes 2-4 blue dot-square box, Figure 3.10D). Interestingly, when Pol IV was added into the reaction at 100 nM and 200 nM. No changes of the product pattern were observed over the incubation time, neither decrement of stalled product nor increment of full-length product (Figure 3.10C, lanes 5-10, red dot-square box, Figure 3.10D). This result showed that the strand displacement reaction by Pol III was perfectly inhibited by the presence of Pol IV. I proposed that when Pol III changed the mode for the strand-displacement reaction, Pol IV quickly took over the primer terminus from Pol III and Pol III was not able to take the primer back from Pol IV as long as it needed to carry out the strand displacement reaction.
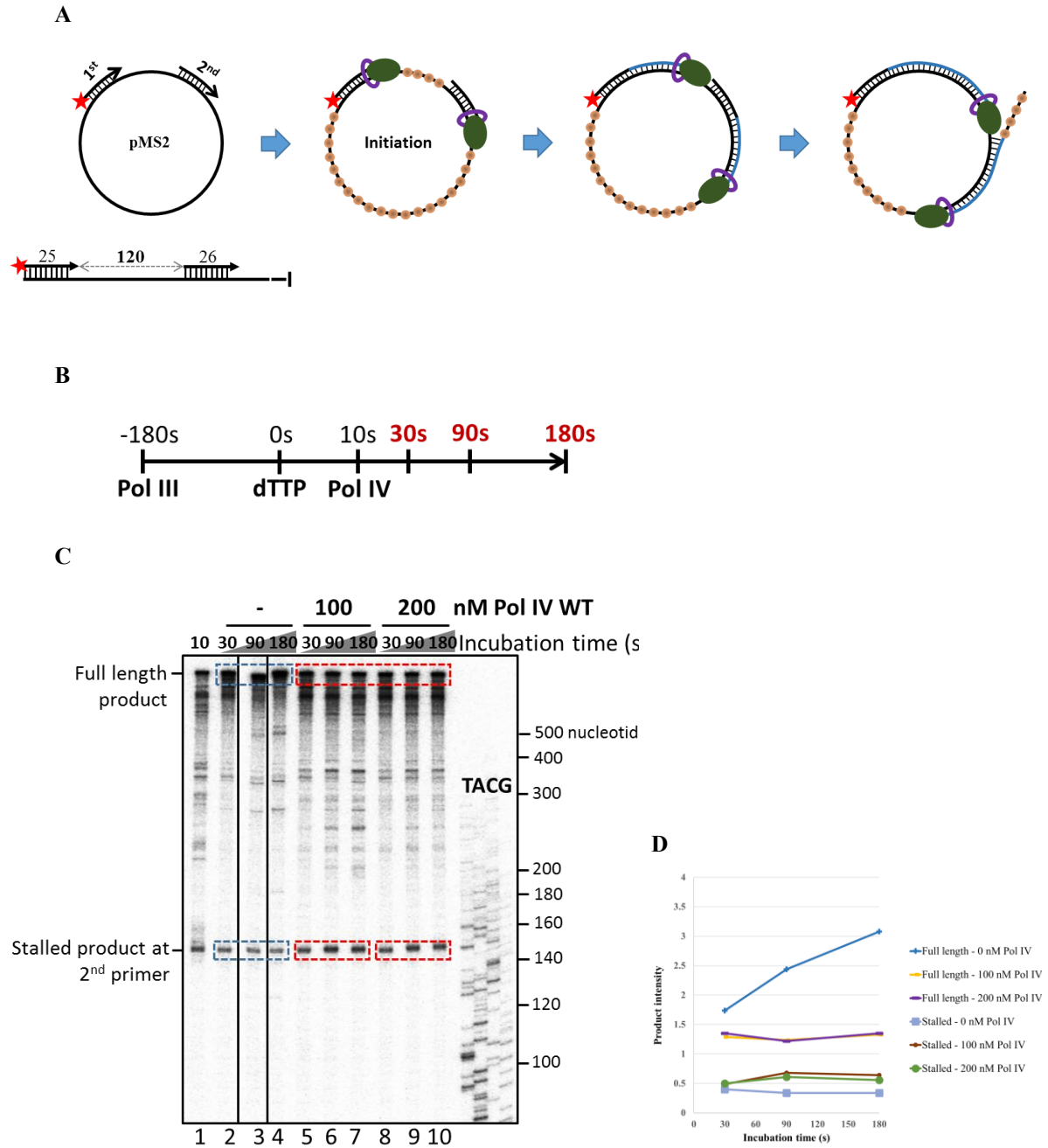
Figure 3.10. Checking the relationship between strand displacement reaction of Pol III and Pol III-pol IV switch. (**A**) Simple schematic diagram representing the experimental design. Two primers were simultaneously annealed to the template pMS2 whereby the first primer was labeled at 5' end by γ -^{32}P. The distance from the first primer to the second primer was 120 nucleotides. In this experiment, a double amount of Pol III was added to the reaction mixture to allow the chain-elongation process proceeds from both primer's ends. Since the chain-elongation complex of the first primer collided the second primer, Pol III needed to do strand displacement reaction. To investigate effect of Pol IV to the strand displacement reaction of Pol III, Pol IV was added to the reaction mixture when Pol III was doing strand displacement activity (after 10 seconds elongation).

(**B**) Schematic diagram representing the experimental procedure. The initiation complex was formed in the absence of dTTP for 3 min. After that, dTTP was added to start elongation. After 10 sec elongation, Pol IV was added to

the reaction mixture and the reaction was further incubated for 30, 90, 180 seconds. The reaction was stopped by adding 140 µl of Stop solution containing 50 mM EDTA, 0.15% SDS, pH 8.0.

(**C**) The replication products were analyzed by 7.5% sequencing gel electrophoresis. Lane 1: 10 seconds elongation without addition of Pol IV. Lanes 2, 3, 4: continuous 30, 90, 180 seconds elongation without addition of Pol IV, respectively. Lanes 5, 6, 7: 100 nM of the wild type Pol IV was added after 10s elongation, and continued to incubate for 30, 90, 180 sec, respectively. Lanes 8, 9, 10: 200 nM of the wild type Pol IV was added after 10s elongation, and continued to incubate for 30, 90, 180 sec, respectively.

(**D**) Graph representing the dynamic changes in amount of the stalled-product at the 2nd primer and the full-length product over the incubation time in the absence or presence of Pol IV.

I.2.2. How does Pol IV gain access to the primer terminus when Pol III binds to it?

It was clear that Pol IV exchanged with the ongoing Pol III at the hairpin structure when Pol III was doing strand displacement reaction. So far the detailed mechanism of the strand displacement reaction was not defined yet, but it was revealed that the interaction between the ε subunit and the cleft of the β clamp is required. Therefore, I speculated that during strand displacement reaction, Pol III might change the conformational mode from elongation to proofreading, and this conformational transition could be a trigger for Pol III-Pol IV switch.

Pol III DnaE173 mutant has a an amino acid substitution in the α subunit that makes the polymerase becomes hyper-processive hence the exchange between the α subunit and the ε subunit is severely impaired and the enzyme cannot enter the proof reading mode even the exonuclease activity is perfectly retained (Sugaya, Ihara, Masuda, Ohtsubo, & Maki, 2002; Yanagihara, Yoshida, Sugaya, & Maki, 2007). Thus, to examine the above hypothesis, using the hairpin-mediated polymerase switch reaction by Pol IV in Burst DNA synthesis assay as previous experiments, I compared the efficiency of Pol III-Pol IV switch between wild-type Pol III and DnaE173 Pol III at the hairpin site. In this experiment, to avoid the unspecific Pol III-Pol IV switch upstream of the hairpin, instead of adding Pol IV from the initiation step, I added Pol IV to the reaction mixture together with dTTP when the chain-elongation was started. Both time course experiment (Figure 3.11 B) and Pol IV-titration experiment (Figure 3.11 C) was carried out. In the time course experiment, 100 nM of Pol IV was added to the reaction mixture together with dTTP and chain-elongation process was conducted for 10, 30, 60, 90, 150 seconds, respectively. In the Pol IV-titration experiment, Pol IV was added to the reaction mixture

together with dTTP to the final concentration of 0, 50, 100, 200, 400 nM, respectively. Chain-elongation process was conducted for 10 seconds. As the result, it was clearly shown in both experiments that Pol III DnaE173 was much more resistant against Pol IV at the hairpin structure compared to the wild type Pol III, therefore resulted in less amount of paused products (Figure 3.11 B, C, black dot-square box). These results support my above hypothesis that the conformational transition from elongation- to proof reading mode of Pol III on the β clamp is the key of Pol IV's action for the polymerase switch.

A

B
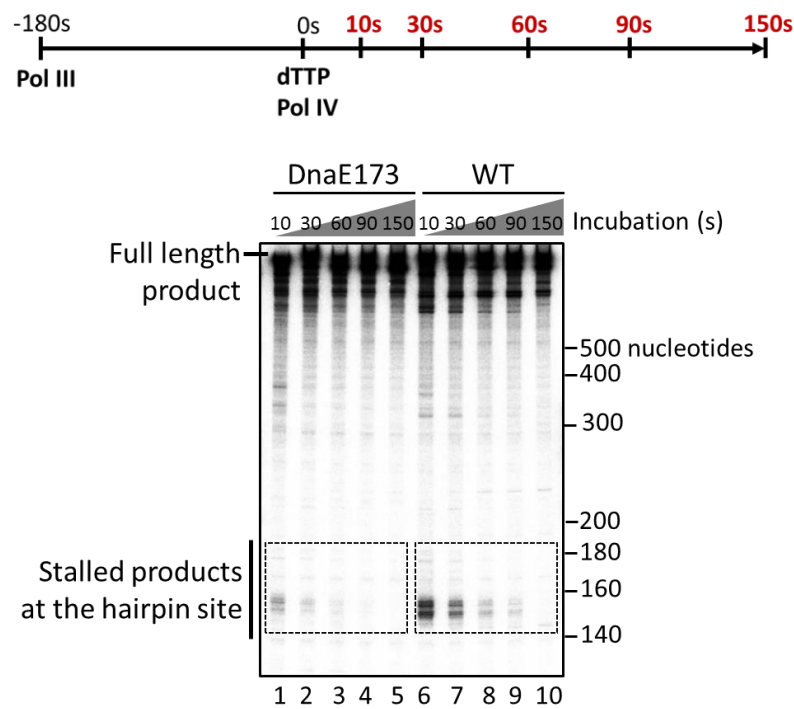
C
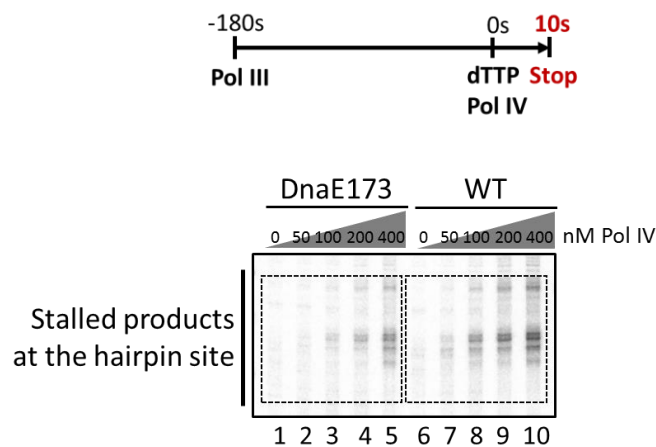
Figure 3.11. Comparison between the effect of Pol IV to the wild type Pol III and the mutant DnaE173 at the hairpin structure.

(**A**) Simple schematic diagram representing for the primer/template design. A 25-nucleotides, 5' γ-^{32}P labeled primer was annealed to the template pMS2-AIR23-23 whereby the distance from the 3' end of the primer to the

62

hairpin was 120 nucleotides.

(**B**) Time course experiment. Upper panel: Schematic diagram representing the experimental procedure. The initiation complex was formed in the absence of dTTP for 3 min. After that, 100 nM of the wild type Pol IV was added together with dTTP to start chain-elongation. Chain-elongation process was carried out for 10, 30, 60, 90 and 150 seconds, respectively. Lower panel: The replication products were analyzed by 7.5% sequencing gel electrophoresis. Lanes 1-5: DnaE173 was used and the chain-elongation time was 10, 30, 60, 90, 150 seconds, respectively. Lanes 6-10: wild type Pol III was used and the chain-elongation time was 10, 30, 60, 90, 150 seconds, respectively.

(**C**) Pol IV concentration titration experiment. Upper panel: Schematic diagram representing the experimental procedure: Different concentrations of Pol IV was added together with dTTP and the chain-elongation process was lasted for 10 sec. Lower panel: The replication products were analyzed by 7.5% sequencing gel electrophoresis. Lanes 1-5: DnaE173 was used and the final concentration of Pol IV was 0, 50, 100, 200, 400 nM, respectively. Lanes 6-10: wild type Pol III was used and the final concentration of Pol IV was 0, 50, 100, 200, 400 nM, respectively.

Part II: Study of the molecular action of Pol IV at the replication fork using *oriC* assay

To study the molecular action of Pol IV at the replication fork, I used *oriC* assay that precisely reconstitutes the bidirectional DNA replication synstem of *E. coli* cell *in vitro*. As described in chapter 2 "Materials and methods", a 4.4 kb-supercoiled plasmid carries a replication origin site - *oriC* and a termination site - *terB* of *E. coli* was used as template DNA (named as pMOL7). First, the replication reaction was assembled in the presence of pMOL7 and all of the *E. coli* replication components such as SSB, primase, helicase, polymerase III holoenzyme, DNA gyrase, Tus, ATP, rNTPs, dNTPs, … except the initiator protein DnaA. When DnaA was added, DNA replication proceeded from *oriC* to *terB* in both directions, generating two replication forks, the clock-wise fork and the counter clock-wise fork. During the natural genomic replication process in *E. coli* cell, two replication forks travel equally and stop when they encounter each other or the termination site - *terB* after half way of the circular genome, therefore results in a similar product pattern of two replication forks. In the *oriC* assay, to distinguish the leading product between two replication forks, *terB* site was put asymmetrically on pMOL7 (Figure 3.12). Hence, the clock-wise replication fork stops earlier, after running 0.9 kb, allowing the counter clock wise-fork can move longer (3.5 kb).
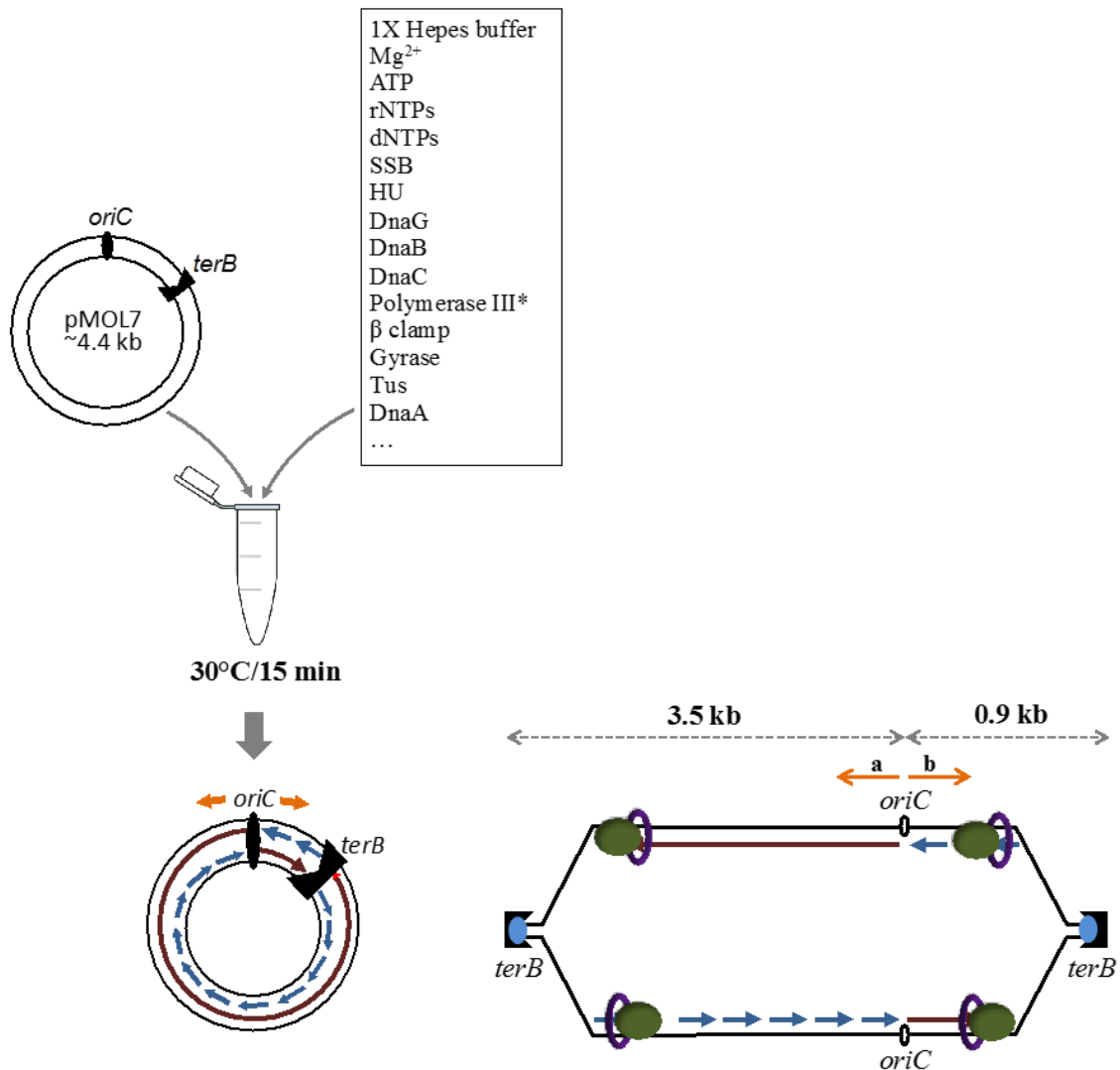
Figure 3.12. *oriC* assay reconstitutes the bidirectional replication machinery of *E. coli* cell *in vitro*. Reaction mixture containing the *oriC-terB*-plasmid (pMOL7) and the *E. coli* replication components was incubated at 30°C for 15 minutes. There were two replication forks (the counter clock-wise fork and the clock-wise fork) proceeded from the origin site - *oriC* and stopped at the termination site – *terB*. Because *terB* site was put assymetrically on the circular template pMOL7, the clock-wise replication fork stopped first, after moving 0.9 kb of pMOL7, allowed the counter clock-wise replication fork moved longer (3.5 kb). The orrange arrows represent for directions of two replication forks, the counter clock-wise fork (a) and the clock-wise fork (b). The green ellipses represent for Pol III, the purple ring-shaped symbols represent for β clamp. The dark red arrows represent for leading products. The blue arrows represent for Okazaki fragments.

II.1. Study of the effect of Pol IV on the normal replication fork

In order to investigate whether Pol IV has an ability to enter the normal replication fork and if it is the case, how Pol IV effects the replication fork progression, I carried out *oriC* assay in the presence of Pol IV. To avoid the confusion when the replication products of Pol III were analyzed, the Pol IV mutant D8A, which loses the polymerase activity but still retains the polymerase-switching activity was used. Pol IV D8A was added together with the *oriC* proteins to the final concentration of 0, 10, 50, 100, 200, 400, 800 nM. After addition of DnaA, the replication reaction was incubated at 30ºC for 15 minutes. The newly synthesized strands were radiolabeled by [α-^{32}P] dATP incorporation and analyzed by 0.9% alkaline agarose gel electrophoresis (Figure 3.13).

In the absence of Pol IV, the DNA synthesis in both replication forks was performed as normal, resulted in a normal replication product pattern, including the 3.5 kb-counter clock-wise leading product, the 0.9 kb-clock-wise leading product and the 0.1-0.6 kb-Okazaki fragments (Figure 3.13A, lane 1). However, when Pol IV was present, the enzyme inhibited the replication product's formation in a concentration-dependent manner. When the concentration of Pol IV was higher than 200 nM, it perfectly inhibited DNA synthesis as no signal of the product was detected (Figure 3.13A, lanes 5, 6, 7). From 10 nM to 100 nM, DNA synthesis by Pol III could occur, but the amount of the leading products of both replication forks was strongly decreased (Figure 3.13A, lanes 2, 3, 4, Figure 3.13B). Interestingly, the amount of the Okazaki fragments product seemed to be not reduced much compared to the leading product (Figure 3.13A, lanes 2, 3, 4, Figure 3.13B). In addition, the size of the Okazaki fragments seemed to be shorter by presence of Pol IV (Figure 3.13A, lanes 2, 3, 4; Figure 3.13B). These evidences suggest that Pol IV inhibited the DNA replication in *oriC* assay, with the stronger effect on the leading synthesis and perhaps produced a shorter type of Okazaki fragments. However, because in this experiment all the products were analyzed in the same gel, therefore it was unclear whether the short products, which were migrated at the bottom of the gel were actual Okazaki fragments or the early stalled-leading products.

A

Counter clock-wise leading product (3.5 kb)

Clock-wise leading product (0.9 kb)

Okazaki fragments

0 10 50 100 200 400 800 nM **Pol IV**

4.3 kb
3.5
2.7
1.9
1.5
0.9
0.4

1   2   3   4   5   6   7

B

Counter clock-wise leading product

Clock-wise leading product

Okazaki fragments
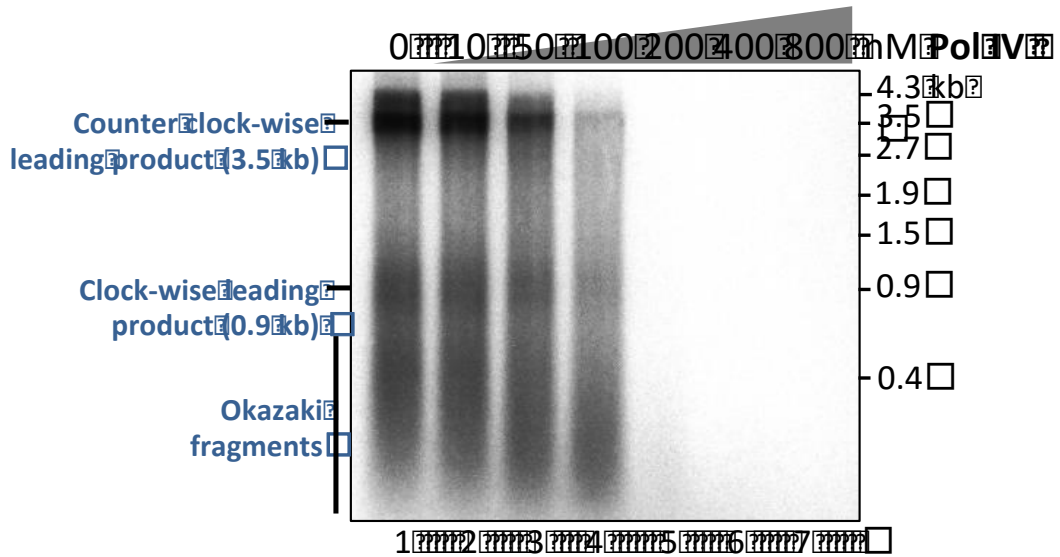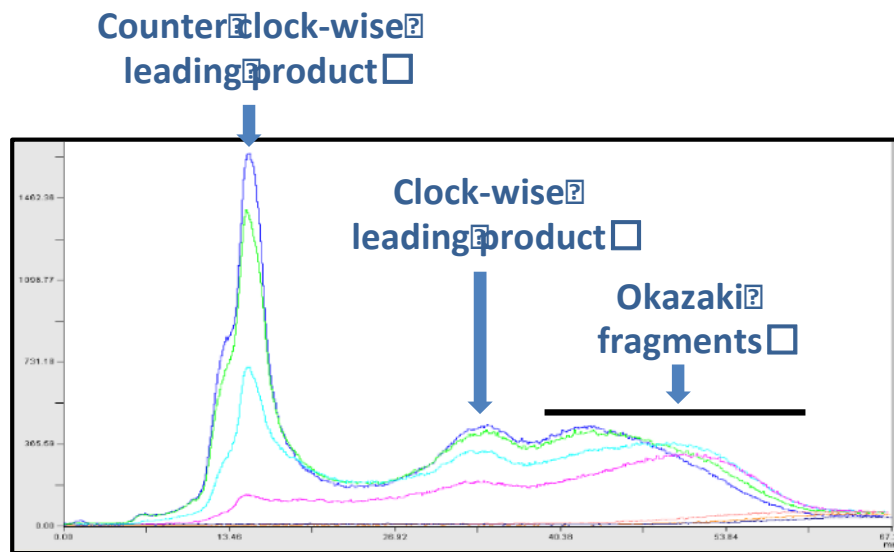
Figure 3.13. Checking the effect of Pol IV to the DNA synthesis of *oriC* assay. *oriC* assay was carried out at 30°C for 15 min in the presence of various concentrations of Pol IV D8A (10, 50, 100, 200, 400 and 800 nM). Replication products were labeled by [α-^{32}P] dATP. (**A**) The replication products were analyzed by 0.9% alkaline agarose gel electrophoresis. Lanes 1-7: Pol IV concentration was 0, 10, 50, 100, 200, 400, 800 nM, respectively. (**B**) The profile represents the intensity of the replication products pattern.

To clearly clarify the difference between the effect of Pol IV to leading strand synthesis and lagging strand synthesis, the same experiment as above was performed, excepted that the final Pol IV concentration added into the *oriC* assay was 0, 10, 50, 100, 200 and 400 nM. Dynamic of the counter clock-wise fork was monitored. However, instead of total product analysis by [α-^{32}P] dATP incorporation, the leading product and Okazaki fragments was individually analyzed using Southern blot analysis (Figure 3.14). Probe A and A', which are located nearby the *oriC* site in the counter clock-wise direction were used for detecting the leading product and Okazaki fragment, respectively (Figure 3.14A). Notably, not all of the Okazaki fragments were detected in this experiment. Similar to the previous result, here it clearly showed that at high concentrations (higher than 200 nM), Pol IV absolutely blocked DNA synthesis (Figure 3.14B, lanes 5, 6 and 11, 12). At lower concentrations of Pol IV, compared to the control sample which was without addition of Pol IV (Figure 3.14B, lane 1), a significant reduction of the leading product was observed and the shorter type of Okazaki fragments was produced (Figure 3.14B, lanes 2, 3 and 8, 9, 10). However, no early stalled-leading product was detected, indicating that the short products migrated at the bottom of the previous gel (Figure 3.13A) were the actual Okazaki fragments. Remarkably, at 100 nM of Pol IV, since no detectable leading product was obtained (Figure 3.14B, lane 4), a quite high amount of Okazaki fragment was still replicated (Figure 3.14B, lane 10), suggesting that in this condition, even the leading Pol III was utterly blocked, the lagging Pol III still proceeded forward together with helicase. During the normal DNA replication, the two polymerase III cores on the leading- and lagging strands are coordinated together with helicase at the replication fork, that makes leading- and lagging strand synthesis are always coupled (Lewis et al., 2016; McHenry, 2011). Taken together, these findings imply that Pol IV could enter the replication fork. The enzyme blocked DNA synthesis of Pol III with the stronger effect on the leading strand synthesis, produced shorter type of Okazaki fragments and induced uncoupling synthesis at the replication fork.
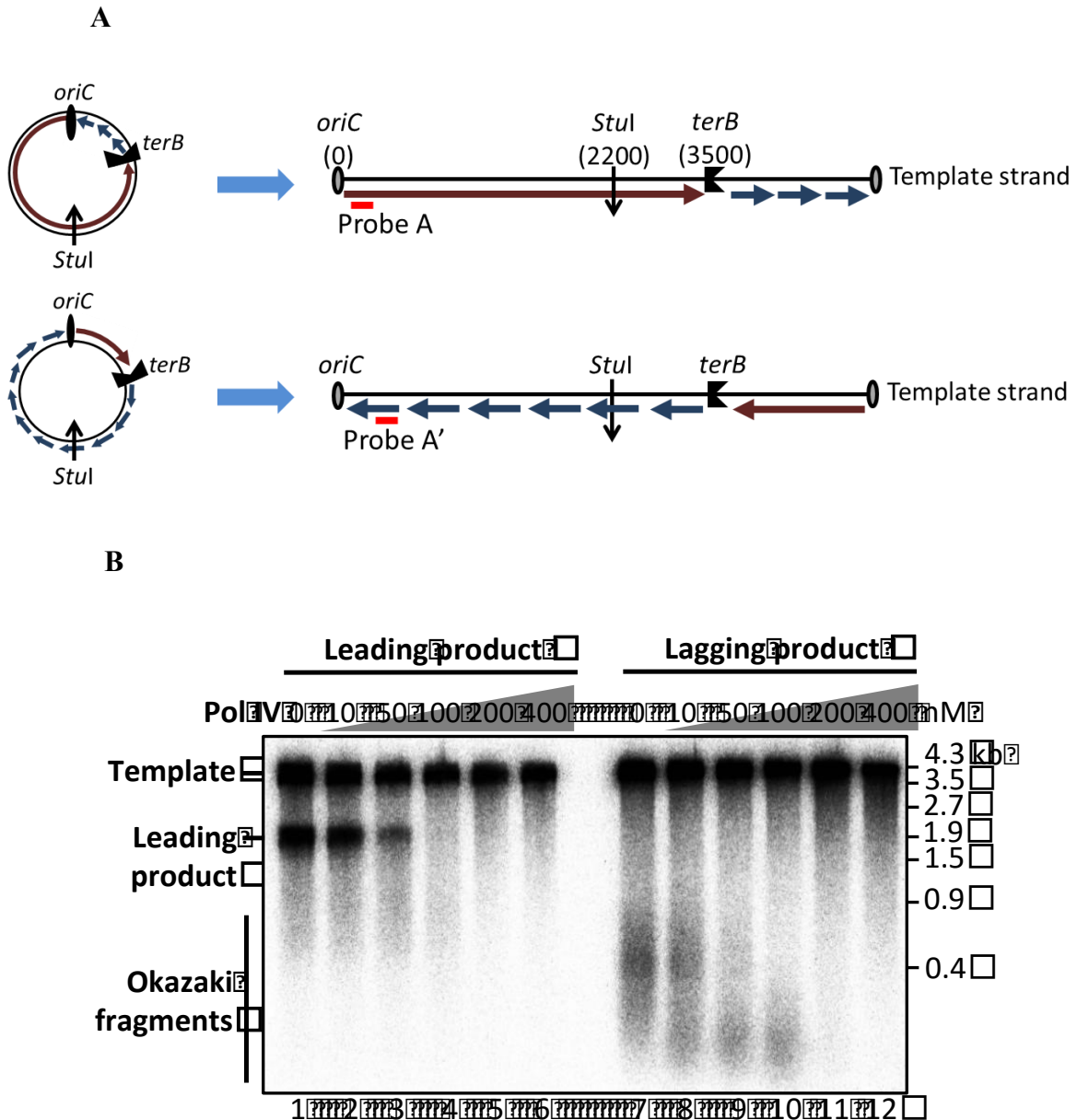
Figure 3.14. Checking the effect of Pol IV to DNA synthesis of *oriC* assay whereby the leading- and lagging product was separately analyzed using Southern blot analysis. Briefly, *oriC* assay was carried out at 30°C for 15 min in the presence of various concentrations of Pol IV D8A (10, 50, 100, 200 and 400nM). After that, the replication products were digested with *Stu*I, then loaded on a 0.9% alkaline agarose gel electrophoresis and subjected to Southern blot analysis. (**A**) Schematic diagram showing the replication product pattern formed on pMOL7 and the location of the probes. The dark red arrows represent the leading products, the blue arrows represent the Okazaki fragments and the scarlet lines represent the probes. (**B**) Result of Southern blot analysis, lanes 1-6: detecting the leading product by probe A, Pol IV concentration was 10, 50, 100, 200 and 400 nM, respectively. Lanes 7-12: detecting the Okazaki fragment by probe A', Pol IV concentration was 10, 50, 100, 200 and 400 nM, respectively.

II.2. Study of the fate of Pol III after Pol III-Pol IV switching at the replication fork

During the translesion synthesis by Pol IV, two turns of polymerase switch are occurred. In the first switch, Pol IV replaces the stalled Pol III at the lesion site and synthesizes the DNA across the lesion. Subsequently, Pol III takes back the primer terminus from Pol IV and resumes the genomic DNA synthesis (the second polymerase switch). The central but still remain unknown question is, after the first polymerase switch, whether the stalled Pol III still stays on replisome, or dissociated. Knowing the answer for this question is very important, because if Pol III is pushed out from the replisome, in the second polymerase switch, recruitment of a new Pol III is needed to re-form the replisome structure.

To answer the question above, a novel system was designed based on the *oriC* assay, as summarized in Figure 3.15. Briefly, first, the stalled replication forks were synchronized and accumulated by omission of DNA gyrase in the *oriC* assay. After that, a sufficient amount of Pol IV was added into the reaction mixture to allow Pol III-Pol IV switch occur at a high efficiency. To prove whether after Pol III-Pol IV switch, Pol III still stays on the replisome or pushed out, the Pol IV-switched replication forks were isolated from the reaction mixture. The purpose of this step was to remove all the unused Pol III in the reaction mixture. Subsequently, the isolated Pol IV-switched replications forks were restarted. Because the polymerase IV dead mutant D8A was used to produce Pol III-Pol IV switch, the restarted product represents for the presence of Pol III at the replication fork. If Pol III still stays on the replisome, the enzyme quickly comes back to the primer terminus and restarts synthesizing the DNA, hence prolongs the stalled product.
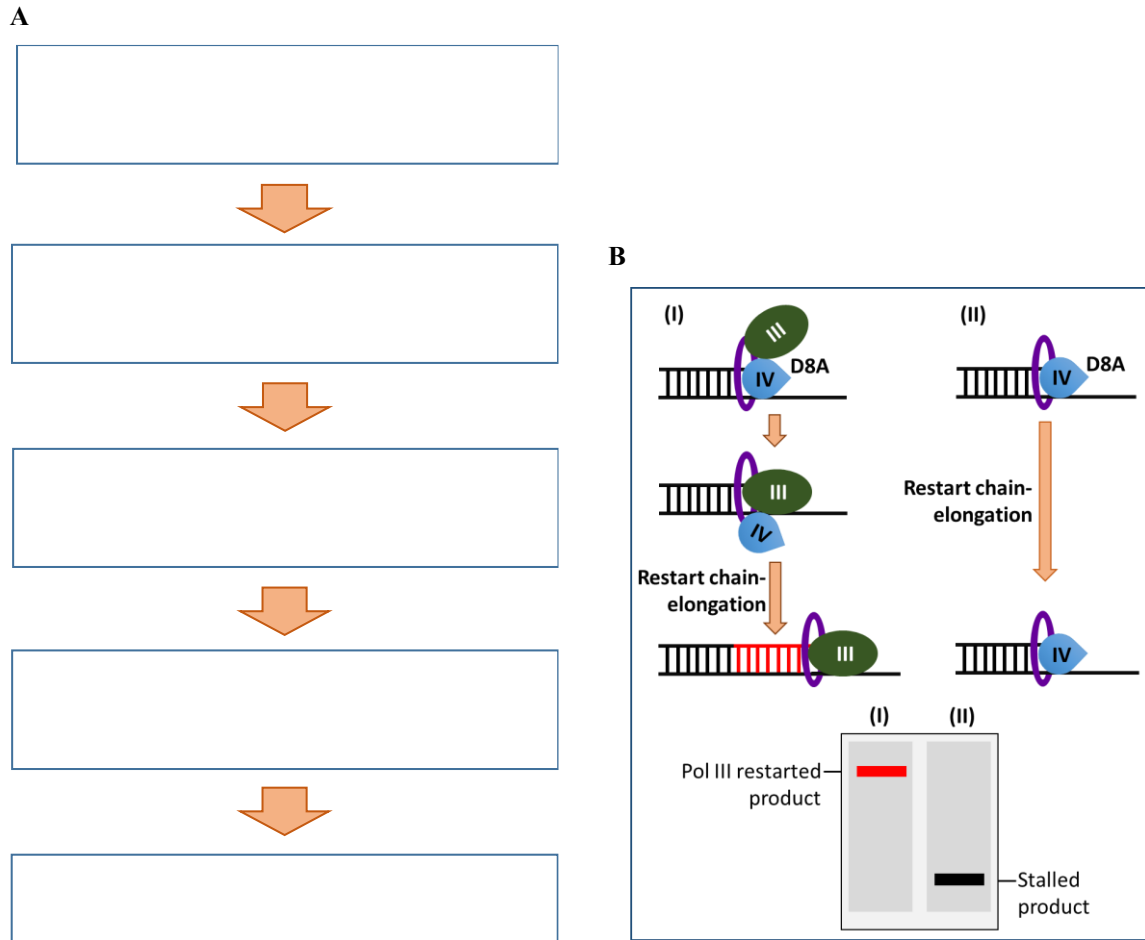
Figure 3.15. Design of a novel system to study the fate of Pol III after Pol III-Pol IV switch at the replication fork. (**A**) Foremost, the stalled replication forks were accumulated by omission of DNA gyrase in the *oriC* assay. After that, Pol III-Pol IV switch at the accumulated stalled replication forks was produced by addition of a sufficient amount of Pol IV. In the next step, the Pol IV-switched replication forks were isolated from the unused Pol III. The isolated Pol IV-switch-replication forks were then restarted by addition of DNA gyrase and other replication components required for chain-elongation process. Finally, the restarting product was analyzed. (**B**). Because the Pol IV mutant D8A which loses the polymerase activity was used to introduce Pol III-Pol IV switch, therefore, the restarted product represents for Pol III product. If after Pol III-Pol IV switch, Pol III is still on the replisome, the enzyme quickly comes back to the primer terminus and prolongs the stalled product. In contrast, if Pol III is pushed out, the length of the stalled product is remained.

II.2.1. Accumulation of the stalled replication forks by omission of DNA gyrase in the *oriC* assay

During the chain-elongation process of DNA replication, the parental strand separation by helicase generates positive supercoil DNA in front of the replication fork. This positive supercoil is a torsional stress, which needs to be released for further chain-elongation because helicase is unable to unwind this kind of DNA substrate. In *E. coli* cell, a DNA topoisomerase II - DNA gyrase is involved in removal of this stress, by introducing the positive supercoiled DNA into the negative supercoiled DNA, as the normal substrate DNA for helicase (Alberts et al., 2002; Reece & Maxwell, 1991).

To evaluate how the replication fork behaves in the absence of DNA gyrase and find a condition to accumulate a sufficient amount of the stalled replication forks, *oriC* assay without addition of DNA gyrase was carried out at 30°C for 3, 5, 7, 10, 15 and 20 min. The DNA sample was then digested by *Alw*NI, separated by a 0.9% alkaline agarose gel electrophoresis and further subjected to Southern blot analysis. The counter clock-wise replication fork was analyzed. To monitor how far the replisome could proceed, the leading product was detected by probe A (Figure 3.16A).

Because in the *oriC* assay, since the origin was fired, replication of the full-length product rapidly done within several seconds. However, when DNA gyrase was omitted, after 3 min incubation, only a band of ~0.6 kb leading product was observed, no signal of full-length leading product was discovered (Figure 3.16B, lane 1). The amount of this 0.6 kb leading product was accumulated after 5 min incubation and became saturated after 7 min incubation (Figure 3.16B, lanes 2, 3, 4, 5, 6), suggesting that in the absence of DNA gyrase, the replisome proceeded 0.6 kb far away from the *oriC* and was unable to go forward even after 20 min incubation due to the existence of a torsional stress in front of. A fain band of the full-length leading product was detected after 5 min incubation indicates that the super-helical stress in some template DNA was released even in the absence of DNA gyrase, probably due to the formation of some nicks in the template DNA. To avoid the uncontrolled formation of the full-length leading product, 3 min incubation without addition of DNA gyrase was chosen as a condition to accumulate the stalled replication forks.
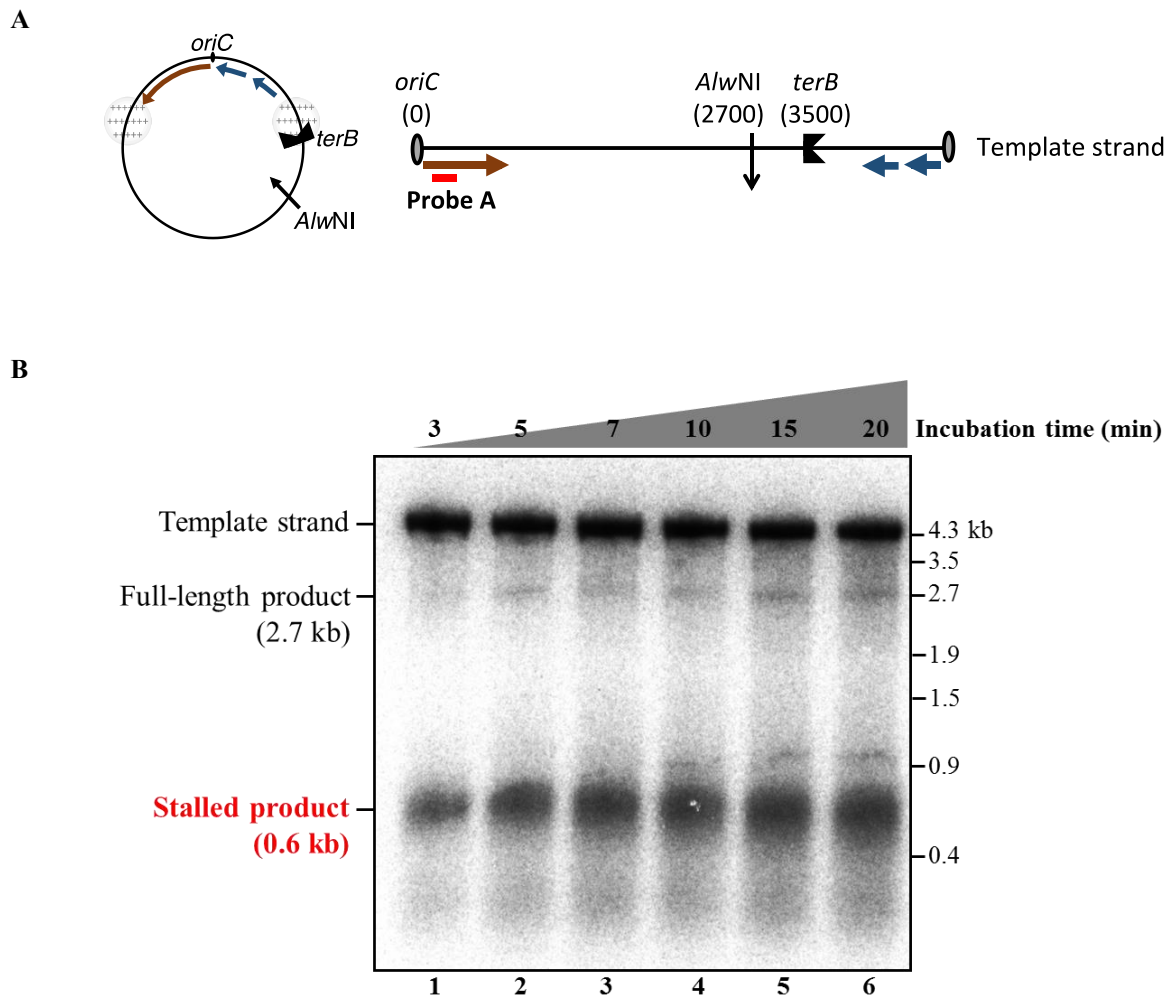
Figure 3.16. Accumulation of the stalled replication forks by omission of DNA gyrase in *oriC* assay. *oriC* assay was carried out in the absence of DNA gyrase at 30°C for 3, 5, 7, 10, 15 and 20 min. After that, the DNA samples were digested with *Alw*NI, then loaded on a 0.9% alkaline agarose gel electrophoresis and subjected to Southern blot analysis. (**A**) Schematic diagram showing the replication product pattern and the location of probe A. The dark red arrows represent the leading product, the blue arrows represent the Okazaki fragments, the circle containing the cross marks represents the accumulation of the positive supercoiled in front of the replication fork, the scarlet line represent probe A. (**B**) Result of Southern blot analysis. Lanes 1-6: *oriC* assay without addition of gyrase for 3, 5, 7, 10, 15, 20 min incubation, respectively.

I speculated that if DNA gyrase is added back, the torsional stress in front of the stalled replication forks could be released. Consequently, helicase unwinds the duplex DNA toward and Pol III is able to further elongate the replication product. To test this speculation and find a condition to rapidly restart the stalled replication forks, 5-fold or 10-fold more excessive than the standard amount of DNA gyrase in *oriC* assay was added into the stalled replication forks and further incubated for the indicated time points (Figure 3.17B). As a result, after 3 min incubation without DNA gyrase, only the 0.6 kb stalled product was observed (Figure 3.17B, lane 1). The control sample with further 5 min incubation without addition of DNA gyrase resulted in some full-length product but it was not significant (Figure 3.17B, lane 2).

However, when 5-fold excessive amount of DNA gyrase was added, after 3, 5, 7 min incubation, the amount of the stalled product was significantly decreased together with the appearance of the full-length product (Figure 3.17B, lanes 5, 6, 7), indicating that the stalled replication forks were restarted by the action of DNA gyrase. After 7 min further incubation, almost of all the stalled replisome were resumed (Figure 3.17B, lane 7). On the other hand, if 10-fold excessive amount of DNA gyrase was used, a sufficient level of fork restarting could be obtained just after 5 min incubation (Figure 3.17B, lane 4). From this data, 10-fold excess amount with further 5 min incubation was chosen for next experiments to restart the stalled replication forks that caused by omitting gyrase.

A
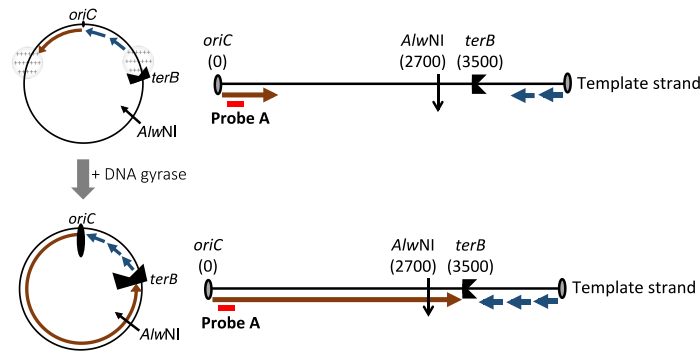
B
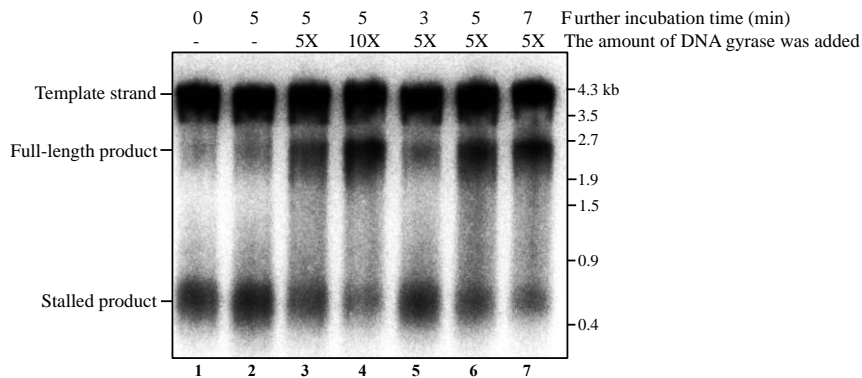
Figure 3.17. Restarting of the stalled replication forks by adding back DNA gyrase into the reaction mixture. 5-fold or 10-fold excessive amount of DNA gyrase was added into the stalled replication forks and further incubated for the indicated time points. After that, the DNA samples were digested with *Alw*NI then separated by a 0.9% alkaline agarose gel electrophoresis and subjected to Southern blot analysis. (**A**) Schematic diagram showing the replication product pattern and location of probe A. The dark red arrows represent the leading product, the blue arrows represent the Okazaki fragments, the circle containing the cross marks represents the accumulation of the positive supercoiled in front of the replication fork, the scarlet line represent probe A. Upper panel: the dynamic of *oriC* assay in the absence of DNA gyrase. Lower panel: the dynamic of *oriC* assay when DNA gyrase was added back to restart the chain-elongation process. (**B**) Result of Southern blot analysis. Lane 1: *oriC* assay without DNA gyrase for 3 min. Lanes 2, 3, 4: the reaction was further incubated for 5 min after addition of 0X, 5X or 10X excessive amount of DNA gyrase, respectively. Lanes 5, 6, 7: 5X excessive amount of DNA gyrase was added back and further incubated for 3 min, 5 min or 7 min, respectively.

As summary, to obtain the accumulated stalled replication forks, *oriC* assay was carried out in the absence of DNA gyrase for 3 min. As the result, all the replisome stalled after proceeding 0.6 kb far away from the *oriC*. To efficiently restart the stalled replication fork, 10X excessive amount of DNA was added back and further incubated for 5 min.

II.2.2. The ability of Pol IV to switch with the stalled Pol III at the torsional stress induced-stalled replication forks

As described previously, to study the fate of Pol III after Pol III-Pol IV switch at the replication fork, a novel system was designed. In this designate system, the stalled replication forks were accumulated by omission of DNA gyrase in *oriC* assay. After that, I aimed to make Pol III-Pol IV switch at these stalled replication fork by providing a sufficient amount of Pol IV. However, it was unknown whether Pol IV has an ability to exchange with these torsional stress induced-stalled Pol III.

To confirm this point, *oriC* assay was executed without addition of DNA gyrase for 3 min at 30°C. After that, the wild type (WT) Pol IV or the mutant D8A was added into the reaction to the final concentration of 200 nM and incubated for 1 min. Subsequently, 10X excessive amount of DNA gyrase was added back, and further incubated for 5 minutes. The DNA samples were then digested by *Alw*NI, loaded on a 0.9% alkaline agarose gel electrophoresis and subjected to Southern blot analysis. The counter clock-wise replication fork was analyzed whereby the leading product was detected using probe A (Figure 3.18A). As previously showed, when DNA gyrase was absent, the replisome stalled at 0.6 kb far-away from the *oriC* (Figure 3.18B, lane 1). When DNA gyrase was added back, in the absence of Pol IV, the replisome smoothly restarted, generated a significant amount of the full-length product (Figure 3.18B, lane 1). Interestingly, when Pol IV was supplied, either the wild type Pol IV or the mutant D8A did inhibit the full-length product formation (Figure 3.18B, lanes 3, 4). Remarkably, in the case of the mutant D8A, the 0.6 kb stalled product just remained the same length (Figure 3.18B, lane 4), but in the case of the wild type Pol IV, the 0.6 kb stalled product was prolonged to approximate 0.9 kb (Figure 3.18B, lane 3). This observation implies that Pol IV efficiently took over the primer terminus from the stalled Pol III (which was caused by omission of DNA gyrase in the *oriC* assay) at the replication fork. However, in this condition, the concentration of Pol IV was very high (200-fold excess than Pol III), therefore Pol III was unable to take back the primer terminus from Pol IV. Pol IV (the wild type or the mutant D8A) utterly kept the primer template junction whereas the wild type Pol IV slowly synthesized the DNA instead of Pol III.

As summary, 200 nM of Pol IV efficiently produced Pol III-Pol IV switch at the torsional

stress induced-stalled replication forks.
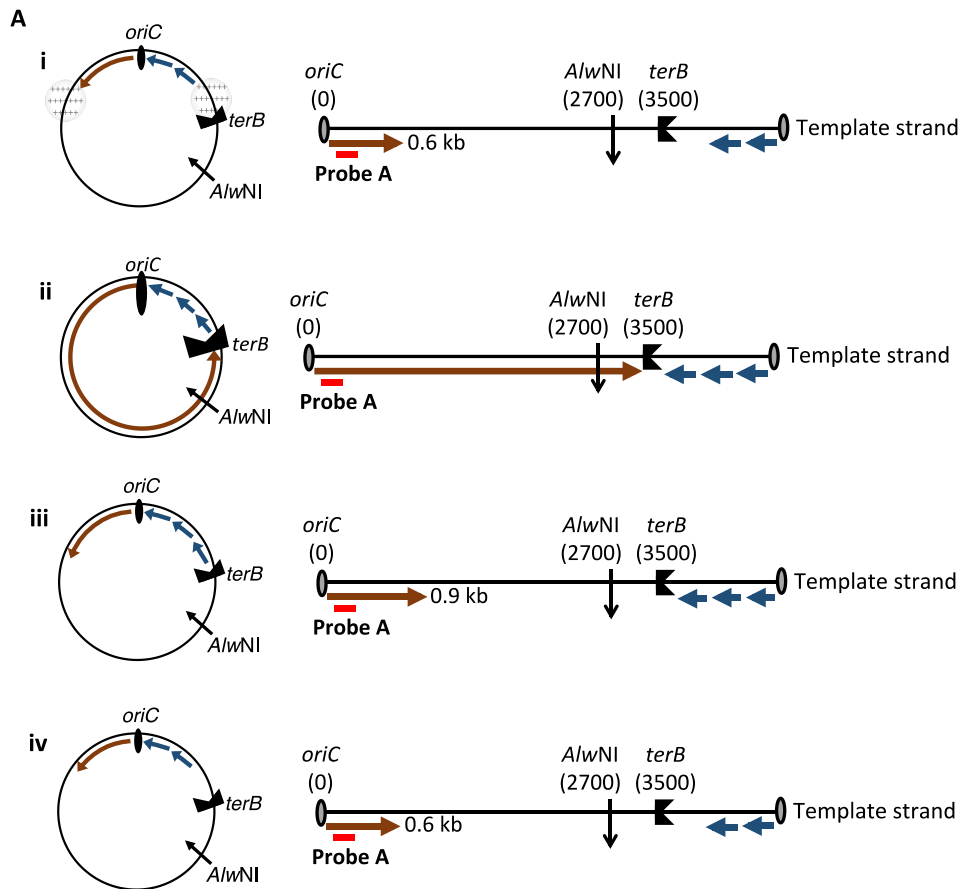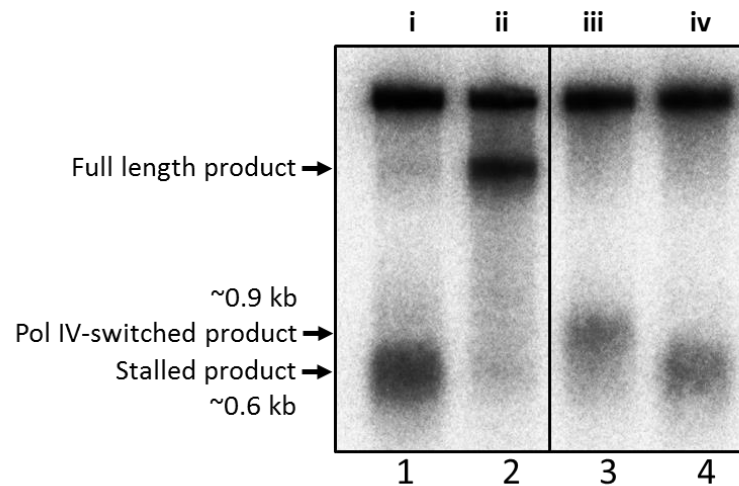
Figure 3.18. Checking the ability of Pol IV to replace the stalled Pol III at the torsional stress induced-stalled replication forks. *oriC* assay was performed in the absence of DNA gyrase at 30°C for 3 min. Afterwards, Pol IV (Wild type or the mutant D8A) was supplied into the reaction to the final concentration of 200 nM and incubated for 1 min. Subsequently, 10X excessive amount of DNA gyrase was put back, and further incubated for 5 minutes.

To analyze the result, the DNA samples were digested by *Alw*NI, then separated by a 0.9% alkaline agarose gel electrophoresis and subjected to Southern blot analysis. The leading product of the counter clock-wise replication fork was detected using probe A.

(**A**) Schematic diagram representing the product pattern and location of the probe A. The dark red arrows represent the leading product, the blue arrows represent the Okazaki fragments, the circle containing the cross marks represents the accumulation of the positive supercoiled in front of the replication fork, the scarlet line represent probe A. i, *oriC* assay without addition of DNA gyrase as the beginning sample. ii, after 3 min incubation in the absence of DNA gyrase, 0.5 μl of Pol IV storage buffer was added and incubated for 1 min. After that, 10X excess amount of DNA gyrase was supplied and further incubated for 5 min. iii, after 3 min incubation in the absence of DNA gyrase, the wild type Pol IV was added to the final concentration of 200 nM and incubated for 1 min. After that, 10X excess amount of DNA gyrase was supplied and further incubated for 5 min. iv, after 3 min incubation in the absence of DNA gyrase, the Pol IV mutant D8A was added to the final concentration of 200 nM and incubated for 1 min. After that, 10X excess amount of DNA gyrase was supplied and further incubated for 5 min.

(**B**) Result of Southern blot analysis. Lanes 1, 2, 3, 4 represent for sample of i, ii, iii, iv, respectively.

II.2.3. Establishment of a novel method to quickly isolate the replication intermediate

So far, I showed that the accumulation of the stalled replication forks could be observed by omission of DNA gyrase in the *oriC* assay. I also confirmed that if DNA gyrase was added back, the stalled replication forks efficiently restarted. Moreover, Pol IV exhibited its ability to efficiently replace the stalled Pol III at the torsional stress induced-stalled replication forks. In term of studying the fate of Pol III after Pol III-Pol IV switch, the next step was to find a method to isolate the Pol IV switched-replication forks from the unused Pol III.

During DNA replication process in *E. coli* cell, the termination protein Tus tightly binds the termination sequence *terB*, leading to the stop of DNA replication when the replication machinery encounters the *terB*/Tus complex (Neylon et al., 2005). It has been believed that among the protein-nucleic acid interactions, Tus/*terB* is known as one of the strongest protein-DNA bindings. In the other hand, the affinity between the biotin and streptavidin compound is also very high (Chivers, Koner, Lowe, & Howarth, 2011). Therefore, to isolate the replication intermediates from the reaction mixture, the Tus protein was biotinylated. I speculated that using the streptavidin coated magnetic bead, the replication intermediates could be pulled down together with the biotinylated Tus by Pull down assay.

II.2.3.1. Preparation of the biotinylated Tus

i. Purification of the biotinylated Tus.

The *tus* gene, which encodes for Tus protein was amplified from MG1655 genome by PCR amplification and inserted into the plasmid pAviTag SUMO (Lucigen), resulting an overexpression plasmid as called as pAvi-*tus*. In this overexpression plasmid, a 6-His tag was located at the 5' end of the *tus* gene and an Avi tag, which is the biotinylation recognition site, was located at the 3' end of the *tus* gene. The plasmid pAvi-*tus* was transformed into the *E. coli* strain Biotin Xcell (Lucigen). Notably, the genome of the Biotin Xcell strain contains *birA* gene, which encodes for the biotin ligase - BirA. Therefore, it was speculated that inside the Biotin Xcell, since the protein Tus is expressed, BirA adds Biotin to the C terminal of Tus via the AviTag (Figure 319A).

The expression of Tus from the vector pAvi-*tus* was induced by rhamnose and the expression of BirA from Biotin Xcell's genome was induced by arabinose. Therefore, overexpression coupled with biotinylation of Tus was carried out at 37°C for 4 hours in the medium containing 0.2% Rhamnose, 0.01% Arabinose and 50 μM Biotin. After that, this modified Tus (38 kDa) was firstly purified by Hitrap chelating column resulting fraction II (Figure 319B, lane 1), and further purified by Hitrap DEAE column resulting fraction III with very high purity (Figure 319B, lane 2).
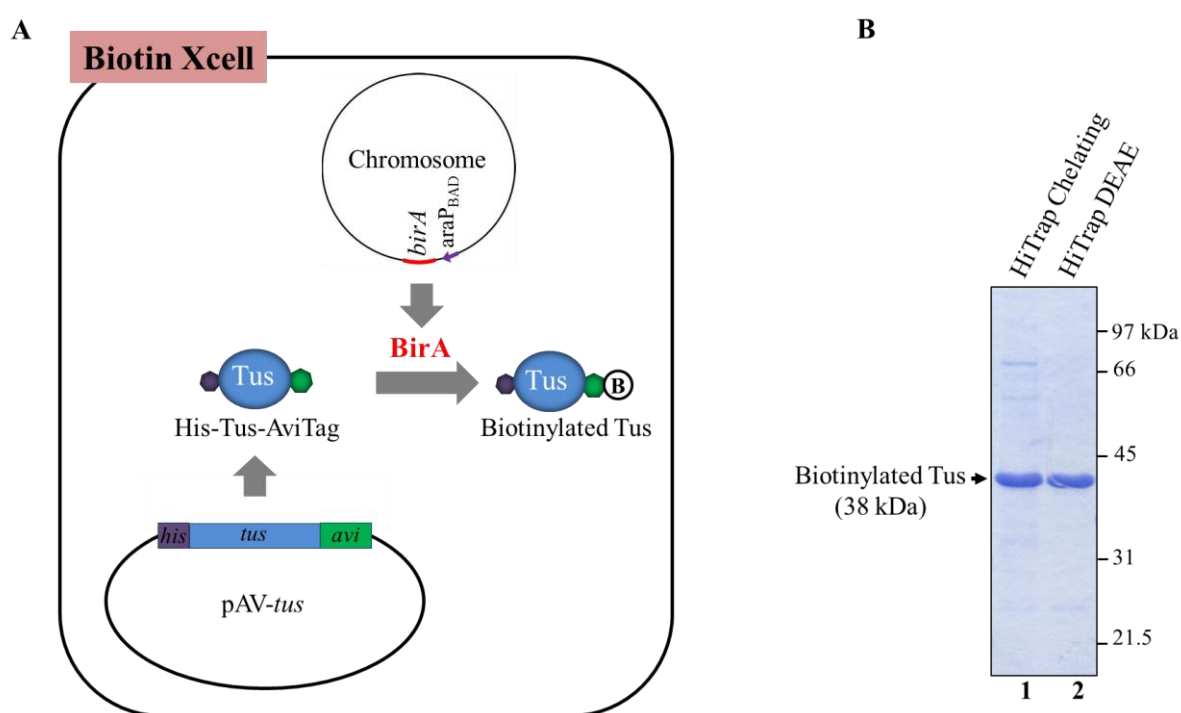
Figure 3.19. Preparation of biotinylated Tus. (A) Schematic diagram showing the strategy for preparation of the biotinylated Tus. The gene encoding for Tus was amplified from MG1655 genome by PCR amplification and inserted into the vector pAviTag SUMO (Lucigen), resulting the overexpression vector pAvi-*tus*. Inside the vector, there is a 6-His tag at the 5' end of the *tus* gene and an Avi tag, which is the biotinylation recognition site at the 3' end of the *tus* gene. The plasmid carrying the *tus* gene fragment was transformed into the *E. coli* strain Biotin Xcell (Lucigen). Because genome of the Biotin Xcell strain contains the gene encoding for the biotin ligase – BirA, therefore, it was speculated that since the protein Tus is expressed, BirA couples Biotin to the C terminal of Tus via the AviTag. (**B**) 12% SDS polyacrylamide gel electrophoresis checking the quality of protein after each column purification. The protein was stained by Coomassie brilliant blue. Lane 1: Hitrap chelating column purification, lane 2: Hitrap DEAE column purification.

ii. Checking the biotinylation of the modified Tus

After purification, the biotinylation of the modified Tus, which was temporally called as biotinylated Tus was determined by Pull down assay (Figure 3. 20A). Briefly, the Tus protein (100 ng of the wild type Tus or the biotinylated Tus) was mixed with the Dynabeads M280 streptavidin (30 μl, Thermo Fisher Scientific) for 5 min at room temperature. After that, the reaction mixture was put on a magnetic separation rack. Because the beads were coated by Streptavidin compound, which exhibited a very strong affinity to the Biotin radical, thus if the purified Tus was biotinylated, it tightly bound to the beads and pulled down in the pellet. In contrast, the non-biotinylated Tus was eluted in the supernatant. Both samples from the pellet and the supernatant were analyzed by a 15% SDS polyacrylamide gel electrophoresis (Figure 3. 20A).

As the result, for the control wild type Tus, the protein just stayed in the supernatant and no significant signal was detected in the pellet (Figure 3. 20B, lanes 1, 2). However, in the case of the biotinylated Tus fraction II, the protein was mainly recovered in the pellet and no protein was detected in the supernatant (Figure 3. 20B, lanes 3,4). Compared to the protein standard concentration (Figure 3. 20B, lanes 5, 6, 7, 8, 9), the amount of protein recovered in the pellet was counted as 70%. This result suggests that 70% of the Tus protein was biotinylated. Because the biotinylated Tus was further purified by Hitrap DEAE column, I also tested whether this step of purification affected the biotinylation efficiency using the same experiment as described above. As shown in Figure 3. 20C, the protein from Hitrap DEAE column purification (fraction III) was also mainly recovered in the pellet (Figure 3. 20C, lane 6) as same as the protein from Hitrap chelating column (Figure 3. 20C, lane 3). It indicates that DEAE colum purification enhanced the protein purity but did not affect the biotinylation efficiency of the protein.

Figure 3.20. Checking the biotinylation efficiency of the modified Tus by Pull down assay. (**A**) Schematic diagram showing the experimental procedure. Briefly, 100 ng of the Tus protein (wild type Tus or the biotinylated Tus) was mixed with 30 μl washed-Dynabeads M280 streptavidin (Thermo Fisher Scientific) for 5 min at room temperature. The reaction mixture was then put on a magnetic separation rack and the supernatant and the pellet was separated. After that, the protein in the pellet was released from the bead. Sample of both supernatant and the pellet was analyzed by 15% SDS polyacrylamide gel electrophoresis. The protein was stained by PlusOne Silver Staining Kit (GE healthcare). (**B**), (**C**) SDS polyacrylamide gel electrophoresis showing the result of Pull down assay. (**B**) Checking the biotinylation and determination of the biotinylation efficiency of the biotinylated Tus fraction II. Lanes 1, 2: wild type Tus – supernatant and pellet, respectively. Lanes 3, 4: biotinylated Tus fraction II – supernatant and pellet, respectively. Lanes 5-9: 5, 10, 25, 50, 100 ng of the biotinylated Tus fraction II was loaded, respectively. (**C**) Checking the biotinylation of the biotinylated Tus fraction III (after Hitrap DEAE column purification) compared to the biotinylated Tus fraction II. Lanes 1-3: biotinylated Tus fraction II, lane 1: control without Pull down assay, 100 ng of the protein was directly loaded on the gel. Lanes 2, 3: Pull down assay - supernatant and pellet, respectively. Lanes 4-6: biotinylated Tus fraction III, lane 4: control without Pull down assay, 100 ng of the protein was directly loaded on the gel. Lanes 5, 6: Pull down assay - supernatant and pellet, respectively.

iii. Evaluation of the activity of the purified biotinylated Tus in oriC assay

During DNA replication, function of Tus is known to bind the termination site - *terB* therefore blocks the replication fork movement when the replisome collides the Tus/*terB* complex (Neylon et al., 2005). As explained from the beginning of this chapter, to distinguish the product pattern of two replication forks of the *oriC* assay, *terB* site was put asymmetrically on the plasmid pMOL7, resulted in a 0.9 kb-long way for the clock-wise fork, and a 3.5 kb-long way for the counter lock-wise fork (Figure 3. 21A). Therefore, after purification, I tested whether the biotinylated Tus still remained the activity to bind *terB* sequence and stop DNA replication process.

In a standard *oriC* assay, to block the replication fork movement, Tus protein was added to the final concentration of 118 nM. In order to check the activity of the biotinylated Tus, *oriC* assay was carried out by addition of various concentrations of Tus (0 nM, 59 nM, 118 nM and 236 nM) at 30°C for 15 min. The replication products were labeled by [α-^{32}P] dATP incorporation, and analyzed by 0.9% alkaline agarose gel electrophoresis (Figure 3. 21B).

When Tus was absent in *oriC* assay, it was predicted that two replication forks, the counter clock-wise fork and the clock-wise fork travel evenly therefore will collide and stop after half way of the circular template pMOL7, resulting the same 2.2 kb-leading product (1/2C) and the Okazaki fragments. However, in the sample when Tus was omitted, beside the 2.2 kb leading product (1/2C), some significant amount of the one-circle products (1C) and the rolling circle products (RC) were detected (Figure 3. 21B, lane 1), suggesting that perhaps one of the replisome pushed out the other when they collided and proceeded forward without stalling, probably due to strand displacement activity of Pol III. When the wild type Tus was added, the enzyme exhibited its ability to block the replication fork movement, therefore resulted in the 3.5 kb counter clock-wise leading product (3/4C), the 0.9 kb clock-wise product (1/4C) and the Okazaki fragments (Figure 3. 21B, lanes 2, 3, 4). Importantly, the biotinylated Tus also provided the same product pattern as the wild type Tus (Figure 3. 21B, lanes 5, 6, 7). This data suggests that the biotinylated Tus functioned in *oriC* assay as normal.
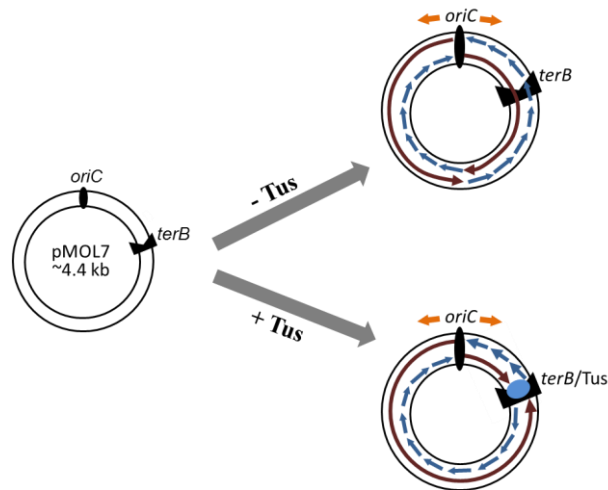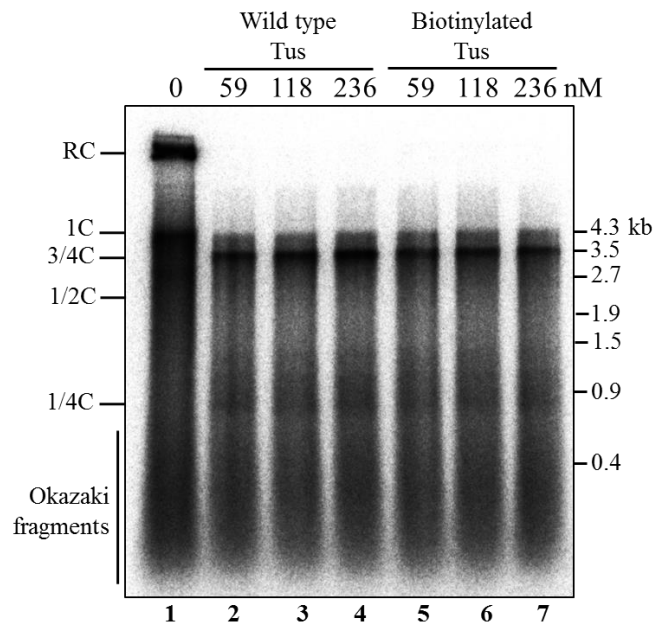
Figure 3.21. Checking activity of the purified biotinylated Tus in *oriC* assay. The *oriC* assay was carried out with different concentrations (0 nM, 59 nM, 118 nM and 236 nM) of the wild type Tus or the biotinylated Tus at 30°C for 15 min. The replication products were labeled by [α-^{32}P] dATP incorporation. (**A**) The schematic diagram showing the replication product pattern in the absence (upper panel) and presence (lower panel) of Tus. The orrange arrows represent for directions of two replication forks, the counter clock-wise fork and the clock-wise fork. The dark red arrows represent for leading products. The blue arrows represent for Okazaki fragments. The blue ellipse represents for Tus. (**B**) The products were analyzed by 0.9% alkaline agarose gel electrophoresis. Lane 1: *oriC* assay in the absence of Tus. Lanes 2, 3, 4: the wild type Tus was added to the final concentration of 59 nM, 118 nM and 236 nM, respectively. Lanes 4, 5, 6: the biotinylated Tus was added to the final concentration of 59 nM, 118 nM and 236 nM, respectively.

II.2.3.2. Isolation of the replication intermediates by Pull down assay using the biotinylated Tus

After getting the biotinylated Tus, I tried to isolate the replication intermediates by the previously described procedure. The *oriC* replication mixture observed after 3 min incubation at 30ºC in the absence of DNA gyrase was mixed with the Dynabeads M280 streptavidin for 1 min at room temperature. Subsequently, the mixture was placed on a magnetic separation rack, then the supernatant and the pellet was separated. I expected that the replication intermediates which contains the biotinylated Tus was pulled down in the pellet, whereas the other unused components including the unused Pol III stayed in the supernatant. The DNA in the pellet was released from the beads. After that, the DNA sample in both supernatant and pellet was purified, separated by a 0.9% alkaline agarose gel electrophoresis and subjected to Southern blot analysis. The counter clock-wise fork was monitored whereby the leading product was detected using probe A (Figure 3. 22). As a result, it clearly showed that some of the replication intermediates were stayed in the supernatant (Figure 3. 22B, lane 3), however more than 50% of the DNA was pulled down in the pellet (Figure 3. 22B, lane 4).

To evaluate whether the isolated replication intermediates were still active or not, after Pull down, a solution containing 10-fold excess amount of DNA gyrase and the components required for chain-elongation process of both leading- and lagging strand synthesis (as described in chapter 2.2.4) was added to the pellet and incubated at 30ºC for 5 min. Notably, neither Pol III nor helicase was added. Interestingly, compared to the control sample without restoration of the replication intermediates, a significant amount of the 0.6 kb stalled product was reduced and a band of the 2.7 kb restarted full-length product was produced (Figure 3. 22B, compared lanes 4 and lane 6, red triangles). This result suggests that the isolated replication intermediates observed by Pull down assay were active. Pol III and helicase stably stayed on the replisome throughout the isolation steps and had an ability to restore when the components required for chain-elongation process was provided.
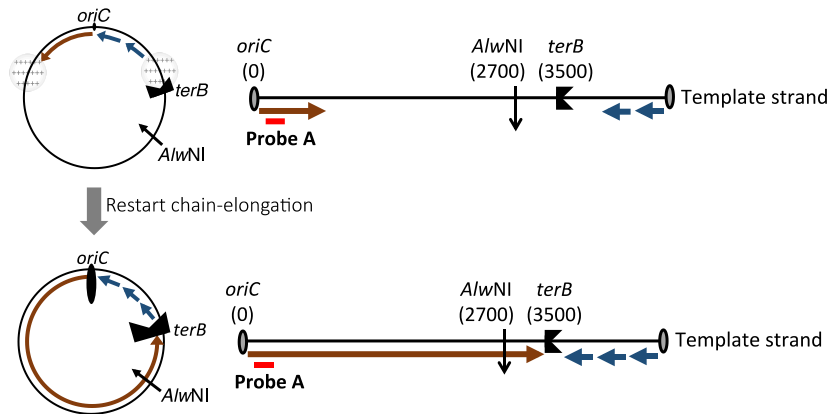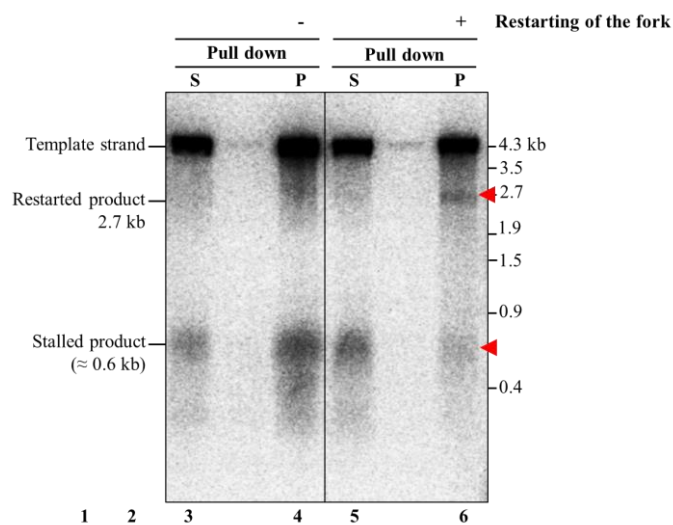
Figure 3.22. Isolation of the replication intermediates by Pull down assay using the biotinylated Tus. The *oriC* replication mixture observed by omission of DNA gyrase was mixed with the Dynabeads M280 streptavidin for 1 min at room temperature. The mixture was then placed on a magnetic separation rack, and the supernatant and the pellet was separated. To confirm whether the isolated replication intermediates were still active, after Pull down, 15 μl of the solution containing 10-fold excess amount of DNA gyrase and the components required for chain-elongation process was added to the pellet and incubated at 30ºC for 5 min. The DNA samples were digested by *Alw*NI, separated by a 0.9% alkaline agarose gel electrophoresis and subjected to Southern blot analysis. The leading product of the counter clock-wise fork was detected by probe A. (**A**) Schematic diagram representing the product pattern and location of the probe A. The dark red arrows represent the leading product, the blue arrows represent the Okazaki fragments, the circle containing the cross marks represents the accumulation of the positive supercoiled in front of the replication fork, the scarlet line represent probe A. Upper panel: the dynamic of *oriC* assay in the absence of DNA gyrase. Lower panel: the dynamic of *oriC* assay when the chain-elongation process was restarted (**B**) Result of Southern blot analysis. Lanes 1-2: Pull down assay without restoration of chain-elongation for the pellet, supernatant and pellet, respectively. Lanes 3-4: Pull down assay with the restoration of chain-elongation for the pellet, supernatant and pellet, respectively.

II.2.4. Study of the fate of Pol III after Pol III-Pol IV switch at the replication fork

Finally, the established novel system above was applied to study the fate of Pol III after Pol III-Pol IV switch at the replication fork, whether Pol III still remain on the replisome or dissociated.

Foremost, *oriC* assay was carried out in the absence of DNA gyrase at 30ºC for 3 min. After that, the polymerase dead mutant Pol IV D8A was added to the final concentration of 200 nM, and incubated for 1 min. The Pol IV-switched replication forks were isolated from the unused components including Pol III by Pull down as previously described (chapter 2.3.1). Subsequently, a the solution containing 10-fold excess amount of DNA gyrase and the components required for chain-elongation process of both leading- and lagging strand synthesis was added to the pellet containing the Pol IV-switched replication forks and incubated at 30ºC for 5 min or 10 min (as described in chapter 2.2.4). Remarkably, neither Pol III nor helicase was added. I expected that if Pol III still remained on the replisome, the enzyme rapidly returns to the primer terminus and restarts the chain-elongation process because in this isolated mixture, the unbound Pol IV was also removed. The restarted product was analyzed by Southern blot, in which the restarted leading product of the counter clock-wise fork was detected using probe A (Figure 3.23).

As the result, in the control experiments without addition of Pol IV, a faint, but detectable amount of restarted full-length product was observed together with a reduction of the stalled product after 5 min or 10 min incubation (Figure 3.23B, lanes 1, 2, red triangles), representing for the presence and restoration of Pol III at the replication fork. However, when Pol III-Pol IV switched was introduced, compared to the control, none of the restarted full-length product was detected, representing for the absence of Pol III. This observation suggests that after Pol III-Pol IV, Pol III was pushed away from the replisome.
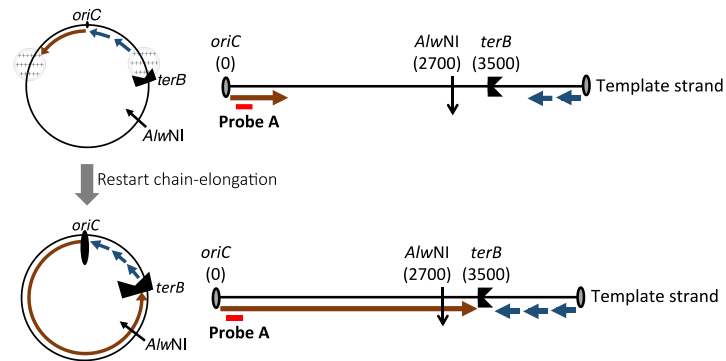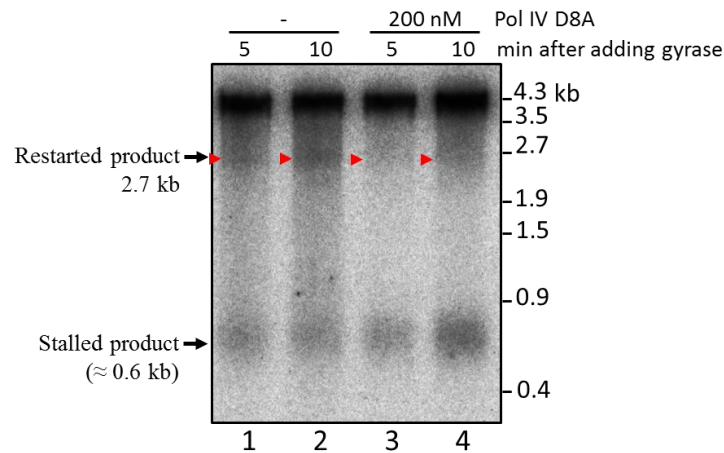
Figure 3.23. Studying the fate of Pol III after Pol III-Pol IV switch at the replication fork using the established novel system. Briefly, 30 μl of the *oriC* assay was carried out in the absence of DNA gyrase at 30ºC for 3 min. After that, the polymerase dead mutant Pol IV D8A was added to the final concentration of 200 nM, and incubated for 1 min. The Pol IV-switched replication forks were isolated from the unused components including Pol III by Pull down. Subsequently, 30 μl of the solution containing 10-fold excess amount of DNA gyrase and the components required for chain-elongation process of both leading- and lagging strand synthesis was added to the pellet containing the Pol IV-switched replication forks and incubated at 30ºC for 5 min or 10 min. DNA samples were separated by a 0.9% alkaline agarose gel electrophoresis and subjected to Southern blot analysis. The restarted leading product of the counter clock-wise fork was detected by probe A. (**A**) Schematic diagram representing the product pattern and location of the probe A. The dark red arrows represent the leading product, the blue arrows represent the Okazaki fragments, the circle containing the cross marks represents the accumulation of the positive supercoiled in front of the replication fork, the scarlet line represent probe A. Upper panel: the dynamic of *oriC* assay in the absence of DNA gyrase. Lower panel: the dynamic of *oriC* assay when the chain-elongation process was restarted. (**B**) Result of Southern blot analysis. Lanes 1-2: The control experiments without addition of Pol IV, the restoration of chain-elongation was lasted for 5, 10 min, respectively. Lanes 3-4: Pol III-Pol IV switched was introduced at the replication fork and the restoration of chain-elongation was lasted for 5, 10 min, respectively.

Chapter 4: Discussions and conclusions

4.1. Pol IV switches with an ongoing Pol III at the hairpin structure

Using Burst DNA synthesis assay, I found that a hairpin structure is a trigger for the polymerase switch between Pol III and Pol IV. At the hairpin site, Pol IV rapidly took the primer terminus from Pol III and synthesized the DNA instead of Pol III (Figure 3.6). However, this polymerase switch action by Pol IV was very transient, Pol III soon took back the primer terminus from Pol IV and resumed the processive DNA synthesis (Figure 3.7).

It was confirmed that in the presence of the single stranded-DNA binding protein (SSB), Pol III readily overcame the hairpin structure (Figure 3.1). Therefore, the observation that the polymerase switch between Pol III and Pol IV was stimulated at the hairpin site in the presence of SSB suggests that Pol IV has an ability to switch with an ongoing Pol III. Moreover, my data showed that there were more triggers for Pol III-Pol IV switch rather than the hairpin structure throughout the template DNA (Figure 3.3).

4.2. Pol III - Pol IV switch occurs when Pol III is acting strand displacement

Next, using the hairpin structure as an efficient trigger for Pol III – Pol IV switch, I studied how Pol IV gains access to the primer terminus from Pol III. To overcome the hairpin structure, Pol III needs to utilize the strand displacement activity. I found that Pol IV switches with the ongoing Pol III when Pol III is catalyzing the strand displacement reaction (Figure 3.10). This finding indicates that any obstacles on the template DNA that stimulates changing of the replication mode of Pol III from the normal synthesis to the strand displacement mode also facilitate Pol III-Pol IV switch.

4.3. Molecular mechanism for Pol IV to gain access to the primer terminus from Pol III

During processive chain-elongation by Pol III, α-polymerase subunit of the polymerase core stably stays on the primer terminus by the tight interactions with the cleft of the β clamp and the single stranded DNA template (Scotland et al., 2015). In addition, the ϵ-exonuclease subunit also occupies the second remaining protein-binding pocket on the cleft of the β clamp (Scotland et al., 2015). Therefore, in theory, there are two possibilities for Pol IV to take over

the protein-binding pocket on the cleft of the β clamp and to gain access to the primer terminus: Pol IV initiatively weakens the Pol III core-β clamp complex by itself; or the Pol III core-β clamp complex itself becomes weaker by some reasons and that provides a chance for entering of Pol IV. So far the molecular mechanism underlying the strand displacement activity of Pol III is not clear yet, but it was revealed that the interaction between ε subunit and β clamp is required (Jergic et al., 2013). Therefore, I speculated that during the strand displacement reaction, the enzyme might change the conformational state on the primer terminus from 5'-3' polymerization- to 3'-5' editting mode, probably to allow the enzyme idle in front of the hairpin. That change would make the interactions between Pol III and the cleft of the dimeric β clamp weaker, and Pol IV may enter to the primer terminus as a consequence of this transition. To test this speculation, I used a Pol III mutant DnaE173, which retains both polymerase- and exonuclease activities but the affinity between α subunit and the template DNA was enhanced, leading to a hyper-processive chain-elongation mode therefore less chance for the proofreading mode (Sugaya et al., 2002; Yanagihara et al., 2007). The observation that the mutant DnaE173 was more resistant to Pol IV at the hairpin site compared to the wild type Pol III (Figure 3.11) suggests that the conformational transition from polymerization mode to editing mode of Pol III on the primer terminus might be the trigger for Pol III-Pol IV switch. Within this point, there are also two possibilities. In the first possibility, Pol IV might take the primer terminus from Pol III during the process when Pol III performs the conformational transition (α and ε subunits transiently release from β clamp). In the second possibility, during Pol III is in the proofreading mode, because the affinity between ε subunit and β clamp is weaker, Pol IV may compete the protein-binding pocket on the cleft of β clamp with the ε subunit and access easily to the primer terminus (Figure 4.1).

The crystal structure of Pol IV revealed that the enzyme has an ability to contact with both the hydrophobic cleft and the rim of the dimeric β clamp (Bunting et al., 2003). While the interaction of Pol IV with the cleft of the β clamp is required for DNA synthesis of Pol IV, the second interaction of Pol IV with the clamp at the rim is believed to be required for polymerase switching (J. M. Heltzel et al., 2009; J. M. Heltzel, Maul, Wolff, & Sutton, 2012; Sale et al., 2012; Scotland et al., 2015). In addition, it was also hypothesized that the sliding β clamp could

bear two different polymerases at the same time during DNA synthesis (Indiani et al., 2005). Moreover, my data from the Burst DNA synthesis showed that Pol IV rapidly switched with almost of all the ongoing Pol III at the hairpin structure within several seconds (Figure 3.7). Taken all the evidence together, I propose that during Pol III synthesis, while both α and ε subunits of Pol III interact to both protein-binding pockets on the cleft of the dimeric β clamp, Pol IV keeps interacting with the rim of the dimeric β clamp in an inactive mode and translocates together with Pol III along the template DNA. When the ternary complex meets an obstacle such as a lesion or DNA secondary structure, Pol IV takes over the primer terminus when Pol III changes the mode from polymerization to proofreading (Figure 4.1).
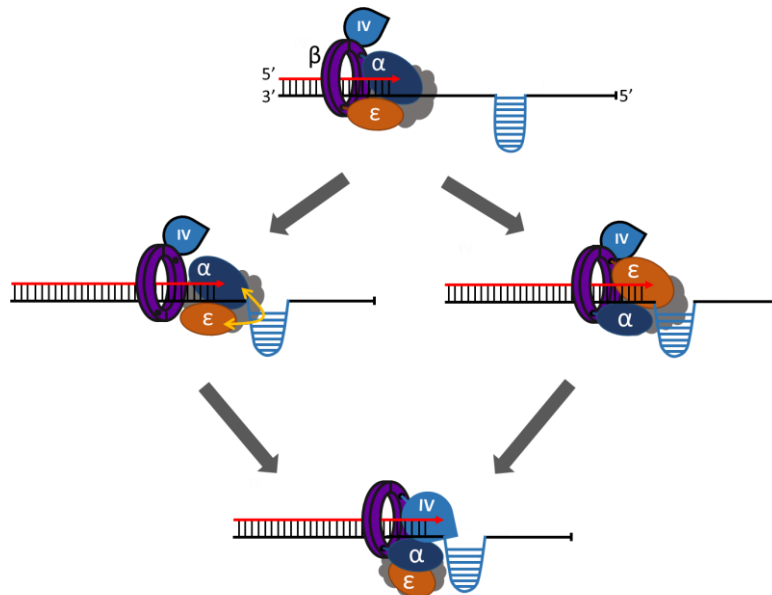
Figure 4.1. Model of how Pol IV gain access to the primer terminus from Pol III at the hairpin structure. During DNA synthesis, both α and ε subunits of Pol III occupy two protein-binding pockets on the cleft of β clamp whereas α subunit takes the primer terminus and performs normal chain-elongation process. Pol IV binds to the rim of β clamp and stays in an inactive form. When the ternary complex encounters the hairpin, Pol III changes the conformational mode from elongation (by α subunit) to proofreading (by ε subunit). There are two possibilities: i, during the conformational change, α and ε subunits may transiently release from β clamp and Pol IV may occupy the protein-binding pocket on the cleft of the β clamp and gain access to the primer terminus; ii, during proofreading mode, because the interaction between ε subunit and β clamp is weaker, Pol IV may compete with ε subunit and gain access to the primer terminus.

4.4. Effect of Pol IV on the normal replication fork

In the result of part II, Using the *in vitro oriC* replication assay that precisely mimics the bidirectional replication machinery of *E. coli*, I found that Pol IV has an ability to enter to the normal replication fork and inhibits DNA synthesis by Pol III. Moreover, my data suggested that Pol IV broke the coupling synthesis of leading- and lagging strand by Pol III at the replication fork, as the leading polymerase was more susceptible to Pol IV than the lagging polymerase. While the leading synthesis was blocked, the lagging synthesis still kept proceeding forward together with helicase and produced a shorter size of Okazaki fragments (Figure 3.12, 3.13). During the dis-continuous lagging strand synthesis, after an Okazaki fragment completion, the lagging polymerase dissociates from the β clamp and binds to the next β clamp on the lagging template strand for next Okazaki fragment synthesis. I suppose that this recycling action may help the lagging polymerase take back the primer terminus from Pol IV easier than the leading polymerase.

From the Burst DNA synthesis result, I found that there are many triggers for Pol III-Pol IV switch rather than the indicated hairpin along the template DNA. I speculate that they may be some particular sequences such as restriction enzyme recognition sites or the GC rich sequences, those likely exist in the *oriC* assay's template, pMOL7. Therefore, I propose that the inhibitory effect of Pol IV on Pol III at the replication fork was caused by Pol III-Pol IV switch. In the *oriC* assay condition, 50-100 nM of Pol IV was the threshold to see the negative effect of Pol IV on Pol III. Below this concentration, even if Pol IV takes over the primer terminus from Pol III, probably Pol III could return to the primer terminus and recover DNA synthesis. However, at high concentration of Pol IV, I speculate that the competition between Pol III and Pol IV becomes harder and Pol III is unable to come back to the primer terminus.

Since Pol IV is known as a low fidelity, low speed and low processivity polymerase, the possible participation of Pol IV during DNA synthesis explains the *in vivo* data why the overexpression of Pol IV strongly slowed down the replication fork speed and increased mutation frequency (Ikeda et al., 2012; Kuban et al., 2005; Kuban et al., 2006; Mori et al., 2012; Tan et al., 2015). During SOS induction, the cellular concentration of Pol IV is highly

upregulated (Fijalkowska, Schaaper, & Jonczyk, 2012a), hence the participation of Pol IV during genomic synthesis may serve for adaptive mutagenesis.

4.5. Establishment of a method to synchronize and isolate the replication intermediates from the reaction mixture

In this study, I succeeded to establish a novel method to synchronize the replisome and rapidly isolate the replication intermediates from the reaction mixture (Chapter 3 – II.2.3). I achieved a very high recovery rate of the replication intermediates (more than 50%) after just 1 minute. This rapid isolation is very meaningful because it avoids the replisome from denaturing or structural change. An earlier study also tried to isolate the replication intermediates from the reaction mixture, however, they used gel filtration method that took very long time but the recovery rate was very low (Yeeles & Marians, 2011). My established system is a very powerful tool for studying replication *in vitro* in future.

4.6. Fate of Pol III after Pol III-Pol IV switch at the replication fork

Using the novel method mentioned above to isolate the Pol IV-switched replication fork from the unused Pol III that remains in the reaction mixture, I observed an unexpected result that at high concentration of Pol IV, Pol III was pushed away from the replisome after Pol III-Pol IV switch at the replication fork (Figure 3.23). As described previously, on the replisome, Pol III holoenzyme also interacts with other replication components such as helicase or SSB. Through the replication fork isolation process, SSB might dissociate from the replisome. It was demonstrated that helicase still stably stayed on the replisome and is able to unwind the duplex DNA when the isolated replication fork was restarted (Figure 3.22). Perhaps the interaction between Pol III and helicase was not strong enough to keep Pol III stays on the replisome under effect of Pol IV.

Taken together, I speculate that when Pol IV is present at a high concentration, the enzyme occupies both protein-binding pockets on the cleft of the β clamp and pushes out Pol III from the replisome. This result indicates that a recruitment of a new Pol III is needed to re-form the replisome structure. Knowing the mechanism for Pol III to be recruited back to the replisome is also interesting. In addition, it is still unclear whether the same phenomenon is observed at

low concentration of Pol IV.

4.7. Conclusions

Collecting all data together, I propose a model for Pol III-Pol IV switch as shown in Figure 4.2. When Pol IV concentration is high, such as under SOS induction, while both α and ε subunits of Pol III bind to both protein-binding pockets on the cleft of the dimeric β clamp and Pol III carri es out the majority of DNA synthesis, Pol IV has an ability to bind to the rim of the dimeric β clamp and to stay in an inactive form. Therefore, Pol IV may translocate together with Pol III. When Pol III is troubled, Pol III changes the conformational state from polymerization to proofreading on the dimeric β clamp, and Pol IV enters to the primer terminus just during this transition or by competing with ε subunit during proofreading mode. Pol IV occupies both protein-binding pockets on the cleft of the β clamp and pushes Pol III away from the replisome. Consequently, a new Pol III is recruited to re-form the replisome structure.

I speculate that during translesion synthesis, when Pol III stalls at the DNA lesions, to avoid the replisome collapse and wait for a recuing pathway, Pol III idles around upstream of the lesion site by playing 3'-5' exonuclease activity. Therefore, Pol IV also takes over the primer terminus from Pol III during this idling process with the mechanism mentioned above.

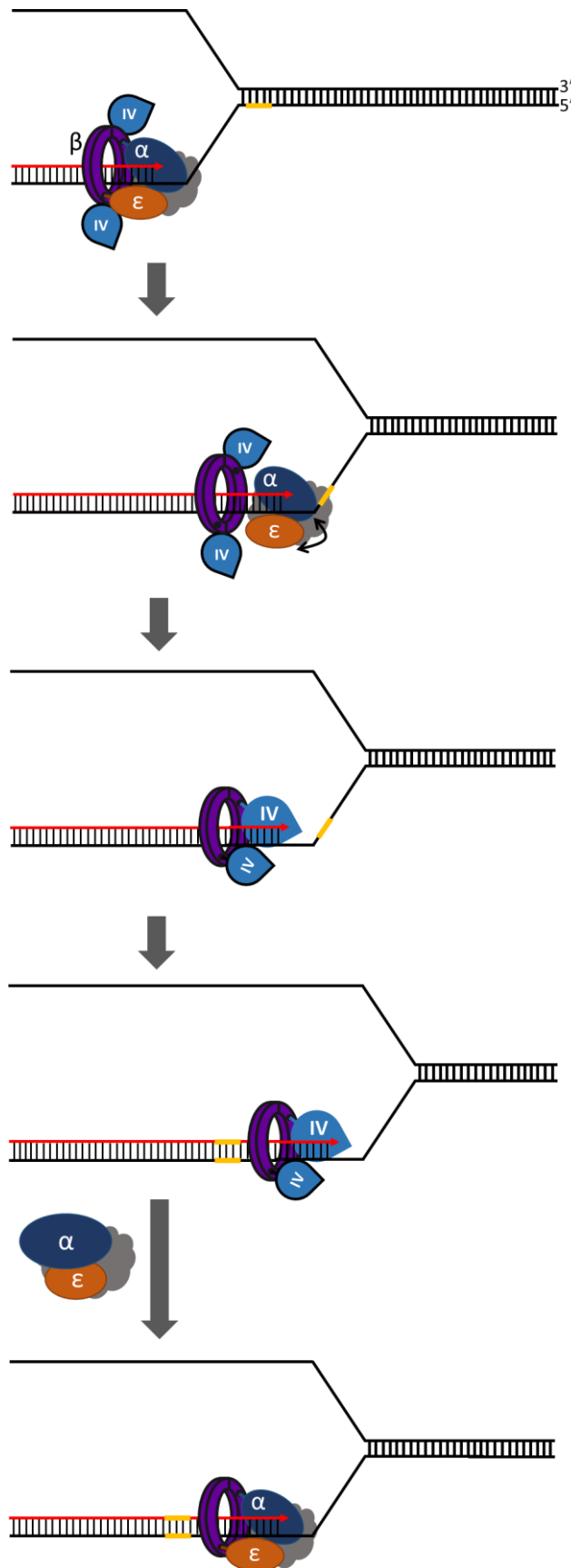**A proposed model for Pol III-Pol IV switch.**

Figure 4.2. A proposed model for Pol III-Pol IV switch. During DNA synthesis, both α and ε subunits of Pol III occupy both protein-binding pockets on the cleft of β clamp whereas α subunit takes the primer terminus and performs chain-elongation process. However, when Pol IV is present at a high concentration, such as under SOS condition, the enzyme binds to the rim of β clamp and translocates together with Pol III during DNA synthesis. When the ternary complex meets an obstacle on the template DNA, Pol III changes the mode from elongation to proofreading. During this transition, α and ε subunits may transiently release from β clamp, hence Pol IV occupies both protein-binding pockets on the cleft of β clamp and pushes away Pol III from the replication fork. In the case of TLS, after bypassing the lesion, a new Pol III is recruited to re-form the replisome structure and resumes the processive DNA synthesis.

Acknowledgements

Firstly, I would like to express my sincere gratitude to my supervisor, Prof. Hisaji Maki for giving me an opportunity to study in his lab, the laboratory of Microbial molecular genetics, graduate school of Biological sciences, Nara institute of science and technology (NAIST) as a PhD student. I am very happy and satisfied to study here, where I have been supporting the best conditions for my research and studying together with great people. During my studying here, his patient and careful guidance made me today. I could not have imagined having a better supervisor.

I would also like to express my profound appreciation to assistant professor, Dr. Asako Furukohri. I am very lucky to work with her during my doctoral project. She not only teaches me precious scientific knowledge but also takes care of me as if she were my oldest sister. She has shown me the light when I have been in the dark. This accomplishment would not have been possible without her continuous encouragement and helps throughout my years of study and through the process of writing this thesis.

I am also grateful to my advisors, Prof. Kimata and Prof. Takagi, who have been following me during my PhD course and giving me many helpful questions as well as insightful comments to complete my research.

My sincere thank also goes to Dr. Satoko Maki. Her precious advices during I prepared the works for Summer Camp and International Workshop improved my presentation skill a lot. I am also grateful to Associate professor Akiyama Masahiro for his thoughtful training at the beginning when I entered Maki lab and his contributions to make the lab's environment becomes better for our works.

Nevertheless, I would also like to acknowledge Mrs. Fukawa, other Maki lab members and my friends, who always listen and willingly to help me during my staying abroad.

I would like to extend my thanks to Nara institute of science and technology and graduate school of Biological sciences for their financial support during my study in Japan.

Last but not the least, I would like to take this opportunity to thank my family for their boundless love and encouragement. My special thanks to my husband, who always beside me, listen to me, support me, share up and down of this life with me.

References

Alberts, B., Johnson, A., & Lewis, J. (2002). Molecular biology of the cell 4th. *Garland Science,*

Bloom, L. B., Chen, X., Fygenson, D. K., Turner, J., O'Donnell, M., & Goodman, M. F. (1997). Fidelity of escherichia coli DNA polymerase III holoenzyme. the effects of beta, gamma complex processivity proteins and epsilon proofreading exonuclease on nucleotide misincorporation efficiencies. *The Journal of Biological Chemistry, 272*(44), 27919-27930.

Bunting, K. A., Roe, S. M., & Pearl, L. H. (2003). Structural basis for recruitment of translesion DNA polymerase pol IV/DinB to the β-clamp. *The EMBO Journal, 22*

Chivers, C. E., Koner, A. L., Lowe, E. D., & Howarth, M. (2011). How the biotin-streptavidin interaction was made even stronger: Investigation via crystallography and a chimaeric tetramer. *The Biochemical Journal, 435*(1), 55-63.

Dewar, J. M., & Walter, J. C. (2017). Mechanisms of DNA replication termination. *Nature Reviews.Molecular Cell Biology,*

Fernandez-Leiro, R., Conrad, J., Scheres, S. H., & Lamers, M. H. (2015). Cryo-EM structures of the E. coli replicative DNA polymerase reveal its dynamic interactions with the DNA sliding clamp, exonuclease and tau. *Elife, 4*, 10.7554/eLife.11134.

Fijalkowska, I. J., Schaaper, R. M., & Jonczyk, P. (2012a). DNA replication fidelity in escherichia coli: A multi-DNA polymerase affair. *FEMS Microbiology Reviews, 36*(6), 1105-1121.

Fijalkowska, I. J., Schaaper, R. M., & Jonczyk, P. (2012b). DNA replication fidelity in escherichia coli: A multi-DNA polymerase affair. *FEMS Microbiology Reviews, 36*(6), 1105-1121.

Fuchs, R. P. (2016). Tolerance of lesions in E. coli: Chronological competition between translesion synthesis and damage avoidance. *DNA Repair, 44*, 51-58.

Furukohri, A., Goodman, M. F., & Maki, H. (2008). A dynamic polymerase exchange with

escherichia coli DNA polymerase IV replacing DNA polymerase III on the sliding clamp. *The Journal of Biological Chemistry, 283*(17), 11260-11269.

Gabbai, C. B., Yeeles, J. T. P., & Marians, K. J. (2014). Replisome-mediated translesion synthesis and leading strand template lesion skipping are competing bypass mechanisms. *J Biol Chem, 289*

Ghosal, G., & Chen, J. (2013). DNA damage tolerance: A double-edged sword guarding the genome. *Translational Cancer Research, 2*(3), 107-129.

Goodman, M. F., & Woodgate, R. (2013). Translesion DNA polymerases. *Cold Spring Harbor Perspectives in Biology, 5*(10), a010363.

Heltzel, J. M., Maul, R. W., Scouten, P. S. K., & Sutton, M. D. (2009). A model for DNA polymerase switching involving a single cleft and the rim of the sliding clamp. *Proceedings of the National Academy of Sciences of the United States of America, 106*

Heltzel, J. M., Maul, R. W., Wolff, D. W., & Sutton, M. D. (2012). Escherichia coli DNA polymerase IV (pol IV), but not pol II, dynamically switches with a stalled pol III* replicase. *Journal of Bacteriology, 194*(14), 3589-3600.

Higuchi, K., Katayama, T., Iwai, S., Hidaka, M., Horiuchi, T., & Maki, H. (2003). Fate of DNA replication fork encountering a single DNA lesion during oriC plasmid DNA replication in vitro. *Genes to Cells, 8*

Ikeda, M., Furukohri, A., Philippin, G., Loechler, E., Akiyama, M. T., Katayama, T., et al. (2014). DNA polymerase IV mediates efficient and quick recovery of replication forks stalled at N2-dG adducts. *Nucleic Acids Research, 42*(13), 8461-8472.

Ikeda, M., Shinozaki, Y., Uchida, K., Ohshika, Y., Furukohri, A., Maki, H., et al. (2012). Quick replication fork stop by overproduction of escherichia coli DinB produces non-proliferative cells with an aberrant chromosome. *Genes & Genetic Systems, 87*(4), 221-231.

Indiani, C., McInerney, P., Georgescu, R., Goodman, M. F., & O'Donnell, M. (2005). A sliding-clamp toolbelt binds high- and low-fidelity DNA polymerases simultaneously. *Molecular Cell,*

19(6), 805-815.

James, E. K., Slobodan Jergic, Justin, M. H. H., Deena, T. J., Nicholas, E. D., Mark, D. S., et al. (2014). Polymerase exchange on single DNA molecules reveals processivity clamp control of translesion synthesis. *Proceedings of the National Academy of Sciences of the United States of America, 111*

Jergic, S., Horan, N. P., Elshenawy, M. M., Mason, C. E., Urathamakul, T., Ozawa, K., et al. (2013). A direct proofreader-clamp interaction stabilizes the pol III replicase in the polymerization mode. *The EMBO Journal, 32*(9), 1322-1333.

Justin, M. H. H., Robert, W. M., David, W. W., & Mark, D. S. (2012). *Escherichia coli* DNA polymerase IV (pol IV), but not pol II, dynamically switches with a stalled pol III* replicase. *Journal of Bacteriology, 194*

Kreuzer, K. N. (2013). DNA damage responses in prokaryotes: Regulating gene expression, modulating growth patterns, and manipulating replication forks. *Cold Spring Harbor Perspectives in Biology, 5*(11), a012674.

Kuban, W., Banach-Orlowska, M., Bialoskorska, M., Lipowska, A., Schaaper, R. M., Jonczyk, P., et al. (2005). Mutator phenotype resulting from DNA polymerase IV overproduction in escherichia coli: Preferential mutagenesis on the lagging strand. *Journal of Bacteriology, 187*(19), 6862-6866.

Kuban, W., Banach-Orlowska, M., Schaaper, R. M., Jonczyk, P., & Fijalkowska, I. J. (2006). Role of DNA polymerase IV in escherichia coli SOS mutator activity. *Journal of Bacteriology, 188*(22), 7977-7980.

LaDuca, R. J., Crute, J. J., McHenry, C. S., & Bambara, R. A. (1986). The beta subunit of the escherichia coli DNA polymerase III holoenzyme interacts functionally with the catalytic core in the absence of other subunits. *The Journal of Biological Chemistry, 261*(16), 7550-7557.

Layton, J. C., & Foster, P. L. (2003). Error-prone DNA polymerase IV is controlled by the stress-response sigma factor, RpoS, in escherichia coli. *Molecular Microbiology, 50*(2), 549-561.

Lewis, J. S., Jergic, S., & Dixon, N. E. (2016). The E. coli DNA replication fork. *The Enzymes, 39*, 31-88.

Maki, H., & Furukohri, A. (2013). DNA polymerase III, bacterial. *Encyclopedia of Biological Chemistry, 2*, 92-95.

Maki, H., Akiyama, M., Horiuchi, T., & Sekiguchi, M. (1990). Molecular mechanisms of replicational fidelity in escherichia coli. *Basic Life Sciences, 52*, 299-308.

Maki, H., & Kornberg, A. (1987). Proofreading by DNA polymerase III of escherichia coli depends on cooperative interaction of the polymerase and exonuclease subunits. *Proceedings of the National Academy of Sciences of the United States of America, 84*(13), 4389-4392.

Masaaki Moriya. (1993). Single-stranded shuttle phagemid for mutagenesis studies in mammalian cells: 8-oxoguanine in DNA induces targeted G·C → T·A transversions in simian kidney cells. *Proceedings of the National Academy of Sciences of the United States of America, 90*

McGlynn, P., & Lloyd, R. G. (2002). Recombinational repair and restart of damaged replication forks. *Nature Reviews.Molecular Cell Biology, 3*(11), 859-870.

McHenry, C. S. (2011). DNA replicases from a bacterial perspective. *Annual Review of Biochemistry, 80*, 403-436.

Mori, T., Nakamura, T., Okazaki, N., Furukohri, A., Maki, H., & Akiyama, M. T. (2012). Escherichia coli DinB inhibits replication fork progression without significantly inducing the SOS response. *Genes & Genetic Systems, 87*(2), 75-87.

Mott, M. L., & Berger, J. M. (2007). DNA replication initiation: Mechanisms and regulation in bacteria. *Nature Reviews.Microbiology, 5*(5), 343-354.

Neylon, C., Kralicek, A. V., Hill, T. M., & Dixon, N. E. (2005). Replication termination in escherichia coli: Structure and antihelicase activity of the tus-ter complex. *Microbiology and Molecular Biology Reviews : MMBR, 69*(3), 501-526.

Ozaki, S., & Katayama, T. (2009). DnaA structure, function, and dynamics in the initiation at the chromosomal origin. *Plasmid, 62*(2), 71-82.

Ozawa, K., Horan, N. P., Robinson, A., Yagi, H., Hill, F. R., Jergic, S., et al. (2013). Proofreading exonuclease on a tether: The complex between the E. coli DNA polymerase III subunits alpha, epsilon, theta and beta reveals a highly flexible arrangement of the proofreading domain. *Nucleic Acids Research, 41*(10), 5354-5367.

Reece, R. J., & Maxwell, A. (1991). DNA gyrase: Structure and function. *Crit Rev Biochem Mol Biol, 26*

Sale, J. E., Lehmann, A. R., & Woodgate, R. (2012). Y-family DNA polymerases and their role in tolerance of cellular DNA damage. *Nature Reviews.Molecular Cell Biology, 13*(3), 141-152.

Scotland, M. K., Heltzel, J. M., Kath, J. E., Choi, J. S., Berdis, A. J., Loparo, J. J., et al. (2015). A genetic selection for dinB mutants reveals an interaction between DNA polymerase IV and the replicative polymerase that is required for translesion synthesis. *PLoS Genetics, 11*(9), e1005507.

Shrivastav, N., Fedeles, B. I., Li, D., Delaney, J. C., Frick, L. E., Foti, J. J., et al. (2014). A chemical genetics analysis of the roles of bypass polymerase DinB and DNA repair protein AlkB in processing N2-alkylguanine lesions in vivo. *PloS One, 9*(4), e94716.

Stukenberg, P. T., Studwell-Vaughan, P. S., & O'Donnell, M. (1991). Mechanism of the sliding beta-clamp of DNA polymerase III holoenzyme. *The Journal of Biological Chemistry, 266*(17), 11328-11334.

Sugaya, Y., Ihara, K., Masuda, Y., Ohtsubo, E., & Maki, H. (2002). Hyper-processive and slower DNA chain elongation catalysed by DNA polymerase III holoenzyme purified from the dnaE173 mutator mutant of escherichia coli. *Genes to Cells : Devoted to Molecular & Cellular Mechanisms, 7*(4), 385-399.

Tan, K. W., Pham, T. M., Furukohri, A., Maki, H., & Akiyama, M. T. (2015). Recombinase and translesion DNA polymerase decrease the speed of replication fork progression during the DNA damage response in escherichia coli cells. *Nucleic Acids Research, 43*(3), 1714-1725.

Toste Rego, A., Holding, A. N., Kent, H., & Lamers, M. H. (2013). Architecture of the pol III-clamp-exonuclease complex reveals key roles of the exonuclease subunit in processive DNA synthesis and repair. *The EMBO Journal, 32*(9), 1334-1343.

Uchida, K., Furukohri, A., Shinozaki, Y., Mori, T., Ogawara, D., Kanaya, S., et al. (2008). Overproduction of escherichia coli DNA polymerase DinB (pol IV) inhibits replication fork progression and is lethal. *Molecular Microbiology, 70*(3), 608-622.

Yanagihara, F., Yoshida, S., Sugaya, Y., & Maki, H. (2007). The dnaE173 mutator mutation confers on the alpha subunit of escherichia coli DNA polymerase III a capacity for highly processive DNA synthesis and stable binding to primer/template DNA. *Genes & Genetic Systems, 82*(4), 273-280.

Yeeles, J. T., & Marians, K. J. (2011). The escherichia coli replisome is inherently DNA damage tolerant. *Science (New York, N.Y.), 334*(6053), 235-238.

Yuan, Q., & McHenry, C. S. (2009). Strand displacement by DNA polymerase III occurs through a tau-psi-chi link to single-stranded DNA-binding protein coating the lagging strand template. *The Journal of Biological Chemistry, 284*(46), 31672-31679.